Space-Time Geostatistical Assessment of Hypoxia in the Northern Gulf of Mexico

V. Rohith Reddy Matli, Shiqi Fang, Joseph Guinness, Nancy. N. Rabalais, J. Kevin Craig, and Daniel R. Obenour

SEDAR74-RD85

September 2021

Environmental Science & Technology

Article

Cite This: Environ. Sci. Technol. XXXX, XXX, XXX−XXX

pubs.acs.org/est

Space-Time Geostatistical Assessment of Hypoxia in the Northern Gulf of Mexico

V. Rohith Reddy Matli,[†] Shiqi Fang,[†] Joseph Guinness,[‡] Nancy. N. Rabalais,[§] J. Kevin Craig,[∥] and Daniel R. Obenour*[,†]

[†]Department of Civil, Construction & Environmental Engineering, North Carolina State University, Raleigh, North Carolina 27607, United States

[‡]Department of Statistical Science, Cornell University, Ithaca, New York 14853, United States

[§]Department of Oceanography and Coastal Sciences, Louisiana State University Baton Rouge, Louisiana 70803, United States

[∥]NOAA Southeast Fisheries Science Center Beaufort North Carolina 28516, United States

Supporting Information

ABSTRACT: Nearly every summer, a large hypoxic zone forms in the northern Gulf of Mexico. Research on the causes and consequences of hypoxia requires reliable estimates of hypoxic extent, which can vary at submonthly time scales due to hydro-meteorological variability. Here, we use an innovative space-time geostatistical model and data collected by multiple research organizations to estimate bottom-water dissolved oxygen (BWDO) concentrations and hypoxic area across summers from 1985 to 2016. We find that 27% of variability in BWDO is explained by deterministic trends with location, depth, and date, while correlated stochasticity accounts for 62% of observational variance within a range of 185 km and 28 days. Space-time modeling reduces uncertainty in estimated hypoxic area by 30% when compared to a spatial-only model, and results provide new insights into the temporal variability of hypoxia. For years with shelf-wide cruises in multiple months, hypoxia is most severe in July in 59% of years, 29% in August, and 12% in June. Also, midsummer cruise estimates of hypoxic area are only modestly correlated with summer-wide (June-August) average estimates (r^2 = 0.5), suggesting midsummer cruises are not necessarily reflective of seasonal hypoxic severity. Furthermore, summer-wide estimates are more strongly correlated with nutrient loading than midsummer estimates.

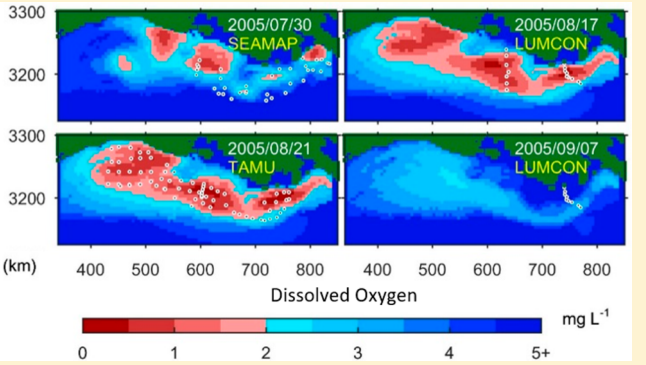

INTRODUCTION

Increasing anthropogenic activities across the world have led to increased nutrient loading to aquatic ecosystems from both point and nonpoint sources.[1] One major effect of nutrient loading is enhanced algal production and eutrophication in receiving waters.[2,3] As the produced organic matter settles to bottom waters and decomposes, dissolved oxygen (DO) levels can be depleted to levels that are harmful to many aquatic taxa.[4−6] This phenomenon, known as hypoxia, occurs when DO levels fall below a critical threshold, typically taken as 2 mg L^{-1} (63 μM). Due to the absence of many forms of aquatic life, hypoxic zones are often referred to as "dead zones". The number of coastal dead zones has increased over the past few decades, and particularly large hypoxic zones are observed in the Baltic Sea, Black Sea, Gulf of Mexico, and East China Sea.[7,8]

The Louisiana−Texas shelf of the northern Gulf of Mexico experiences one of the largest anthropogenically driven hypoxic zones worldwide, at times exceeding 20 000 km^2 in areal extent.[4,9] Hypoxia in the Gulf has been linked to nutrient loadings from the Mississippi−Atchafalaya river system,[10] which is the largest drainage system of the United States, covering more than 3.22 million square kilometers.[11,12] River discharge usually peaks in the spring (March−May) and coastal currents carry the nutrient-rich water westward over the Louisiana−Texas shelf.[13] Freshwater discharge and warming surface waters promote stratification of the water column, while high nutrient concentrations stimulate growth of phytoplankton.[10,14−16] The decomposition of this autochthonous organic matter below the pycnocline produces a substantial hypoxic zone nearly every summer.[4] The high primary production derived from riverine nutrients has historically supported major fisheries in the region via bottom-up effects.[17−19] However, overlap in time and space with severe hypoxia has led to negative effects on aquatic species,[20−22] that have implications for economically important

Received: June 25, 2018
Revised: September 17, 2018
Accepted: September 28, 2018
Published: September 28, 2018

DOI: 10.1021/acs.est.8b03474
Environ. Sci. Technol. XXXX, XXX, XXX−XXX

fisheries.[21,23] As a result, there is considerable interest in reducing the severity of Gulf hypoxia.[24]

Nearly every year, several organizations conduct cruises in the Gulf of Mexico for monitoring hydrographic conditions including hypoxia, as well as other aspects of the ecosystem. These cruises have been conducted by Louisiana Universities Marine Consortium (LUMCON), Southeast Area Monitoring and Assessment Program (SEAMAP), Texas A&M University (TAMU), University of Maryland Center for Environmental Sciences (UMCES), U.S. Environmental Protection Agency (EPA), and Nutrient Enhanced Coastal Productivity Program (NECOP). In addition to shelf-wide cruises, LUMCON and Louisiana Department of Wildlife and Fisheries (LDWF) conducted smaller transect cruises at selected locations along the shelf. However, the hypoxic area has typically been estimated only for midsummer LUMCON shelf-wide cruises. These midsummer estimates have been determined through simple interpolation and contouring[10] and through geostatistical modeling.[9] The latter approach was developed to provide a systematic methodology for determining hypoxic extent (including volume) with quantified uncertainty, while addressing potential biases associated with changes in cruise coverage and instrumentation over time.

Estimates of hypoxic extent are critical to both nutrient and fisheries management. These annual estimates are the standard for assessing progress toward the Hypoxia Task Force goal of reducing the area of hypoxia in the Gulf to 5000 km^2 over a five-year running average by 2035[24] and have also been used to assess effects on fisheries.[21,25−27] While early work focused on single factor correlations between coarse measures of hypoxic severity and annual fisheries landings,[25,26] recent studies have found that significant hypoxia effects emerge when analyses are conducted at higher spatial and temporal resolution over the course of a fishing season.[21,27,28] Estimates of hypoxic area are also essential for calibrating a number of statistical[29−31] and parsimonious mechanistic models[32,33] that forecast hypoxic severity based primarily on nutrient loading and river flow.[34] In addition, relatively complex hydrodynamic and water quality models use hypoxic area estimates for verification.[35,36] Current estimates of hypoxic area reflect only midsummer conditions, and are of limited value for verification of models that simulate the entire summer season[36] or for assessing effects on seasonally dynamic fisheries. Thus, hypoxia modeling and prediction could potentially be enhanced through development of empirical hypoxia estimates that capture the evolution of hypoxia throughout the summer.

Geostatistics can be used to model data that are spatially and temporally correlated in a statistically rigorous framework.[37] Geostatistics was originally developed in the field of mining, and is now widely used in meteorology,[38−40] environmental science,[41−43] and agriculture.[44−46] A number of studies have demonstrated that geostatistical methods often outperform simpler interpolation methods.[47−49] Murphy et al.[50] used geostatistics for modeling hypoxia in Chesapeake Bay and discussed the advantages of using universal kriging for interpolation.[37] Zhou et al.[51] developed a geostatistical model for bottom-water dissolved oxygen (BWDO) in Lake Erie and Obenour et al.[9] developed coupled geostatistical models for BWDO and hypoxic thickness to estimate both hypoxic area and volume. Zhou et al.[52] also developed a three-dimensional geostatistical model for modeling hypoxic volume in Chesapeake Bay. The models developed by Obenour et al.[9] and Zhou et al.[51,52] provide robust estimates of hypoxic extent with quantified uncertainties using conditional realizations (CRs).[37]

Temporal dynamics have received limited attention in geostatistical modeling, due to the data requirements and computational demands associated with adding the temporal dimension to geospatial estimation.[53] Space-time geostatistics, which is a subclass of spatial statistics,[54] allows for probabilistic interpolation in time as well as space. Additionally, temporal trends can be rigorously analyzed within a framework that addresses autocorrelation in the response variable. Some of the earliest space-time geostatistical models were used to model acid rains[55] and groundwater.[56] Space-time geostatistics has also been applied in other fields,[41,57,58] although applications to aquatic systems have been limited. The present study explores, for the first time, the utility of space-time geostatistical modeling for characterizing environmental dynamics within a large-scale aquatic system.

The objectives of this study are to develop a space-time geostatistical model for BWDO in the northern Gulf of Mexico and to use the model to explore the intra- and interannual variability in hypoxic areal extent. The model integrates BWDO samples from seven organizations, comprising over 7000 sampling events from 1985 to 2016, and considers large-scale spatial trends with respect to easting, northing, and bathymetry. Advantages of incorporating temporal trends and temporal covariance within the geostatistical model to constrain estimation uncertainty are evaluated. The resulting model is used to develop estimates of hypoxic area at a 3-day time step from May through September of each year. Intra-annual variability in hypoxia is characterized, and interannual variability is compared to hypoxia estimates from previous studies and seasonal nutrient loading.

METHODOLOGY

Data and Study Boundaries. We compiled DO data collected by LUMCON, SEAMAP, TAMU, EPA, LDWF, UMCES, and NECOP from the years 1985 to 2016 (section S1 of the Supporting Information, SI). DO was sampled using rosette-mounted DO probes by all organizations except LDWF and sometimes LUMCON. In addition to rosette-mounted DO probes, LUMCON also used hand-held DO probes in most years, and LDWF used only hand-held DO probes. These data reflect ship-based measurements conducted during monitoring cruises of various spatial extent and temporal duration. A summary of cruises is presented in Figures 1, 2, S1, and S2. While most cruises covered large portions of the shelf (i.e., shelf-wide cruises), LUMCON transect (LUMCON-T) and LDWF cruises had relatively limited spatial coverage.

Sampling locations (latitude, longitude) were converted to Universal Transverse Mercator (UTM) Zone 15N to estimate geographic distances.[59] The depth at each location was determined using digital elevation data obtained from NOAA.[60] Sampling events with unusually erratic profiles or unrealistic DO values indicating instrument malfunction, were omitted from this analysis. Processed data were synthesized to extract maximum depth and BWDO from each profile. Hand-held probes are capable of sampling at lower depths (closer to the sea floor) compared to rosette-mounted DO probes. To correct the bias in these measurements, the data collected by rosette-mounted probes were adjusted using the methodology defined by Obenour et al.[9] when performing CRs (described below). On average, the BWDO from rosette-mounted DO probes were scaled by a factor of 0.95 ($BWDO_{corrected} = 0.95 \times$

DOI: 10.1021/acs.est.8b03474
Environ. Sci. Technol. XXXX, XXX, XXX−XXX

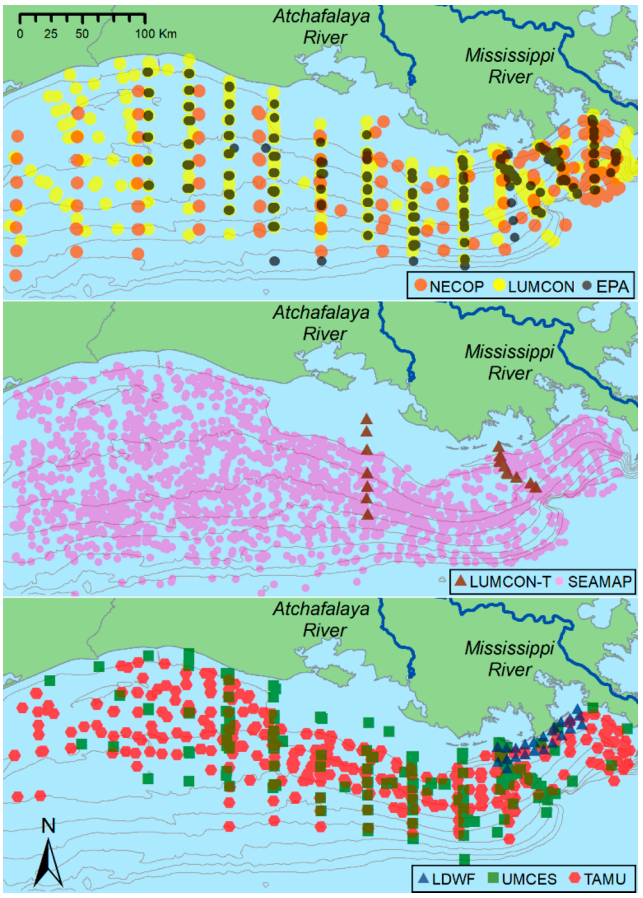

Figure 1. Locations of bottom water dissolved oxygen (BWDO) sampling from 1985 to 2016 within the study area, color-coded by monitoring program.

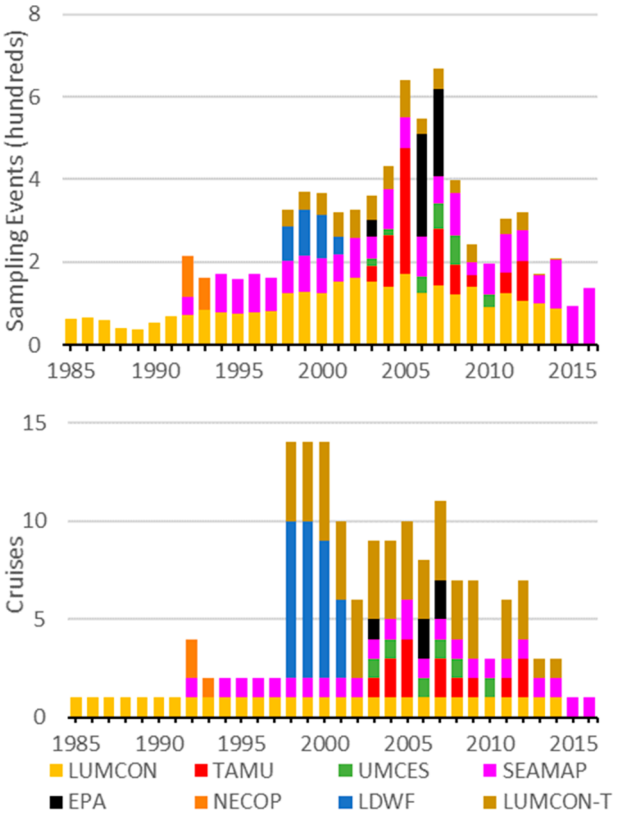

Figure 2. Number of sampling events and cruises by year, color-coded by monitoring program.

$BWDO_{Rosette}$), and this simple scaling factor was applied when characterizing deterministic trends (described below).

The spatial extent of this study is limited to the Louisiana–Texas shelf of the northern Gulf of Mexico between 342.5 and 837.5 km UTM easting (east Galveston Bay to Mississippi River Delta) and between 3122.5 and 3292.5 km UTM northing,[9] where most of the sampling occurred. Samples that were collected at depths beyond 100 m were omitted from the model as hypoxia occurs at shallower depths.[14] Predictions were further limited to depths between 3 and 80 m for computational efficiency, as hypoxia is very rare beyond 80 m, and sampling outside of this depth range is sparse.[9] We modeled data from May to September of each year when hypoxia is most common. Geospatial prediction was conducted on a 5 km^2 grid.

Model Formulation. In the geostatistical model, response variable z (i.e., BWDO) is determined by a linear combination of deterministic and stochastic components:

$$z = \mathbf{X}\beta + \eta + \varepsilon \quad (1)$$

where $\mathbf{X}\beta$ denotes the deterministic component, η represents spatially and temporally correlated stochasticity, and ε uncorrelated stochasticity (i.e., white noise) in the response. The deterministic component is similar to a multiple linear regression (MLR), including predictor variables $\mathbf{X}$ and their corresponding regression coefficients β. The $\mathbf{X}$ matrix can include both categorical variables (represented by a matrix of zeros and ones) and trend variables, also known as "drift" variables.[37] The β vector includes intercept coefficients corresponding to categorical variables and slope coefficients corresponding to trend variables. Categorical intercepts allow the deterministic trends (with space and intra-annually with time) to shift up or down to best fit the observations in each category, where categories can be years or individual cruises.

Spatiotemporal geostatistical models can be developed by incorporating temporal trend variables in the deterministic part of the model or by adding time as an additional dimension in the stochastic component of the model.[61,62] The model developed for this study uses both approaches, as described by Guinness and Stein[63] and Guinness.[64] The stochastic portion of eq 1, $\eta + \varepsilon$, is represented by a space-time covariance function. Space-time covariance functions are broadly classified into separable and nonseparable functions.[62] Separable functions do not allow for space-time interactions within the model,[53,65,66] which does not generally hold true in the case of large-scale environmental phenomenon.[67] Therefore, a non-separable exponential covariance function with a nugget effect is used (eq 2). If the time lag is zero, then this function reduces to an exponential spatial covariance function, as used by Obenour et al.[9]

$$Q(s_{i,j}, t_{i,j}) = \begin{cases} \sigma_\eta^2 + \sigma_\varepsilon^2, & s_{i,j} = t_{i,j} = 0 \\ \sigma_\eta^2 \times \exp\left(-\sqrt{\frac{s_{i,j}^2}{a^2} + \frac{t_{i,j}^2}{b^2}}\right), & s_{i,j} \text{ or } t_{i,j} > 0 \end{cases} \quad (2)$$

Here, Q is the covariance between a pair of observations (z_i and z_j) sampled at times (t_i and t_j) and locations (s_i and s_j), and thus separated by distance ($s_{i,j}$) and time lag ($t_{i,j}$). The parameters σ_η^2 and σ_ε^2 are the variances of stochasticity that are

DOI: 10.1021/acs.est.8b03474
Environ. Sci. Technol. XXXX, XXX, XXX−XXX

Table 1. Geostatistical Covariance Function Parameters σ_ε^2(Nugget), σ_η^2 (Partial Sill), α (Spatial Anisotropy Ratio), a (Spatial Range Parameter), b (Temporal Range Parameter), and BIC-Selected Trend Variables for Different Model Versions[a]

model version	σ_ε^2 (mg^2 L^{-2})	σ_η^2 (mg^2 L^{-2})	α	a (km)	b (days)	BIC-selected variables	deterministic R^2 (%)
A	0.59	2.03	2.26	49		E,N,D,D^2	41
B	0.50	2.75	2.26	68	10	E,N,D,D^2	22
C	0.49	2.60	2.27	62	9	E,N,D,D^2,T,T^2	27

[a]Note: Spatial and temporal ranges are approximately three times their respective range parameters.

spatiotemporally correlated and uncorrelated, respectively. Scaling parameters a and b are approximately equal to one-third the spatial and temporal ranges of correlation, respectively. To account for spatial anisotropy in the model, $s_{i,j}$ is scaled using parameter α, representing the ratio of east–west to north–south correlation ranges.[9,37] Covariance parameters including α are estimated using residual maximum likelihood estimation.[68,69]

Potential deterministic trends for BWDO include linear and quadratic trends with time (T and T^2), depth (D and D^2), easting (E and E^2), and northing (N and N^2). Bayesian Information Criterion (BIC),[70,71] which penalizes model complexity relative to model fit, was used to select among these candidate variables. We first used BIC to perform variable selection from MLR[72] ignoring spatial and temporal covariance. Covariance function parameters were estimated based on the residuals obtained from the BIC-selected model. Subsequently, geostatistical BIC[69] was used to repeat the variable selection accounting for spatial and temporal correlation (SI S3) and deterministic parameters were estimated using generalized least-squares.[69] Previous research indicated that the overall trend between depth and BWDO did not continue beyond 40 m, such that a maximum value of 40 m was used for trend formulation.[9] Deterministic model residuals were found to be normally distributed around these trends with minimal heteroscedasticity, thereby justifying this approach (SI S5).

The covariance function and selected deterministic trend variables were used to determine the geostatistical kriging weights ($\mathbf{\Lambda}_d$) for the estimation grid on a given date (d) through the following system of linear equations:[37]

$$\begin{bmatrix} \mathbf{Q}_{oo} & \mathbf{X}_o \\ \mathbf{X}_o^{\mathrm{T}} & \mathbf{0} \end{bmatrix} \begin{bmatrix} \mathbf{\Lambda}_d \\ -\mathbf{G}_d \end{bmatrix} = \begin{bmatrix} \mathbf{Q}_{oe,d} \\ \mathbf{X}_{e,d}^{\mathrm{T}} \end{bmatrix} \tag{3}$$

where $\mathbf{Q}_{oo}$ is the variance-covariance matrix of observations from all cruises determined using eq 2, $\mathbf{X}_o$ is the matrix of deterministic trend variables associated with the observations, $\mathbf{G}_d$ is a matrix of Lagrange multipliers, $\mathbf{X}_{e,d}$ is the matrix of trend variables associated with the estimation locations and date, and $\mathbf{Q}_{oe,d}$ is the variance-covariance matrix of observations and estimation locations. For n observations and p predictors (trend variables plus categorical variables), $\mathbf{Q}_{oo}$ is a matrix of size $n \times n$ and $\mathbf{X}_o$ is $n \times p$. For m estimation grid locations, $\mathbf{\Lambda}_d$ is an $n \times m$ matrix and $\mathbf{G}_d$ is $p \times m$.

Hypoxic area is probabilistically estimated using geostatistical Monte Carlo simulations, known as "conditional realizations".[37] A CR is performed by first creating an unconditional realization (i.e., a simulation of a Gaussian random function) with covariance from eq 2:

$$\begin{bmatrix} \mathbf{z}_{e,d}^{\mathrm{u}} \\ \mathbf{z}_{o,d}^{\mathrm{u}} \end{bmatrix} = \mathbf{C}\left(\begin{bmatrix} \mathbf{Q}_{ee} & \mathbf{Q}_{oe,d}^{\mathrm{T}} \\ \mathbf{Q}_{oe,d} & \mathbf{Q}_{oo} \end{bmatrix} \right)^{\mathrm{T}} \mathbf{u} \tag{4}$$

where $\mathbf{z}_{o,d}^{u}$ is an $n \times 1$ vector of simulated values at observation locations, $\mathbf{z}_{e,d}^{u}$ is an $n \times 1$ vector of simulations at estimation grid locations, $\mathbf{Q}_{ee}$ is an $m \times m$ variance-covariance matrix of estimation grid locations, and $\mathbf{u}$ is an $m \times 1$ vector of random independent samples from the standard normal distribution. The function $\mathbf{C}(\ )$ returns the Cholesky decomposition of the constructed matrix. The unconditional realizations are then conditioned to the observed data and deterministic trends using the kriging weights:

$$\mathbf{z}_{e,d}^{c} = \mathbf{\Lambda}_d^{\mathrm{T}}(\mathbf{z}_o - \mathbf{z}_{o,d}^{\mathrm{u}}) + \mathbf{z}_{e,d}^{\mathrm{u}} \tag{5}$$

where $\mathbf{z}_o$ is the $n \times 1$ vector of all BWDO observations, and the resulting $\mathbf{z}_{e,d}^{c}$ is the vector of conditionally simulated values across the estimation grid on date d. One thousand simulations were performed for each 3-day time step over the study period to develop probabilistic estimates of hypoxic area (see SI S4 for details on processing of simulations).

Alternate Temporal Formulations. We compared three different formulations of the geostatistical model for BWDO, each using a different approach for handling temporal variability. In the first version (A), temporal correlation and temporal trends were not considered. Instead, each cruise was assigned a unique intercept value (using cruise-specific categorical variables) within the deterministic component of the model. This approach is similar to Obenour et al.,[9] where geostatistical estimation was performed only at the times of LUMCON shelf-wide cruises. In the second version (B), data were modeled as temporally correlated within each summer season, and a single deterministic intercept value was applied to each year. In the third version (C), intra-annual temporal trends were considered, in addition to the temporal correlation and yearly intercepts of version B. The temporal trends included linear and quadratic trends with respect to date of collection. All model versions included spatial correlation and considered linear and quadratic trends with respect to space and bathymetry as potential covariates. In brief, version A uses cruise-specific intercepts to account for temporal variability, version B uses a space-time covariance function with year-specific intercepts, and version C adds intraseasonal deterministic temporal trends to B.

RESULTS AND DISCUSSION

Variable Selection and Parameter Estimation. Model parametrization is the first step in comparing and evaluating the three temporal formulations described above. Version A assigns a unique intercept to each cruise in the data set, and this flexibility allows 41% of variability in BWDO to be explained by the deterministic component of the model (R^2 = 0.41). However, some cruises are comprised of relatively few

DOI: 10.1021/acs.est.8b03474
Environ. Sci. Technol. XXXX, XXX, XXX–XXX

observations (e.g., LDWF and LUMCON transect cruises), which results in substantial uncertainty in their cruise-specific intercepts (S6). For version A, covariates E, N, D, and D^2 are selected as deterministic trend variables (Table 1). The total variance of stochastic components is found to be 2.62 $mg^2\ L^{-2}$, of which 77.5% is spatially correlated (Table 1). The spatial range of correlation is 148 km in the east−west direction ($3 \times a$ parameter in Table 1) and 65 km in the north−south direction, owing to spatial anisotropy. Version A does not consider temporal correlation and cannot be used for interpolating temporally (i.e., between cruises).

Model version B uses a more rigid deterministic framework, assigning a single categorical intercept to all cruises in a given year, thereby reducing the number of parameters to be estimated, when compared to version A. This rigidity decreases the variance explained by the deterministic component to 22% (from 41% in version A) and increases the total variance of stochastic components to 3.25 $mg^2\ L^{-2}$, of which 84.6% is spatially and temporally correlated (Table 1). The range of spatial correlation also increases relative to version A; and for samples collected at a given location, stochasticity is temporally correlated within a lag of 30 days ($3 \times b$ parameter in Table 1).

Gulf hypoxia is typically expected to peak in July with relatively little hypoxia in May and September.[10,14] To account for this seasonal pattern, linear and quadratic trends based on day-of-year (T, T^2) are considered in model version C. Here, variables E, N, D, D^2, T, and T^2 are selected based on BIC. The temporal trend increases the variance explained to 27% (from 22% in version B) and decreases the variance of the stochastic component modestly (Table 1 and SI S7). Including temporal trend variables also slightly reduces correlation ranges relative to version B (to 185 km and 28 days). We note the correlation ranges (for all three model versions) are longer than those determined previously for the northern Gulf (see SI S7).[73] For version C, quadratic trends indicate minimal BWDO at a depth of 24 m and in late July (SI S8).

Hypoxic Area Estimates. Model versions A, B, and C are used to estimate hypoxic area and associated uncertainty on the mean date of each cruise (Figure 3). Version A, which uses cruise specific intercepts, results in lower confidence interval (CI) widths for cruises with relatively extensive spatial coverage (e.g., 7/27/2005 in Figure 3), but relatively wide CIs for smaller cruises, reflecting substantial uncertainties in the cruise-specific intercepts (noted above). Conversely, versions B and C have lower uncertainties when data coverage is relatively sparse (e.g., 7/30/2005 and 8/17/2005 in Figure 3). There are some exceptions to this observation wherein the estimates from versions B and C have higher uncertainties than version A (e.g., 5/11/2005 and 9/29/2005 in Figure 3) but these disparities are isolated and not observed across all years (SI S9). Overall, CIs for version C are 30% less than for version A and 12% less than for version B, when averaged across all cruises (SI S9). This is expected, because the deterministic quadratic trend with time is found to be informative based on BIC (noted above). While studies using space-time geostatistics are often limited to time periods of abundant observational data,[53] incorporating deterministic trends helps characterize expected seasonal patterns and reduces uncertainty, particularly during periods with limited cruise data. Thus, the advantage of space-time modeling, using both temporal correlation and temporal trends, is quantitatively demonstrated, and version C is employed for mapping BWDO (S10) and estimating hypoxic area across each summer (Figure 4, SI S11). Although the best estimates of hypoxic area vary smoothly over time, the wide CIs determined through CR reflect potential temporal variability.[37] Results are also aggregated as 30-day (monthly) estimates that are less sensitive to short-term variability. Uncertainties are lowest on and around shelf-wide cruise dates, due to the relatively abundant monitoring data. On average, July 95% CIs widths are approximately 4000 km^2 (25%) less than those from other months, as a greater portion of the data were collected in July (SI S12).

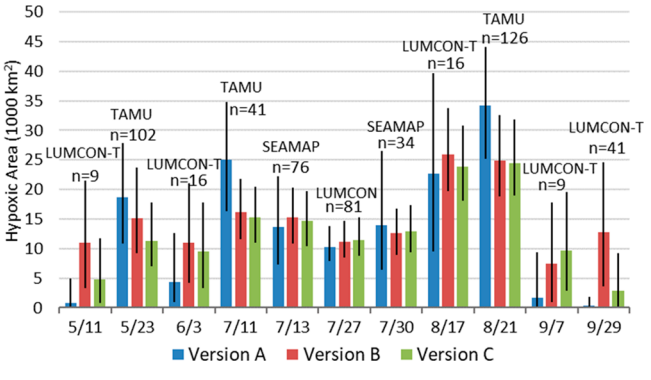

Figure 3. Estimates of hypoxic area obtained from model versions A, B, and C on the mean dates of each 2005 cruise. Error bars represent 95% confidence intervals. Number of samples and monitoring program is noted above the estimates for each cruise. Results for all cruises are tabulated in SI S9.

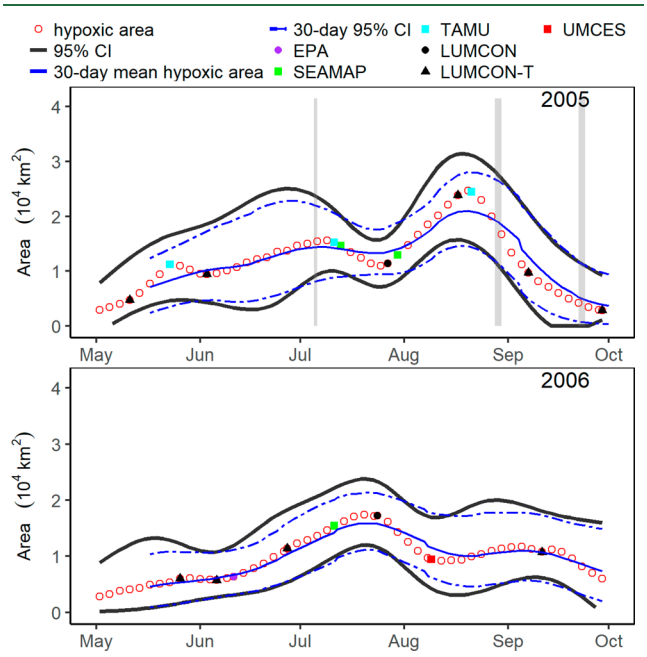

Figure 4. Daily (at 3-day intervals) and 30-day mean hypoxic area estimates with 95% CIs for example years, 2005 and 2006. Solid symbols represent cruise dates. Vertical gray bands represent times of major tropical storms.[74] See SI S11 for all years.

Comparisons among Annual Hypoxia Metrics. Daily estimates of hypoxic area are aggregated to calculate average hypoxic areas for the entire summer (June−August) and for the 30-day period of maximum hypoxia each year. These metrics are compared to estimates of hypoxic area from the

DOI: 10.1021/acs.est.8b03474
Environ. Sci. Technol. XXXX, XXX, XXX−XXX

times of the (LUMCON) midsummer shelf-wide cruises (Figure 5).[9] Over the entire study period, midsummer

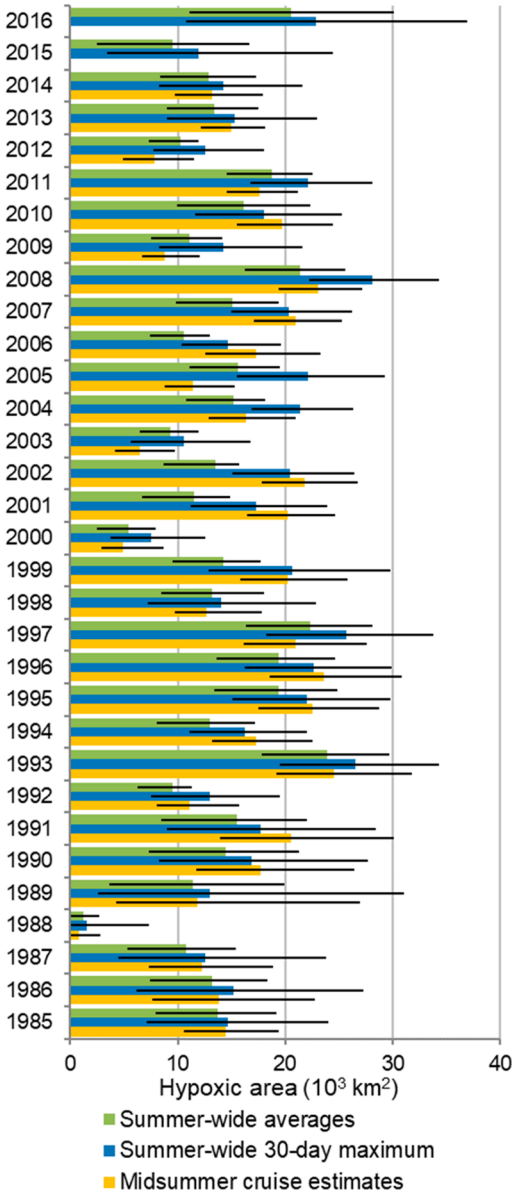

Figure 5. Hypoxic area estimates for the midsummer (LUMCON) shelf wide cruises, 30-day maximum and summer-wide (June–August) average. Error bars represent 95% CIs.

shelfwide cruise estimates are moderately correlated with the 30-day maximums and summer-wide estimates (r^2 of 0.75 and 0.69, respectively). However, in the earlier years of this study (1985–1997), there is little available observational data outside of the month of July, such that summer-wide and 30-day maximum estimates are heavily influenced by the midsummer cruise. The limited data availability in these earlier years is further reflected by relatively wide 95% CIs for these years (Figure 5). Compared to the period of 1998–2014, when shelfwide cruises were consistently conducted across multiple months, the summer-wide CIs for the period of 1985–1997 are 37% wider, on average. For 1998–2014, we note that midsummer cruise estimates are only modestly correlated with summer-wide average estimates (r^2 = 0.50) and 30-day maximum estimates (r^2 = 0.62). In addition, for 1998–2014, hypoxic area is estimated to be largest in the month of July in 10 years (59%), August in 5 years (29%) and June in 2 years (12%). These findings are generally consistent with previous studies indicating Gulf hypoxia is most severe from June through August.[5,75] However, the results demonstrate that estimates determined from one midsummer cruise per year are not necessarily reflective of seasonal hypoxic severity.

Analysis of Temporal Trends and Extrema. Temporal trend analysis was performed to assess whether hypoxia is becoming more or less severe over time, perhaps as a result of anthropogenic or hydroclimatological change. Long-term trend analysis following the procedure described in Obenour et al.,[9] suggests insignificant growth in summer-wide average hypoxic area (64 km^2 yr^{-1}, p = 0.48). A similar trend analysis performed on monthly averages (May–September) also shows no significant long-term trends over our study period.

Significant differences ($p < 0.05$, determined from two-tailed test) in summer-wide hypoxic area estimates (between years) are associated primarily with extreme drought or flood years. Severe droughts reduced freshwater and nutrient loads in 1988, 2000, and 2012,[76,77] corresponding to some of the smallest summer-wide hypoxic areas determined in this study. The estimated hypoxic area for 1988 is significantly lower than all other years, and the 2000 estimate is significantly lower than 83% of other years. The years 1993, 1997, and 2008 had some of the highest inflows of freshwater and nutrient load from Mississippi and Atchafalaya Rivers, with 1993 being an extreme flood year.[78] The highest summer-wide hypoxic area estimate is determined for 1993; however, summer-wide areas for years 1997 and 2008 vary by less than 10% from the 1993 value and their 95% CIs largely overlap. Previous studies did not find hypoxia to be severe in 1997, as the LUMCON midsummer cruise that year followed a tropical storm,[79] which appears to have temporarily disrupted hypoxia (SI S11). The larger 1997 summer-wide estimate provided by this study benefits from a SEAMAP cruise preceding the storm. We also note that 2002 has been reported as the largest hypoxic area measurement (for current study period),[15] but when considering summer-wide data from multiple cruises, other years were likely more severe.

Extreme and unusual hydro-meteorological conditions affect the development of hypoxia in the Gulf.[13,14] Tropical storms often disrupt stratification of the water column and enhance mixing of water layers. Scavia et al.[32] classified 1988, 1989, 1997, and 2003 as storm years based on meteorological records leading up to the times of midsummer shelf-wide cruises. Estimates from our model show sharp declines in hypoxia following many (but not all) major storm events (Figure 4; SI S11). Furthermore, in 1998 and 2009, westerly winds were unusually dominant, reducing midsummer hypoxic area.[30] Our results suggest hypoxia peaked in late June of these years and declined in July (Figures S27 and S30). However, in 1998, hypoxia re-formed in late summer leading to a second peak in August. These results further emphasize that midsummer cruise estimates are not always reflective of seasonal hypoxic severity, and may not be optimal for informing hypoxia and fisheries management.

Wind speed, direction, and duration are expected to play a significant role in hypoxia formation.[31,33,80,81] Future work could focus on developing meteorological inputs as candidate predictor variables for the geostatistical model. Accounting for wind-induced temporal variability could potentially result in more accurate BWDO estimates with reduced uncertainty.[16,21] However, the estimates developed in this study (without wind)

DOI: 10.1021/acs.est.8b03474
Environ. Sci. Technol. XXXX, XXX, XXX–XXX

may be more appropriate for calibrating and validating predictive models. If the geostatistical model incorporates the same (imperfect) wind data used to drive the predictive models, then the geostatistical estimates would no longer provide an independent check on model performance.

Hypoxic Area versus Nutrient Loading. Hypoxic area estimates are often used to calibrate predictive models that inform watershed management and refine our understanding of natural and anthropogenic factors influencing hypoxia formation.[34] These models use nutrient loading as a key predictor, sometimes supplemented with hydro-meteorological variables. To explore the predictability of our new hypoxia estimates, we examine correlations between hypoxic area and nutrient loading. Specifically, we considered bioavailable nitrogen loads (100% of inorganic and 12% of organic nitrogen)[33] based on USGS nutrient flux data.[82] We considered the midsummer cruise, 30-day maximum, and summer-wide mean hypoxic areas (Figure 5) for 1998−2014 (i.e., years with shelf-wide cruises in multiple months) as response variables.

Midsummer hypoxia estimates are most strongly correlated with February through June loads (r^2 = 0.48), and average summer-wide estimates are most strongly correlated with November−June loads (r^2 = 0.66) (Figure 6). Bootstrapping[83]

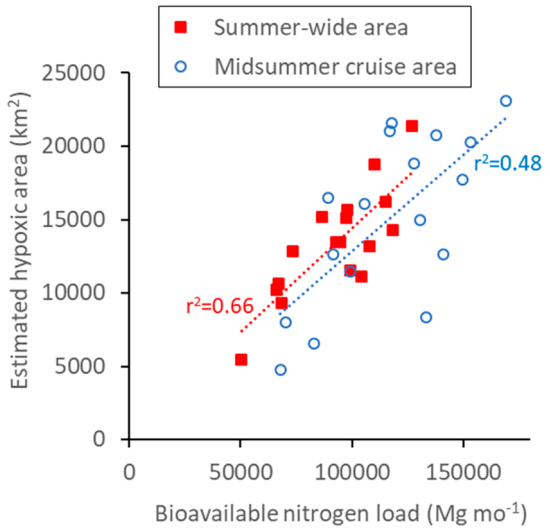

Figure 6. Plots of geostatistically estimated hypoxic area versus mean bioavailable nitrogen load (1998−2014). For midsummer LUMCON cruise and summer-wide (June−August) hypoxia estimates, nitrogen loads are averaged from February−June and November−June, respectively.

indicates that the summer-wide correlation with loading is stronger than the midsummer correlation at an 89% confidence level. Additionally, 30-day maximum hypoxic area is correlated with November−June loads (r^2 = 0.57). These results indicate that summer-wide and 30-day maximum estimates are more predictable than midsummer cruise estimates, likely because temporally integrated estimates are less influenced by meteorological fluctuations that affect hypoxia at specific times and locations.[30] Furthermore, these results suggest that a longer loading period (November−June) may be more relevant to hypoxia management than previously thought, when compared to the shorter period of April−June used in most predictive models.[34] While the November−June period is longer than the expected freshwater residence time on the Gulf Shelf,[84] organic matter can accumulate in the sediment over longer time-scales. Recent studies indicate sediment oxygen demand plays an important role in hypoxia formation[85] and may respond to nutrient loading over longer time-scales.[33] At the same time, the comparison between nutrient loading and hypoxic area presented here does not address the confounding correlation between flow and nutrient loading.[69] Flow and nutrient load tend to be correlated over time,[31] and are both known to promote hypoxia through enhanced water column stratification and organic matter production, respectively.[86] Given the importance of hypoxic area estimates for calibrating and verifying predictive models (see Introduction), we expect these results will be employed to refine our understanding of mechanistic drivers of hypoxia and to improve hypoxia forecast accuracy.

Future Directions. This study focuses on estimation of BWDO and associated bottom-water hypoxic area. For the first time, the utility of space-time geostatistics for synthesizing data from multiple disparate sampling programs to characterize variability in large-scale aquatic phenomena is demonstrated. Our approach complements high-resolution biophysical models that also make predictions across the shelf and explain around one-third of the spatiotemporal variability in BWDO observations.[36] Future Gulf research could focus on fusing geostatistical and biophysical modeling results, considering the uncertainties in each, to produce overall best estimates of BWDO and hypoxic area. Additionally, future research could expand the space-time modeling framework to simulate hypoxic thickness and volume. Similar to the spatial extent of hypoxia, the thickness of the hypoxic layer is expected to vary over inter- and intra-annual time scales.[9,10,16] In addition, the spatially and temporally extensive DO estimates provided here could be leveraged to further elucidate hypoxia effects on nekton, sessile organisms, and fisheries. Studies correlating annual measures of hypoxia severity with metrics of fishery performance have been criticized because they lack statistical power and rarely control for other potentially correlated factors.[26,87,88] Recent studies using higher resolution (daily to weekly temporal scales and 1 to 10 km spatial scales) fisheries catch and DO data have detected significant effects of hypoxia on fisheries not evident in annual correlations.[21,89,90]

■ ASSOCIATED CONTENT

Supporting Information

The Supporting Information is available free of charge on the ACS Publications website at DOI: 10.1021/acs.est.8b03474.

Data summary, model schematic, CR processing procedure, residual plots, parameter estimates, covariance plot, trend plots, summary of results for models A−C, BWDO maps, hypoxic area time series plots, and monthly hypoxic area plots (PDF)

■ AUTHOR INFORMATION

Corresponding Author

*Phone: +1 919-515 7702; e-mail: drobenour@ncsu.edu.

ORCID

Shiqi Fang: 0000-0001-5872-996X

Daniel R. Obenour: 0000-0002-7459-218X

Notes

The authors declare no competing financial interest.

DOI: 10.1021/acs.est.8b03474
Environ. Sci. Technol. XXXX, XXX, XXX−XXX

■ ACKNOWLEDGMENTS

We are grateful to Tiffany Toft (NOAA), Steve DiMarco (TAMU), Michael Harden (LDWF), Klaus Huebert (UMCES), and Michael Murrell (EPA) for assistance with monitoring data. Also, thanks to Dario Del Giudice, Michael Murrell, and Kyle Buck for helpful manuscript reviews. This work was funded by NOAA grant NA16NOS4780203. This is NGOMEX Contribution 236.

■ REFERENCES

(1) Galloway, J. N.; Townsend, A. R.; Erisman, J. W.; Bekunda, M.; Cai, Z.; Freney, J. R.; Martinelli, L. A.; Seitzinger, S. P.; Sutton, M. A. Transformation of the nitrogen cycle: recent trends, questions, and potential solutions. *Science* **2008**, *320* (5878), 889−892.

(2) Nixon, S. W. Coastal marine eutrophication: a definition, social causes, and future concerns. *Ophelia* **1995**, *41* (1), 199−219.

(3) Smith, V. H. Eutrophication of freshwater and coastal marine ecosystems a global problem. *Environ. Sci. Pollut. Res.* **2003**, *10* (2), 126−139.

(4) Rabalais, N. N.; Turner, R. E.; Wiseman, W. J., Jr Gulf of Mexico hypoxia, aka "The dead zone. *Annu. Rev. Ecol. Syst.* **2002**, *33* (1), 235−263.

(5) Rabalais, N. N.; Turner, R. E.; Scavia, D. Beyond Science into Policy: Gulf of Mexico Hypoxia and the Mississippi River: Nutrient policy development for the Mississippi River watershed reflects the accumulated scientific evidence that the increase in nitrogen loading is the primary factor in the worsening of hypoxia in the northern Gulf of Mexico. *BioScience* **2002**, *52* (2), 129−142.

(6) Breitburg, D. Effects of hypoxia, and the balance between hypoxia and enrichment, on coastal fishes and fisheries. *Estuaries* **2002**, *25* (4), 767−781.

(7) Diaz, R. J.; Rosenberg, R. Spreading dead zones and consequences for marine ecosystems. *Science* **2008**, *321* (5891), 926−929.

(8) Breitburg, D.; Levin, L. A.; Oschlies, A.; Grégoire, M.; Chavez, F. P.; Conley, D. J.; Garçon, V.; Gilbert, D.; Gutiérrez, D.; Isensee, K.; Jacinto, G. S.; Limburg, K. E.; Montes, I.; Naqvi, S. W. A.; Pitcher, G. C.; Rabalais, N. N.; Roman, M. R.; Rose, K. A.; Seibel, B. A.; Telszewski, M.; Yasuhara, M.; Zhang, J. Declining oxygen in the global ocean and coastal waters. *Science* **2018**, *359* (6371) DOI: 10.1126/science.aam7240.

(9) Obenour, D. R.; Scavia, D.; Rabalais, N. N.; Turner, R. E.; Michalak, A. M. Retrospective analysis of midsummer hypoxic area and volume in the northern Gulf of Mexico, 1985−2011. *Environ. Sci. Technol.* **2013**, *47* (17), 9808−9815.

(10) Rabalais, N. N.; Turner, R. E.; Justic, D.; Dortch, Q.; Wiseman, Jr, W. J. *Characterization of hypoxia: topic I report for the integrated assessment on hypoxia in the Gulf of Mexico*. NOAA/ National Centers for Coastal Ocean Science: Silver Spring, MD, 1999. https://aamboceanservice.blob.core.windows.net/oceanservice-prod/products/hypox_t1final.pdf.

(11) Goolsby, D. A.; Battaglin, W. A.; Lawrence, G. B.; Artz, R. S.; Aulenbach, B. T.; Hooper, R. P.; Keeney, D. R.; Stensland, G. J. *Flux and Sources of Nutrients in the Mississippi−Atchafalaya River Basin: Topic 3 Report for the Integrated Assessment on Hypoxia in the Gulf of Mexico*; National Centers for Coastal Ocean Science: Silver Spring, MD, 1999.

(12) Turner, R. E.; Rabalais, N. N. Changes in Mississippi River water quality this century. *BioScience* **1991**, *41* (3), 140−147.

(13) Walker, N. D.; Wiseman, W. J., Jr; Rouse, L. J., Jr; Babin, A. Effects of river discharge, wind stress, and slope eddies on circulation and the satellite-observed structure of the Mississippi River plume. *J. Coastal Res.* **2005**, *216* (6), 1228−1244.

(14) Rabalais, N. N.; Turner, R. E. Hypoxia in the northern Gulf of Mexico: description, causes and change. *Coastal Estuarine Stud.* **2001**, *58*, 1−36.

(15) Rabalais, N. N.; Turner, R. E.; Gupta, B. K. S.; Boesch, D. F.; Chapman, P.; Murrell, M. C. Hypoxia in the northern Gulf of Mexico: Does the science support the plan to reduce, mitigate, and control hypoxia? *Estuaries Coasts* **2007**, *30* (5), 753−772.

(16) Bianchi, T. S.; DiMarco, S. F.; Cowan, J. H., Jr; Hetland, R. D.; Chapman, P.; Day, J. W.; Allison, M. A. The science of hypoxia in the Northern Gulf of Mexico: a review. *Sci. Total Environ.* **2010**, *408* (7), 1471−1484.

(17) Gunter, G. The fertile fisheries crescent. *Journal of the Mississippi Academy of Sciences* **1963**, *9*, 286−290.

(18) Caddy, J. F. Toward a comparative evaluation of human impacts on fishery ecosystems of enclosed and semi-enclosed seas. *Rev. Fish. Sci.* **1993**, *1* (1), 57−95.

(19) Breitburg, D. L.; Hondorp, D. W.; Davias, L. A.; Diaz, R. J. Hypoxia, nitrogen, and fisheries: integrating effects across local and global landscapes. *Annual Review of Marine Science* **2009**, *1*, 329−349.

(20) Zhang, H.; Mason, D. M.; Stow, C. A.; Adamack, A. T.; Brandt, S. B.; Zhang, X.; Kimmel, D. G.; Roman, M. R.; Boicourt, W. C.; Ludsin, S. A. Effects of hypoxia on habitat quality of pelagic planktivorous fishes in the northern Gulf of Mexico. *Mar. Ecol.: Prog. Ser.* **2014**, *505*, 209−226.

(21) Purcell, K. M.; Craig, J. K.; Nance, J. M.; Smith, M. D.; Bennear, L. S. Fleet behavior is responsive to a large-scale environmental disturbance: Hypoxia effects on the spatial dynamics of the northern Gulf of Mexico shrimp fishery. *PLoS One* **2017**, *12* (8), e0183032.

(22) Rose, K. A.; Creekmore, S.; Thomas, P.; Craig, J. K.; Rahman, M. S.; Neilan, R. M. Modeling the population effects of hypoxia on Atlantic croaker (Micropogonias undulatus) in the northwestern Gulf of Mexico: part 1—model description and idealized hypoxia. *Estuaries Coasts* **2018**, *41* (1), 233−254.

(23) Langseth, B. J.; Schueller, A. M.; Shertzer, K. W.; Craig, J. K.; Smith, J. W. Management implications of temporally and spatially varying catchability for the Gulf of Mexico menhaden fishery. *Fisheries research* **2016**, *181*, 186−197.

(24) *Mississippi River/Gulf of Mexico Watershed Nutrient Task Force 2017 Report to Congress*; U.S. Environmental Protection Agency, Office of Wetlands, Oceans and Watersheds: Washington, DC, 2017, https://www.epa.gov/sites/production/files/2017-11/documents/hypoxia_task_force_report_to_congress_2017_final.pdf.

(25) Zimmerman, R. J.; Nance, J. M. Effects of hypoxia on the shrimp fishery of Louisiana and Texas. *Coastal Estuarine Stud.* **2001**, *58*, 293−310.

(26) O'Connor, T.; Whitall, D. Linking hypoxia to shrimp catch in the northern Gulf of Mexico. *Mar. Pollut. Bull.* **2007**, *54* (4), 460−463.

(27) Smith, M. D.; Oglend, A.; Kirkpatrick, A. J.; Asche, F.; Bennear, L. S.; Craig, J. K.; Nance, J. M. Seafood prices reveal impacts of a major ecological disturbance. *Proc. Natl. Acad. Sci. U. S. A.* **2017**, *114*, 1512−1517.

(28) Smith, M. D.; Asche, F.; Bennear, L. S.; Oglend, A. Spatial-dynamics of hypoxia and fisheries: The case of Gulf of Mexico brown shrimp. *Marine Resource Economics* **2014**, *29* (2), 111−131.

(29) Greene, R. M.; Lehrter, J. C.; Hagy, J. D., III Multiple regression models for hindcasting and forecasting midsummer hypoxia in the Gulf of Mexico. *Ecological Applications* **2009**, *19* (5), 1161−1175.

(30) Turner, R. E.; Rabalais, N. N.; Justić, D. Predicting summer hypoxia in the northern Gulf of Mexico: Redux. *Mar. Pollut. Bull.* **2012**, *64* (2), 319−324.

(31) Forrest, D. R.; Hetland, R. D.; DiMarco, S. F. Multivariable statistical regression models of the areal extent of hypoxia over the Texas−Louisiana continental shelf. *Environ. Res. Lett.* **2011**, *6* (4), 045002.

(32) Scavia, D.; Evans, M. A.; Obenour, D. R. A scenario and forecast model for Gulf of Mexico hypoxic area and volume. *Environ. Sci. Technol.* **2013**, *47* (18), 10423−10428.

(33) Obenour, D. R.; Michalak, A. M.; Scavia, D. Assessing biophysical controls on Gulf of Mexico hypoxia through probabilistic modeling. *Ecological Applications* **2015**, *25* (2), 492−505.

DOI: 10.1021/acs.est.8b03474
Environ. Sci. Technol. XXXX, XXX, XXX−XXX

(34) Scavia, D.; Bertani, I.; Obenour, D. R.; Turner, R. E.; Forrest, D. R.; Katin, A. Ensemble modeling informs hypoxia management in the northern Gulf of Mexico. *Proc. Natl. Acad. Sci. U. S. A.* **2017**, *114* (33), 8823−8828.
(35) Justić, D.; Wang, L. Assessing temporal and spatial variability of hypoxia over the inner Louisiana−upper Texas shelf: Application of an unstructured-grid three-dimensional coupled hydrodynamic-water quality model. *Cont. Shelf Res.* **2014**, *72*, 163−179.
(36) Fennel, K.; Laurent, A.; Hetland, R.; Justić, D.; Ko, D. S.; Lehrter, J.; Murrell, M.; Wang, L.; Yu, L.; Zhang, W. Effects of model physics on hypoxia simulations for the northern Gulf of Mexico: A model intercomparison. *Journal of Geophysical Research: Oceans* **2016**, *121* (8), 5731−5750.
(37) Chilès, J.-P; Delfiner, P. *Geostatistics: Modeling Spatial Uncertainty*; Wiley: New York, 1999.
(38) Hevesi, J. A.; Istok, J. D.; Flint, A. L. Precipitation estimation in mountainous terrain using multivariate geostatistics. Part I: structural analysis. *Journal of Applied Meteorology* **1992**, *31* (7), 661−676.
(39) Martinez-Cob, A. Multivariate geostatistical analysis of evapotranspiration and precipitation in mountainous terrain. *J. Hydrol.* **1996**, *174* (1−2), 19−35.
(40) Malherbe, L.; Cardenas, G.; Colin, P.; Yahyaoui, A. Using different spatial scale measurements in a geostatistically based approach for mapping atmospheric nitrogen dioxide concentrations. Application to the French Centre region. *Environmetrics* **2008**, *19* (7), 751−764.
(41) Stein, A.; Kocks, C. G.; Zadoks, J. C.; Frinking, H. D.; Ruissen, M. A.; Myers, D. E. A geostatistical analysis of the spatio-temporal development of downy mildew epidemics in cabbage. *Phytopathology* **1994**, *84* (10), 1227−1238.
(42) Liu, W.; Yu, H.; Chung, C. Assessment of water quality in a subtropical alpine lake using multivariate statistical techniques and geostatistical mapping: a case study. *Int. J. Environ. Res. Public Health* **2011**, *8* (4), 1126−1140.
(43) Rossi, R. E.; Mulla, D. J.; Journel, A. G.; Franz, E. H. Geostatistical tools for modeling and interpreting ecological spatial dependence. *Ecol. Monogr.* **1992**, *62* (2), 277−314.
(44) Trangmar, B. B.; Yost, R. S.; Uehara, G. Application of geostatistics to spatial studies of soil properties. *Advances in Agronomy*; Academic Press: 1986, *38*, 45−94.
(45) Oliver, M. A. Precision agriculture and geostatistics: How to manage agriculture more exactly. *Significance* **2013**, *10* (2), 17−22.
(46) Wang, G.; Pang, Z.; Boisvert, J. B.; Hao, Y.; Cao, Y.; Qu, J. Quantitative assessment of mineral resources by combining geostatistics and fractal methods in the Tongshan porphyry Cu deposit (China). *J. Geochem. Explor.* **2013**, *134*, 85−98.
(47) Tabios, G. Q.; Salas, J. D. A comparative analysis of techniques for spatial interpolation of precipitation. *J. Am. Water Resour. Assoc.* **1985**, *21* (3), 365−380.
(48) Goovaerts, P. Performance comparison of geostatistical algorithms for incorporating elevation into the mapping of precipitation. *The IV International Conference on GeoComputation hosted by Mary Washington College in Fredericksburg, VA, USA* 1999, *25*, 28.
(49) Murphy, R. R.; Curriero, F. C.; Ball, W. P. Comparison of spatial interpolation methods for water quality evaluation in the Chesapeake Bay. *J. Environ. Eng.* **2010**, *136* (2), 160−171.
(50) Murphy, R. R.; Kemp, W. M.; Ball, W. P. Long-term trends in Chesapeake Bay seasonal hypoxia, stratification, and nutrient loading. *Estuaries Coasts* **2011**, *34* (6), 1293−1309.
(51) Zhou, Y.; Obenour, D. R.; Scavia, D.; Johengen, T. H.; Michalak, A. M. Spatial and temporal trends in Lake Erie hypoxia, 1987−2007. *Environ. Sci. Technol.* **2013**, *47* (2), 899−905.
(52) Zhou, Y.; Scavia, D.; Michalak, A. M. Nutrient loading and meteorological conditions explain interannual variability of hypoxia in Chesapeake Bay. *Limnol. Oceanogr.* **2014**, *59* (2), 373−384.
(53) Heuvelink, G. B.; Pebesma, E.; Gräler, B. Space-time geostatistics. *Encyclopedia of GIS* **2016**, 1−7.
(54) Gelfand, A. E.; Diggle, P.; Guttorp, P.; Fuentes, M. *Handbook of Spatial Statistics*; CRC Press: Boca Raton, FL, 2010.
(55) Bilonick, R. A. Risk qualified maps of hydrogen ion concentration for the New York state area for 1966−1978. *Atmos. Environ.* **1983**, *17* (12), 2513−2524.
(56) Rouhani, S.; Hall, T. J. *Space-Time Kriging of Groundwater Data*; Springer: Dordrecht, 1989.
(57) Guttorp, P.; Meiring, W.; Sampson, P. D. A space-time analysis of ground-level ozone data. *Environmetrics* **1994**, *5* (3), 241−254.
(58) Heuvelink, G.; Griffith, D. A. Space−Time Geostatistics for Geography: A Case Study of Radiation Monitoring Across Parts of Germany. *Geographical Analysis* **2010**, *42* (2), 161−179.
(59) Bolstad, P. *GIS Fundamentals: A First Text on Geographic Information Systems*; Eider Press: White Bear Lake, MN, 2005.
(60) Northern Gulf 1 arc-second NAVD 88 Coastal Digital Elevation Model; https://www.ngdc.noaa.gov/metaview/page?xml=NOAA/NESDIS/NGDC/MGG/DEM/iso/xml/720.xml&view=getDataView&header=none. (Accessed January, 2018).
(61) Sølna, K.; Switzer, P. Time trend estimation for a geographic region. *J. Am. Stat. Assoc.* **1996**, *91* (434), 577−589.
(62) Kyriakidis, P. C.; Journel, A. G. Geostatistical space−time models: a review. *Math. Geol.* **1999**, *31* (6), 651−684.
(63) Guinness, J.; Stein, M. L. Stein Interpolation of Nonstationary High Frequency Spatial—Temporal Temperature Data. *Annals of Applied Statistics* **2013**, *7* (3), 1684−1708.
(64) Guinness, J. Permutation and Grouping Methods for Sharpening Gaussian Process Approximations. *Technometrics* **2018**, 1.
(65) Gneiting, T. Nonseparable, stationary covariance functions for space−time data. *J. Am. Stat. Assoc.* **2002**, *97* (458), 590−600.
(66) Gneiting, T.; Genton, M. G.; Guttorp, P. Geostatistical space-time models, stationarity, separability, and full symmetry. *Monographs on Statistics and Applied Probability* **2006**, *107*, 151.
(67) Fuentes, M.; Chen, L.; Davis, J. M. A class of nonseparable and nonstationary spatial temporal covariance functions. *Environmetrics* **2008**, *19* (5), 487−507.
(68) Mardia, K. V.; Marshall, R. J. Maximum likelihood estimation of models for residual covariance in spatial regression. *Biometrika* **1984**, *71* (1), 135−146.
(69) Obenour, D. R.; Michalak, A. M.; Zhou, Y.; Scavia, D. Quantifying the impacts of stratification and nutrient loading on hypoxia in the northern Gulf of Mexico. *Environ. Sci. Technol.* **2012**, *46* (10), 5489−5496.
(70) Schwarz, G. Estimating the dimension of a model. *annals of statistics* **1978**, *6* (2), 461−464.
(71) Cavanaugh, J. E. Model Selection: Bayesian Information Criterion. *Wiley StatsRef: Statistics Reference Online*; Wiley: Hoboken, NJ, 2009.
(72) Faraway, J. J. *Linear Models with R*; CRC press: 2014.
(73) Li, Y.; Nowlin, W. D.; Reid, R. O. Mean hydrographic fields and their interannual variability over the Texas-Louisiana continental shelf in spring, summer, and fall. *Journal of Geophysical Research: Oceans* **1997**, *102* (C1), 1027−1049.
(74) Atlantic Hurricane Season; https://www.nhc.noaa.gov/data/tcr/. (Accessed January, 2018).
(75) Rabalais, N. N.; Turner, R. E.; Wiseman, W. J. Hypoxia in the Gulf of Mexico. *J. Environ. Qual.* **2001**, *30* (2), 320−329.
(76) Andreadis, K. M.; Clark, E. A.; Wood, A. W.; Hamlet, A. F.; Lettenmaier, D. P. Twentieth-century drought in the conterminous United States. *Journal of Hydrometeorology* **2005**, *6* (6), 985−1001.
(77) Mallya, G.; Zhao, L.; Song, X. C.; Niyogi, D.; Govindaraju, R. S. 2012 Midwest drought in the United States. *Journal of Hydrologic Engineering* **2013**, *18* (7), 737−745.
(78) Larson, L. W. The great USA flood of 1993. *IAHS Publications-Series of Proceedings and Reports-Intern Assoc Hydrological Sciences* 1997, *239*, 13−20.
(79) *Preliminary Report: Hurricane Danny 16−26 July 1997*; National Hurricane Center: Miami, FL, 1997; http://www.nhc.noaa.gov/1996danny.html.

DOI: 10.1021/acs.est.8b03474
Environ. Sci. Technol. XXXX, XXX, XXX−XXX

(80) Feng, Y.; DiMarco, S. F.; Jackson, G. A. Relative role of wind forcing and riverine nutrient input on the extent of hypoxia in the northern Gulf of Mexico. *Geophys. Res. Lett.* **2012**, *39* (9), L09601.
(81) Rabalais, N. N.; Smith, L. M.; Turner, R. E. The Deepwater Horizon oil spill and Gulf of Mexico shelf hypoxia. *Cont. Shelf Res.* **2018**, *152*, 98−107.
(82) Nutrient Flux for the Mississippi River Basin and Subbasins; https://toxics.usgs.gov/hypoxia/mississippi/nutrient_flux_yield_est.html. (Accessed January, 2018).
(83) Efron, B. *Bootstrap Methods: Another Look at the Jackknife*; Springer: New York, NY, 1992.
(84) Zhang, X.; Hetland, R. D.; Marta-Almeida, M.; DiMarco, S. F. A numerical investigation of the Mississippi and Atchafalaya freshwater transport, filling and flushing times on the Texas-Louisiana Shelf. *Journal of Geophysical Research: Oceans* **2012**, *117* (C11), C11009.
(85) Fennel, K.; Hu, J.; Laurent, A.; Marta-Almeida, M.; Hetland, R. Sensitivity of hypoxia predictions for the northern Gulf of Mexico to sediment oxygen consumption and model nesting. *Journal of Geophysical Research: Oceans* **2013**, *118* (2), 990−1002.
(86) Wiseman, W. J.; Rabalais, N. N.; Turner, R. E.; Dinnel, S. P.; MacNaughton, A. Seasonal and interannual variability within the Louisiana coastal current: stratification and hypoxia. *Journal of Marine Systems* **1997**, *12* (1−4), 237−248.
(87) *Ecological and economic consequences of hypoxia: topic 2 report for the integrated assessment on hypoxia in the Gulf of Mexico*; National Centers for Coastal Ocean Science: Silver Spring, MD, 1999; http://www.cop.noaa.gov/pubs/das/das16.pdf.
(88) Rose, K. A.; Adamack, A. T.; Murphy, C. A.; Sable, S. E.; Kolesar, S. E.; Craig, J. K.; Breitburg, D. L.; Thomas, P.; Brouwer, M. H.; Cerco, C. F. Does hypoxia have population-level effects on coastal fish? Musings from the virtual world. *J. Exp. Mar. Biol. Ecol.* **2009**, *381*, S203.
(89) Huang, L.; Nichols, L. A.; Craig, J. K.; Smith, M. D. Measuring welfare losses from hypoxia: the case of North Carolina Brown Shrimp. *Marine Resource Economics* **2012**, *27* (1), 3−23.
(90) Langseth, B. J.; Purcell, K. M.; Craig, J. K.; Schueller, A. M.; Smith, J. W.; Shertzer, K. W.; Creekmore, S.; Rose, K. A.; Fennel, K. Effect of changes in dissolved oxygen concentrations on the spatial dynamics of the Gulf Menhaden fishery in the northern Gulf of Mexico. *Marine and Coastal Fisheries* **2014**, *6* (1), 223−234.

DOI: 10.1021/acs.est.8b03474
Environ. Sci. Technol. XXXX, XXX, XXX−XXX

Supporting Information

for

"A Space-Time Geostatistical Assessment of Hypoxia in the Northern Gulf of Mexico."

by

V Rohith Reddy Matli, Shiqi Fang, Joseph Guinness, Nancy. N. Rabalais, J. Kevin Craig,

and Daniel R. Obenour*

consisting of

13 sections with 32 figures and 6 tables in 53 pages.

*corresponding author, drobenour@ncsu.edu

Table of Contents

S1: Summary of Gulf monitoring cruises used in this study, 1985-2016

Data were retrieved from National Oceanic and Atmospheric Administration (NOAA) National Centers for Environmental Information.[1-23] TAMU data for the years 2010-2012 were provided by the director of TAMU's Mechanisms Controlling Hypoxia program (personal communication, S. DiMarco, 2017). Similarly, LDWF data were provided by LDWF program staff (personal communication M. Harden, 2017).

Table S1. Summary of available data.

Source	Number of Observations	Start Date	End Date	Mean Date
LUMCON	61	7/15/1985	7/20/1985	7/17/1985
LUMCON	67	7/7/1986	7/17/1986	7/11/1986
LUMCON	60	7/1/1987	7/5/1987	7/2/1987
LUMCON	42	8/12/1988	8/16/1988	8/13/1988
LUMCON	37	8/4/1989	8/9/1989	8/6/1989
LUMCON	54	7/23/1990	7/27/1990	7/24/1990
LUMCON	69	7/16/1991	7/20/1991	7/17/1991
NECOP	36	5/5/1992	5/13/1992	5/8/1992
NECOP	65	5/14/1992	5/20/1992	5/17/1992
SEAMAP	43	6/28/1992	7/7/1992	7/3/1992
LUMCON	71	7/24/1992	7/29/1992	7/25/1992
NECOP	80	7/2/1993	7/12/1993	7/6/1993
LUMCON	83	7/24/1993	7/30/1993	7/26/1993
SEAMAP	92	7/4/1994	7/18/1994	7/11/1994
LUMCON	79	7/24/1994	7/29/1994	7/26/1994
SEAMAP	85	7/6/1995	7/18/1995	7/13/1995
LUMCON	75	7/21/1995	7/26/1995	7/23/1995
SEAMAP	92	7/3/1996	7/16/1996	7/10/1996
LUMCON	78	7/23/1996	7/28/1996	7/25/1996
SEAMAP	80	6/30/1997	7/13/1997	7/6/1997
LUMCON	82	7/23/1997	7/29/1997	7/25/1997
LUMCONT	9	5/12/1998	5/12/1998	5/12/1998
LDWF	7	5/12/1998	5/12/1998	5/12/1998
LDWF	4	5/27/1998	5/27/1998	5/27/1998
LUMCONT	12	6/9/1998	6/10/1998	6/9/1998
LDWF	13	6/23/1998	6/23/1998	6/23/1998
SEAMAP	76	7/1/1998	7/16/1998	7/10/1998
LDWF	6	7/14/1998	7/14/1998	7/14/1998
LDWF	12	7/21/1998	7/21/1998	7/21/1998
LUMCON	84	7/16/1998	7/26/1998	7/22/1998
LDWF	13	8/18/1998	8/18/1998	8/18/1998
LUMCONT	10	8/11/1998	8/19/1998	8/18/1998

Source	Number of Observations	Start Date	End Date	Mean Date
LDWF	17	8/25/1998	8/25/1998	8/25/1998
LUMCONT	9	9/22/1998	9/22/1998	9/22/1998
LDWF	12	9/22/1998	9/22/1998	9/22/1998
LUMCONT	9	5/4/1999	5/4/1999	5/4/1999
LDWF	14	5/18/1999	5/18/1999	5/18/1999
LDWF	10	5/25/1999	5/25/1999	5/25/1999
LDWF	18	6/3/1999	6/3/1999	6/3/1999
LUMCONT	10	6/3/1999	6/9/1999	6/8/1999
LDWF	10	6/17/1999	6/30/1999	6/19/1999
SEAMAP	87	7/4/1999	7/20/1999	7/14/1999
LUMCON	85	7/23/1999	7/30/1999	7/25/1999
LDWF	14	7/29/1999	7/29/1999	7/29/1999
LDWF	19	8/5/1999	8/5/1999	8/5/1999
LUMCONT	9	8/24/1999	8/24/1999	8/24/1999
LDWF	13	8/31/1999	8/31/1999	8/31/1999
LDWF	14	9/9/1999	9/9/1999	9/9/1999
LUMCONT	10	9/7/1999	9/14/1999	9/13/1999
LUMCONT	3	5/8/2000	5/15/2000	5/10/2000
LUMCONT	8	5/15/2000	5/15/2000	5/15/2000
LDWF	17	5/22/2000	5/22/2000	5/22/2000
LUMCONT	2	6/2/2000	6/2/2000	6/2/2000
LUMCONT	9	6/14/2000	6/14/2000	6/14/2000
LDWF	15	6/15/2000	6/15/2000	6/15/2000
LDWF	14	6/27/2000	6/27/2000	6/27/2000
LUMCONT	10	7/5/2000	7/10/2000	7/7/2000
LDWF	19	7/10/2000	7/10/2000	7/10/2000
SEAMAP	84	7/3/2000	7/19/2000	7/12/2000
LUMCON	72	7/22/2000	7/27/2000	7/23/2000
LDWF	14	7/25/2000	7/25/2000	7/25/2000
LDWF	17	8/9/2000	8/9/2000	8/9/2000
LUMCONT	9	8/15/2000	8/15/2000	8/15/2000
LUMCONT	2	8/18/2000	8/18/2000	8/18/2000
LDWF	10	8/30/2000	8/30/2000	8/30/2000
LUMCONT	9	9/13/2000	9/13/2000	9/13/2000
LUMCONT	16	5/7/2001	5/8/2001	5/7/2001
LDWF	11	5/11/2001	5/11/2001	5/11/2001
LDWF	13	6/18/2001	6/18/2001	6/18/2001
LUMCONT	11	6/18/2001	6/19/2001	6/18/2001
SEAMAP	66	6/13/2001	7/25/2001	7/10/2001
LDWF	7	7/6/2001	7/11/2001	7/10/2001
LUMCON	93	7/20/2001	7/26/2001	7/22/2001
LDWF	12	8/8/2001	8/8/2001	8/8/2001
LUMCONT	10	8/15/2001	8/23/2001	8/15/2001
LUMCONT	2	9/6/2001	9/6/2001	9/6/2001
LUMCONT	19	9/17/2001	9/24/2001	9/18/2001
LUMCONT	10	5/7/2002	5/26/2002	5/8/2002
LUMCONT	19	6/8/2002	6/12/2002	6/11/2002

Source	Number of Observations	Start Date	End Date	Mean Date
SEAMAP	94	6/28/2002	7/17/2002	7/9/2002
LUMCON	91	7/20/2002	7/26/2002	7/23/2002
LUMCONT	17	8/7/2002	8/14/2002	8/13/2002
LUMCONT	15	8/26/2002	8/29/2002	8/27/2002
LUMCONT	9	9/20/2002	9/20/2002	9/20/2002
LUMCONT	17	5/13/2003	5/14/2003	5/13/2003
LUMCONT	3	6/4/2003	6/9/2003	6/5/2003
EPA	41	6/12/2003	6/19/2003	6/15/2003
LUMCONT	10	6/16/2003	6/16/2003	6/16/2003
SEAMAP	53	7/3/2003	7/28/2003	7/14/2003
LUMCON	92	7/23/2003	7/28/2003	7/25/2003
UMCES	19	7/30/2003	8/4/2003	8/2/2003
LUMCONT	8	8/14/2003	8/15/2003	8/14/2003
LUMCONT	10	8/22/2003	8/22/2003	8/22/2003
LUMCONT	9	9/9/2003	9/9/2003	9/9/2003
TAMU	37	9/13/2003	9/16/2003	9/14/2003
LUMCONT	2	5/5/2004	5/5/2004	5/5/2004
LUMCONT	9	5/13/2004	5/13/2004	5/13/2004
LUMCONT	2	6/6/2004	6/6/2004	6/6/2004
LUMCONT	16	6/15/2004	6/16/2004	6/15/2004
TAMU	60	6/26/2004	7/1/2004	6/28/2004
SEAMAP	96	6/28/2004	7/14/2004	7/8/2004
LUMCON	84	7/21/2004	7/26/2004	7/23/2004
UMCES	15	7/28/2004	8/1/2004	7/30/2004
LUMCONT	9	8/19/2004	8/19/2004	8/19/2004
TAMU	64	8/20/2004	8/26/2004	8/23/2004
LUMCONT	18	8/30/2004	9/9/2004	9/8/2004
LUMCONT	9	5/11/2005	5/11/2005	5/11/2005
TAMU	102	5/20/2005	5/26/2005	5/23/2005
LUMCONT	16	6/2/2005	6/3/2005	6/2/2005
TAMU	76	7/8/2005	7/14/2005	7/11/2005
SEAMAP	41	7/4/2005	7/16/2005	7/12/2005
LUMCON	81	7/25/2005	7/30/2005	7/26/2005
SEAMAP	34	7/28/2005	7/31/2005	7/29/2005
LUMCONT	16	8/16/2005	8/18/2005	8/16/2005
TAMU	126	8/18/2005	8/24/2005	8/21/2005
LUMCONT	9	9/7/2005	9/7/2005	9/7/2005
LUMCONT	41	9/28/2005	9/30/2005	9/28/2005
LUMCONT	9	5/26/2006	5/27/2006	5/26/2006
LUMCONT	4	6/6/2006	6/6/2006	6/6/2006
EPA	121	6/6/2006	6/18/2006	6/11/2006
LUMCONT	17	6/26/2006	6/27/2006	6/26/2006
SEAMAP	94	6/29/2006	7/16/2006	7/10/2006
LUMCON	87	7/21/2006	7/27/2006	7/24/2006
UMCES	40	8/4/2006	8/13/2006	8/9/2006
LUMCONT	8	9/11/2006	9/11/2006	9/11/2006
EPA	127	9/6/2006	9/18/2006	9/11/2006

Source	Number of Observations	Start Date	End Date	Mean Date
EPA	83	5/1/2007	5/7/2007	5/4/2007
LUMCONT	16	5/12/2007	5/13/2007	5/12/2007
LUMCONT	9	6/6/2007	6/6/2007	6/6/2007
TAMU	63	7/17/2007	7/20/2007	7/18/2007
SEAMAP	66	6/25/2007	8/3/2007	7/22/2007
LUMCON	94	7/22/2007	7/28/2007	7/24/2007
UMCES	60	7/30/2007	8/7/2007	8/3/2007
LUMCONT	9	8/15/2007	8/15/2007	8/15/2007
EPA	130	8/19/2007	8/31/2007	8/23/2007
TAMU	74	9/6/2007	9/10/2007	9/7/2007
LUMCONT	16	9/11/2007	9/12/2007	9/11/2007
LUMCONT	9	5/12/2008	5/13/2008	5/12/2008
LUMCONT	16	6/11/2008	6/13/2008	6/11/2008
SEAMAP	102	6/29/2008	7/16/2008	7/9/2008
TAMU	72	7/17/2008	7/20/2008	7/18/2008
LUMCON	89	7/21/2008	7/28/2008	7/24/2008
UMCES	73	8/1/2008	8/12/2008	8/7/2008
LUMCONT	4	8/15/2008	8/15/2008	8/15/2008
LUMCONT	9	5/26/2009	5/29/2009	5/26/2009
LUMCONT	8	6/12/2009	6/12/2009	6/12/2009
SEAMAP	167	6/23/2009	7/15/2009	7/5/2009
LUMCON	93	7/18/2009	7/23/2009	7/20/2009
TAMU	29	7/28/2009	7/31/2009	7/29/2009
LUMCONT	16	8/10/2009	8/11/2009	8/10/2009
LUMCONT	2	8/24/2009	8/25/2009	8/24/2009
LUMCONT	7	9/21/2009	9/21/2009	9/21/2009
SEAMAP	77	7/13/2010	8/2/2010	7/24/2010
LUMCON	90	7/25/2010	7/31/2010	7/28/2010
UMCES	30	9/2/2010	9/7/2010	9/4/2010
LUMCONT	15	5/16/2011	5/30/2011	5/23/2011
LUMCONT	15	6/17/2011	6/18/2011	6/17/2011
TAMU	48	6/24/2011	6/28/2011	6/26/2011
SEAMAP	95	7/2/2011	7/16/2011	7/10/2011
LUMCON	89	7/24/2011	7/30/2011	7/26/2011
LUMCONT	7	8/22/2011	8/23/2011	8/22/2011
LUMCONT	15	5/1/2012	5/2/2012	5/1/2012
TAMU	46	6/11/2012	6/15/2012	6/13/2012
LUMCONT	15	6/16/2012	6/17/2012	6/16/2012
SEAMAP	76	6/16/2012	6/29/2012	6/23/2012
LUMCON	66	7/22/2012	7/27/2012	7/24/2012
TAMU	49	8/16/2012	8/20/2012	8/17/2012
LUMCONT	10	8/16/2012	8/22/2012	8/21/2012
SEAMAP	66	6/16/2013	6/30/2013	6/22/2013
LUMCON	99	7/21/2013	7/28/2013	7/24/2013
LUMCONT	1	5/26/2014	5/26/2014	5/26/2014
SEAMAP	119	6/17/2014	7/5/2014	6/27/2014
LUMCON	85	7/27/2014	8/2/2014	7/30/2014

Source	Number of Observations	Start Date	End Date	Mean Date
SEAMAP	94	6/17/2015	7/5/2015	6/27/2015
SEAMAP	138	6/16/2016	7/3/2016	6/25/2016

References

1. DiMarco, S. and Texas A&M University (2012). Physical and chemical data collected by bottle and CTD in the Gulf of Mexico from the R/V Gyre and R/V Pelican, April 2004 - July 2009 to help resolve the dominant oceanographic processes that control the timing, duration, and severity of hypoxia of the region (NODC Accession 0088164). Version 1.1. National Oceanographic Data Center, NOAA. Dataset.

2. May, N. L. and US DOC; NOAA; National Marine Fisheries Service (2011). Temperature, salinity, dissolved oxygen measurements collected using CTD, bottle from multiple platforms in the Gulf of Mexico from 1992 through 2008 as part of the Southeast Area Monitoring and Assessment Program (SEAMAP) (NODC Accession 0069702). Version 1.1. National Oceanographic Data Center, NOAA. Dataset.

3. May, Nelson US DOC; NOAA; NMFS; Southeast Fisheries Science Center (2017). Temperature, salinity, dissolved oxygen measurements collected using CTD, bottle from multiple platforms in the Gulf of Mexico from 2009 through 2015 as part of the Southeast Area Monitoring and Assessment Program (SEAMAP) (NCEI Accession 0131259). NOAA National Centers for Environmental Information. Unpublished Dataset.

4. May, Nelson US DOC; NOAA; NMFS; Southeast Fisheries Science Center (2016). Temperature, salinity, dissolved oxygen, and other measurements collected using CTD from NOAA Ship OREGON II in Gulf of Mexico from 2016 as part of the Southeast Area

Monitoring and Assessment Program (SEAMAP) (NCEI Accession 0156169). Version 1.1. NOAA National Centers for Environmental Information. Dataset.

5. Murrell, M. and US Environmental Protection Agency (2015). Profiles of dissolved oxygen, temperature, salinity, nitrate, silicate, chlorophyll, primary production and other biological, chemical, and physical measurements collected in the Northern Gulf of Mexico between 2002 and 2007 (NCEI Accession 0074610). Version 1.1. NOAA National Centers for Environmental Information. Dataset.

6. Rabalais, N. N., Turner, R. E., & Scavia, D. (2002). Beyond Science into Policy: Gulf of Mexico Hypoxia and the Mississippi River: Nutrient policy development for the Mississippi River watershed reflects the accumulated scientific evidence that the increase in nitrogen loading is the primary factor in the worsening of hypoxia in the northern Gulf of Mexico. *AIBS Bulletin*, *52*(2), 129-142.

7. Rabalais, N. N. and Louisiana Universities Marine Consortium (2010_A). Chemical, zooplankton, and phytoplankton data from CTD and other instruments in the Mississippi River and Gulf of Mexico as part of the Nutrient Enhanced Coastal Ocean Productivity (NECOP) project, from 1985-07-15 to 1993-05-12 (NODC Accession 9800129). Version 1.1. National Oceanographic Data Center, NOAA. Dataset.

8. Rabalais, N. N. and Louisiana Universities Marine Consortium (2010_B). Chemical, zooplankton, and phytoplankton data from CTD and other instruments in the Mississippi River and Gulf of Mexico as part of the Nutrient Enhanced Coastal Ocean Productivity (NECOP) project, from 1985-07-15 to 1993-05-12 (NODC Accession 9800129). Version 1.1. National Oceanographic Data Center, NOAA. Dataset.

9. Rabalais, N. N. and Louisiana Universities Marine Consortium (2011$_A$). Louisiana Hypoxia Surveys 1998 - 2002: Physical, biological, and chemical data collected off the coast of Louisiana as part of a long-term study of hypoxia (NODC Accession 0002033). Version 1.1. National Oceanographic Data Center, NOAA. Dataset.

10. Rabalais, N. N. and Louisiana Universities Marine Consortium (2011$_B$). Louisiana Hypoxia Surveys 2007: Biological, chemical, and physical data collected off the coast of Louisiana as part of the Hypoxia Studies in the Northern Gulf of Mexico project in 2007 (NODC Accession 0060060). Version 1.1. National Oceanographic Data Center, NOAA. Dataset.

11. Rabalais, N. N. and Louisiana Universities Marine Consortium (2011$_C$). Louisiana Hypoxia Surveys 2006: Biological, chemical, and physical data collected off the coast of Louisiana as part of the Hypoxia Studies in the Northern Gulf of Mexico project in 2006 (NODC Accession 0049435). Version 1.1. National Oceanographic Data Center, NOAA. Dataset.

12. Rabalais, N. N. and Louisiana Universities Marine Consortium (2011$_D$). Louisiana Hypoxia Surveys 2005: Biological, chemical, and physical data collected off the coast of Louisiana as part of the Hypoxia Studies in the Northern Gulf of Mexico project in 2005 (NODC Accession 0039733). Version 2.2. National Oceanographic Data Center, NOAA. Dataset.

13. Rabalais, N. N. and Louisiana Universities Marine Consortium (2011$_E$). Louisiana Hypoxia Surveys 2004: Biological, chemical, and physical data collected off the coast of Louisiana as part of the Hypoxia Studies in the Northern Gulf of Mexico project in 2004

(NODC Accession 0032050). Version 1.1. National Oceanographic Data Center, NOAA. Dataset

14. Rabalais, N. N. and Louisiana Universities Marine Consortium (2011F). Louisiana Hypoxia Surveys 2003: Biological, chemical, and physical data collected off the coast of Louisiana as part of the Hypoxia Studies in the Northern Gulf of Mexico project in 2003 (NODC Accession 0020956). Version 1.1. National Oceanographic Data Center, NOAA. Dataset.

15. Rabalais, N. N. and Louisiana Universities Marine Consortium (2012). Louisiana Hypoxia Survey 2009: Biological, chemical, and physical data collected off the coast of Louisiana as part of the Hypoxia Studies in the Northern Gulf of Mexico project in 2009 (NODC Accession 0099531). Version 1.1. National Oceanographic Data Center, NOAA. Dataset.

16. Rabalais, N. N. and Louisiana Universities Marine Consortium (2015). Physical, chemical, and biological data collected in the Gulf of Mexico from 02 Feb 2010 to 28 Oct 2010 (NODC Accession 0117436). Version 2.2. National Oceanographic Data Center, NOAA. Dataset.

17. Rabalais, N.N., Turner, R.E. and Wiseman Jr, W.J. (2017A). Hydrographic and chemical water parameters collected by CTD and other instruments from the Pelican and the Tommy Munro in coastal waters of Louisiana from 1994-07-24 to 1997-07-29 (NCEI Accession 0164298). Version 1.1. NOAA National Centers for Environmental Information. Dataset.

18. Rabalais, Nancy (2017_B). Physical (Hydrography), chemical (CTD), and biological (Water Quality) processes of the Texas-Louisiana continental shelf, 2013 (NCEI Accession 0162440). Version 1.1. NOAA National Centers for Environmental Information. Dataset.

19. Rabalais, Nancy (2017_C). Physical (Hydrography), chemical (CTD), and biological (Water Quality) processes of the Texas-Louisiana continental shelf, 2012 (NCEI Accession 0162101). Version 1.1. NOAA National Centers for Environmental Information. Dataset.

20. Rabalais, Nancy (2017_D). Physical (Hydrography), chemical (CTD), and biological (Water Quality) processes of the Texas-Louisiana continental shelf, 2014 (NCEI Accession 0161219). Version 1.1. NOAA National Centers for Environmental Information. Dataset.

21. Roman, M., Boicourt, W., & Pierson, J.J. (2011). Multiyear PELICAN CTD Profile data from 2003 to 2010 collected in NGOMEX project. Biological and Chemical Oceanography Data Management Office (BCO-DMO). Dataset version: 28 September 2011. http://bcodata.whoi.edu/jg/dir/BCO/NGOMEX/.

22. Smith, L. M. and Louisiana Universities Marine Consortium (2015). Louisiana Hypoxia Surveys 2011: Biological, chemical, and physical data collected off the coast of Louisiana as part of the Hypoxia Studies in the Northern Gulf of Mexico project in 2011 (NCEI Accession 0129417). Version 1.1. NOAA National Centers for Environmental Information. Dataset.

23. Widgeon, T. and Louisiana Universities Marine Consortium (2010). Louisiana Hypoxia Surveys 2008: Biological, chemical, and physical data collected off the coast of Louisiana as part of the Hypoxia Studies in the Northern Gulf of Mexico project in 2008 (NODC Accession 0069471). Version 1.1. National Oceanographic Data Center, NOAA. Dataset.

S2: BWDO observation maps for each cruise used in this study

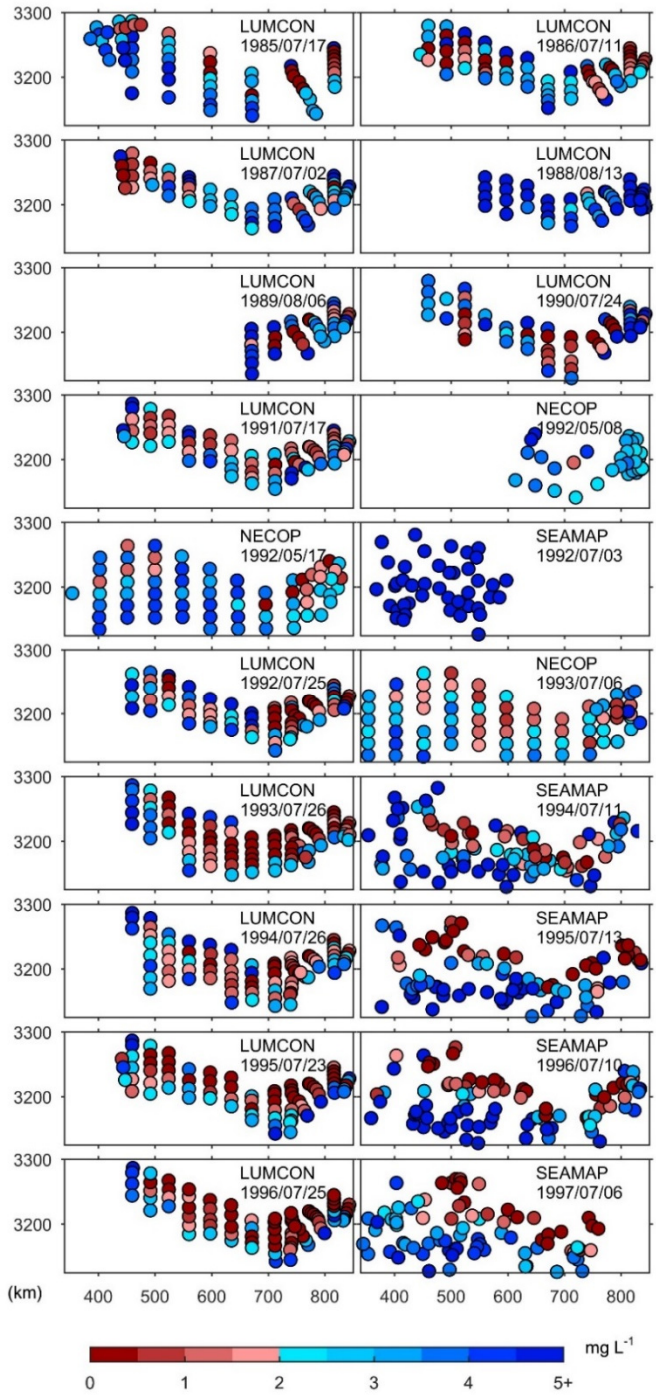

Figure S1. BWDO observed in cruises between 07/1985 and 07/1997.

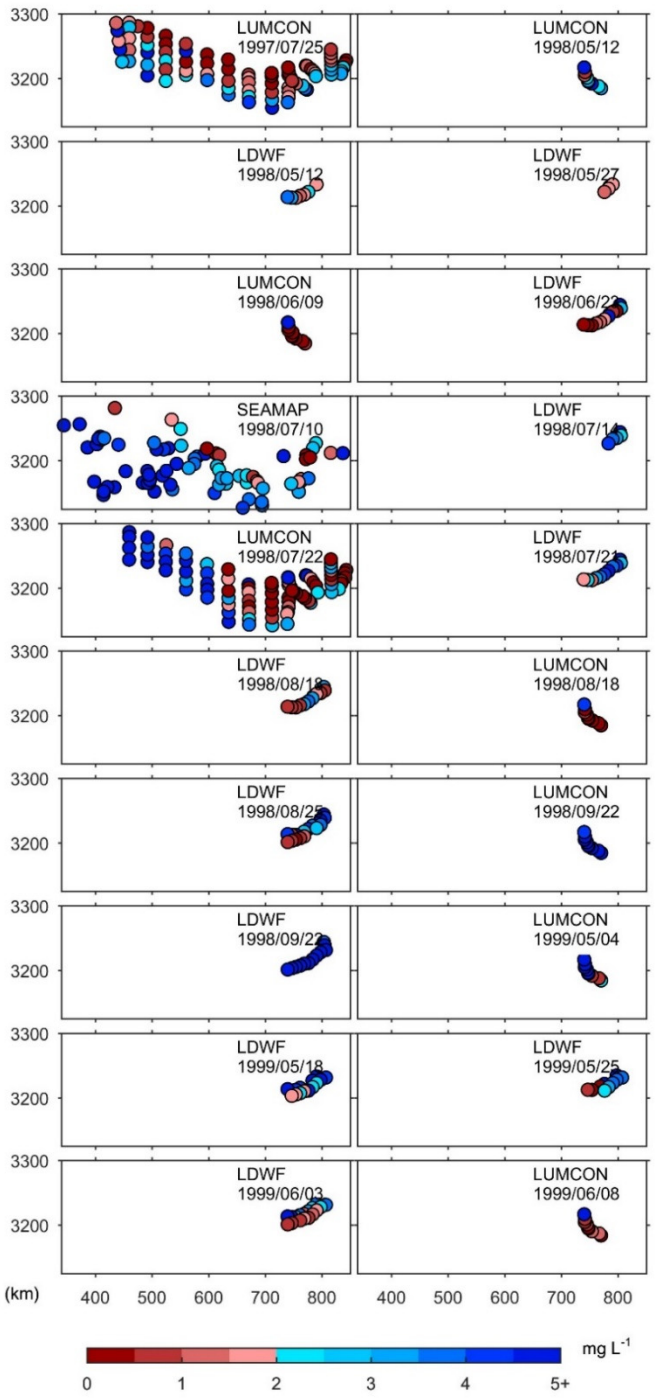

Figure S2. BWDO observed in cruises between 07/1997 and 06/1999.

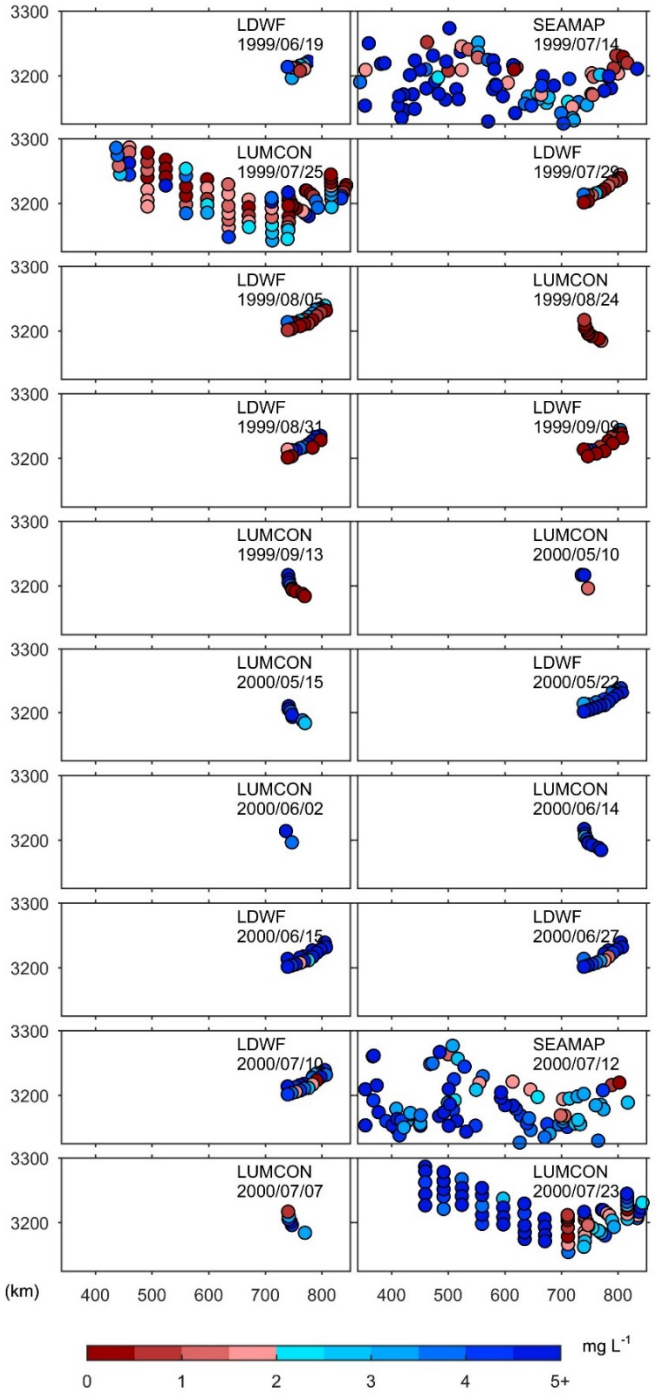

Figure S3. BWDO observed in cruises between 06/1999 and 07/2000.

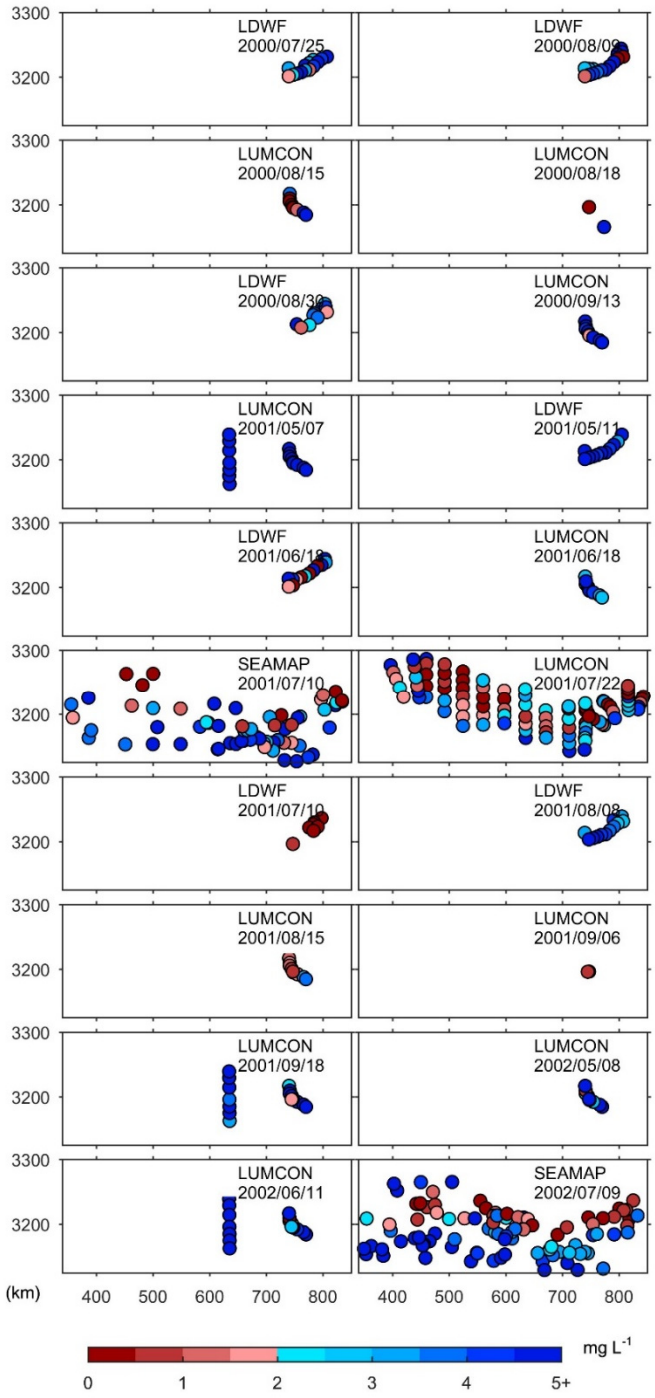

Figure S4. BWDO observed in cruises between 07/2000 and 07/2002.

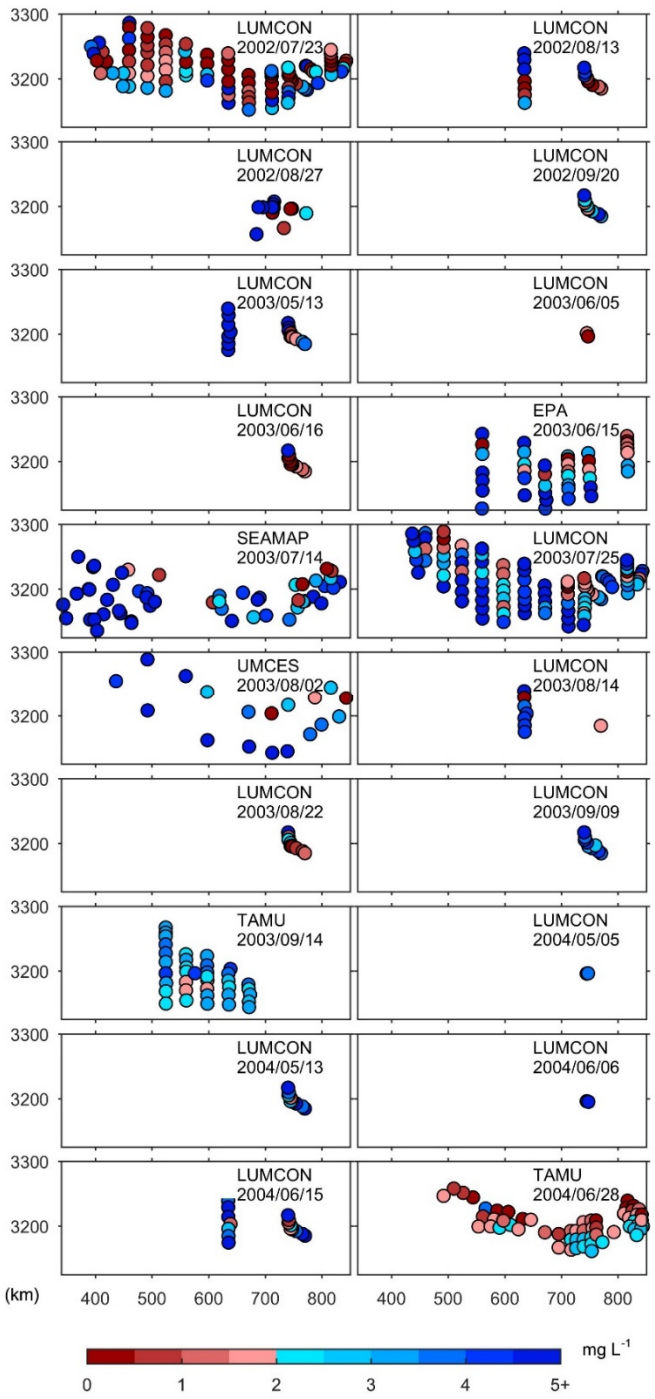

Figure S5. BWDO observed in cruises between 07/2002 and 06/2004.

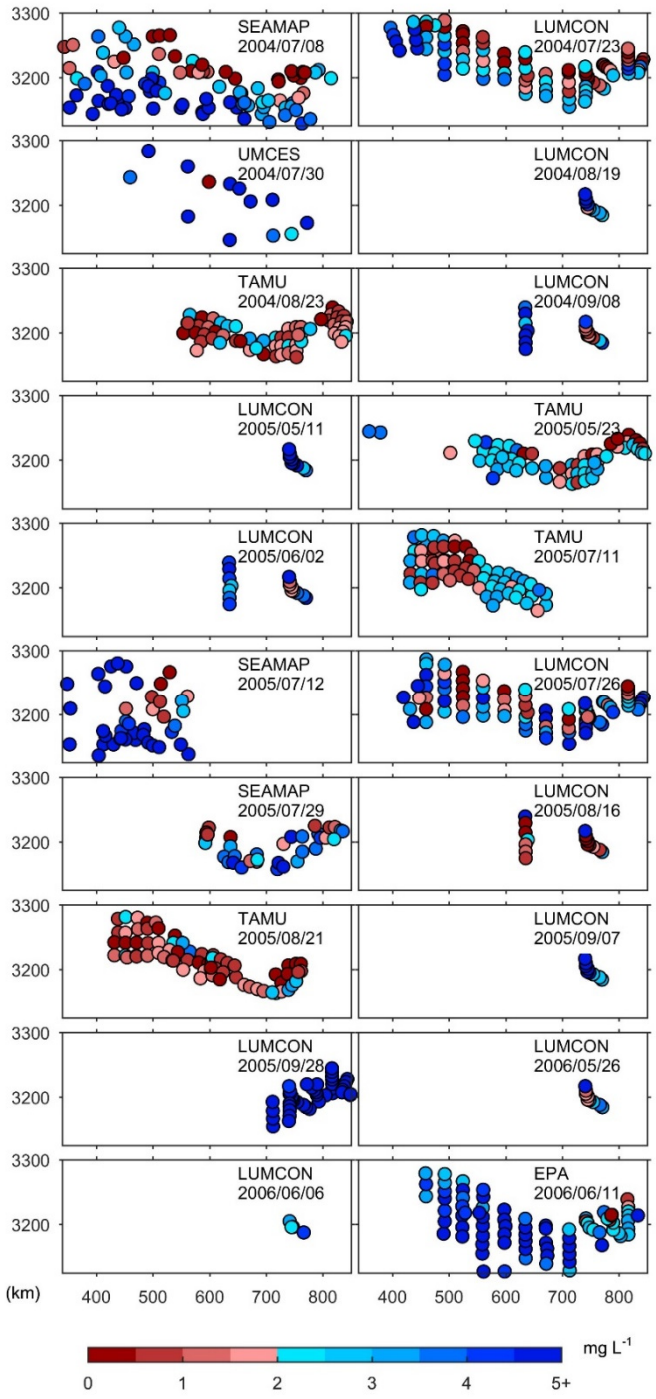

Figure S6. BWDO observed in cruises between 07/2004 and 06/2006.

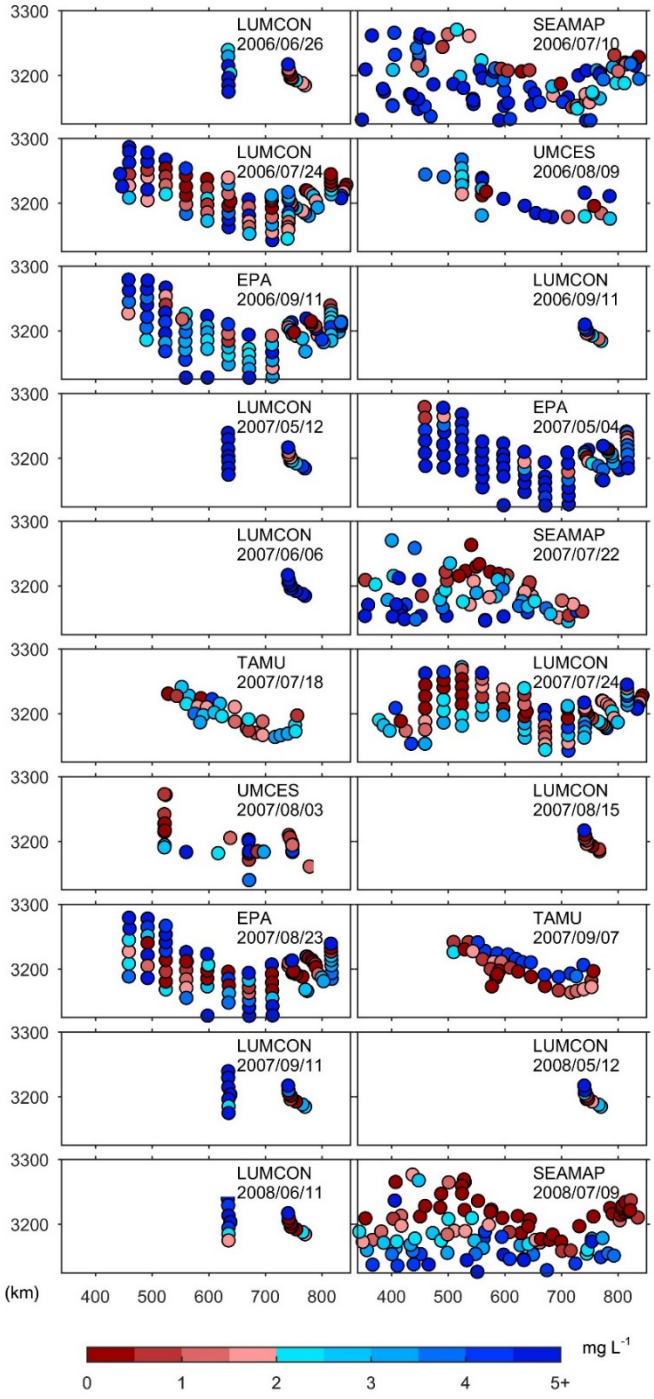

Figure S7. BWDO observed in cruises between 06/2006 and 07/2008.

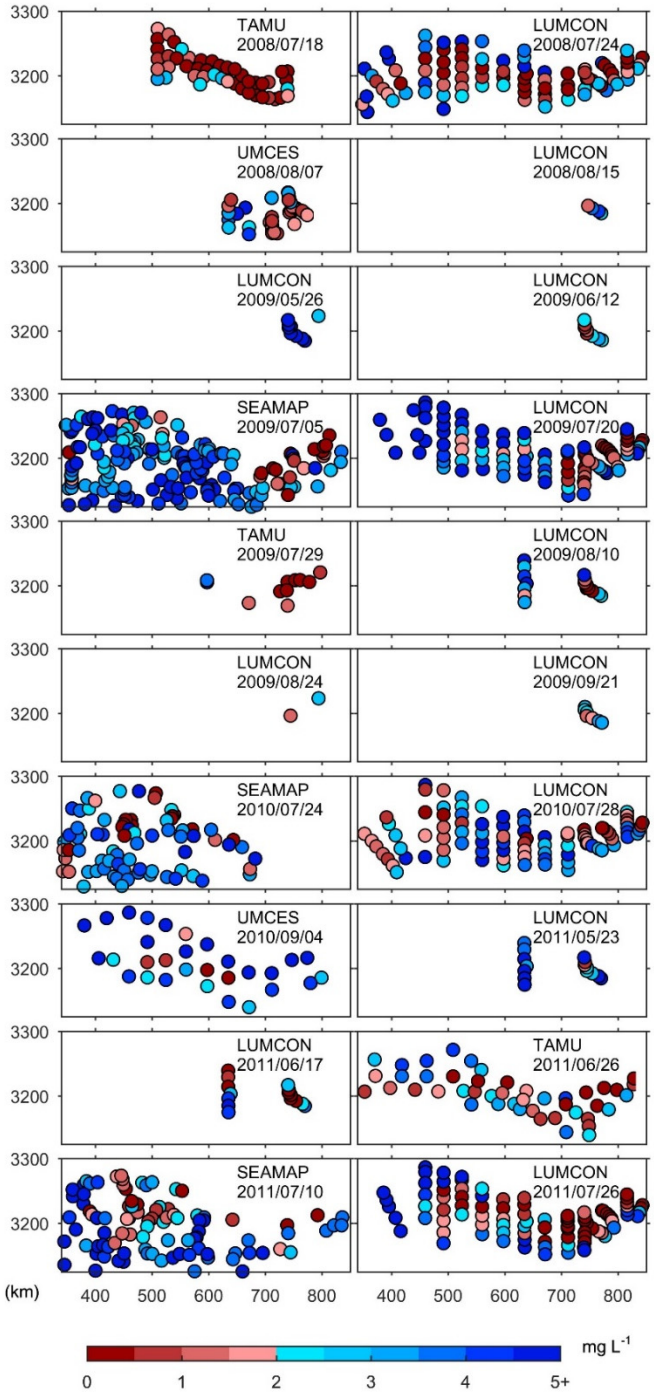

Figure S8. BWDO observed in cruises between 07/2008 and 07/2011.

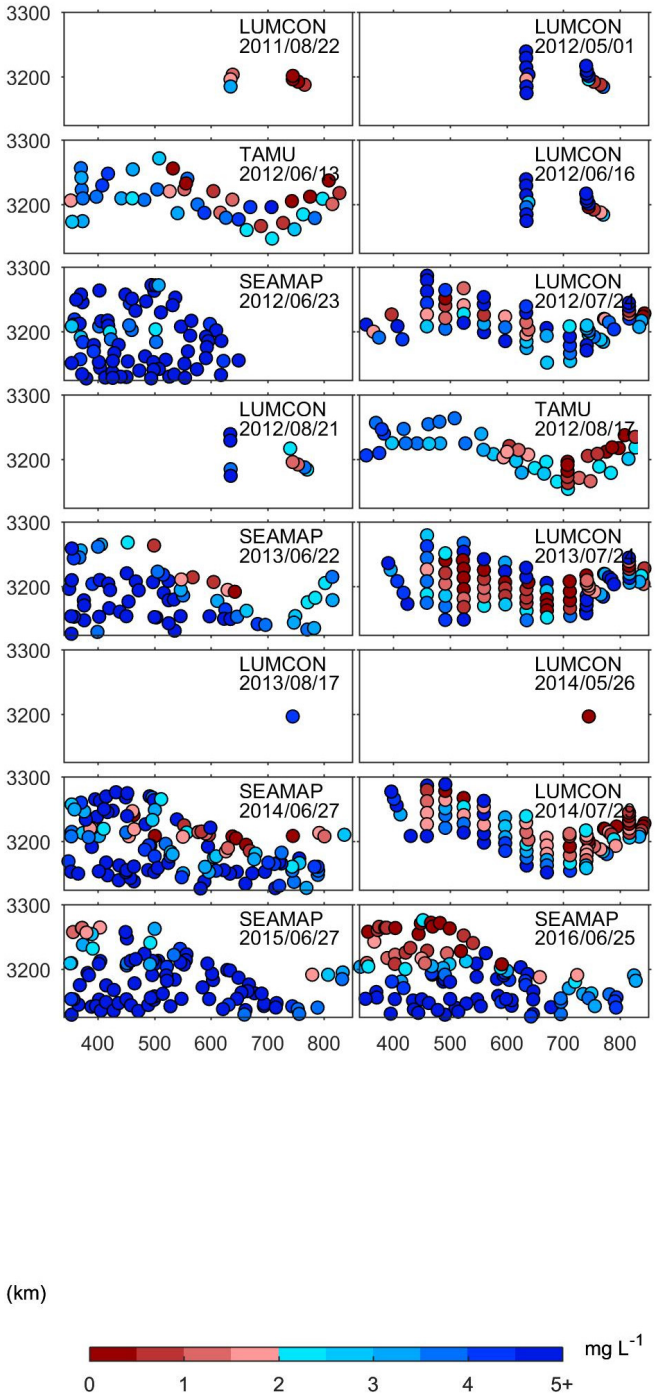

Figure S9. BWDO observed in cruises

between 08/2011 and 06/2016.

S3: Modeling process schematic

The figure below outlines the various steps involved in the geostatistical model developed for this study.

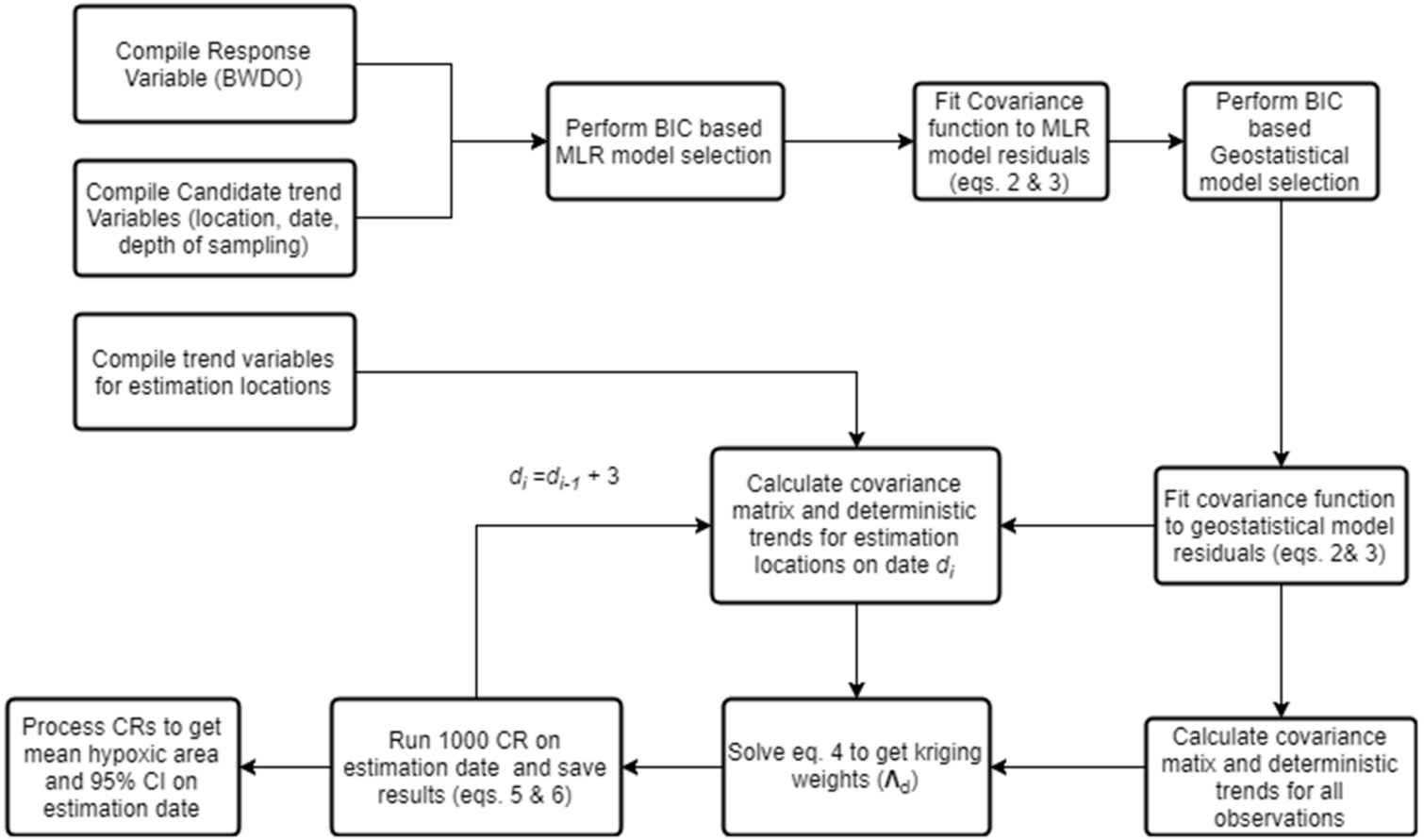

Figure S10. Model schematic.

S4: Processing of simulations

One thousand CRs are performed on each date when an estimate of hypoxic area is required. Here, we developed estimates at 3-day intervals across the summer of each year. For each realization, hypoxic area is calculated by multiplying the number of hypoxic grid cells (BWDO less than 2 mg L^{-1}) by the grid cell size (25 km^2). Using the 1000 simulated values of hypoxic area (at each 3-day interval), we determined the mean, median, standard deviation, and 95% confidence intervals (CIs). CIs of estimates obtained from CR were smoothed using GGPLOT2.[1] 30-day and summer-wide (June-August) mean hypoxic areas are also determined based on these simulations. CIs for 30-day and summer-wide mean hypoxic areas are determined by summing variances using the properties of correlated random variables.[2] Temporal correlations among the 3-day estimates is determined based on lagged correlation coefficients (i.e., the autocorrelation function[3]) for each year. Furthermore, all variance aggregations are performed following a Box-Cox transformation[4] of simulated hypoxic area values, which tend to be mildly right-skewed. The Box-Cox transformation is parameterized for each year to maximize the normality of the transformed dataset.[5] CIs for 30- and summer-wide mean hypoxic areas are determined on this Box-Cox scale, and then back-transformed to the original scale.

All computations discussed in this section were performed in MATLAB[6] and R was used for some post processing.[1, 3] Due to the number of observations (7273 observations) used in model development, and the size of the estimation grid (2498 estimation locations), a minimum of 64 GB memory was required to run the model.

References

1. Wickham, H. *GGPLOT2: elegant graphics for data analysis.* Springer: 2016.

2. Kottegoda, N.T.; Rosso, R. *Applied statistics for civil and environmental engineers.* Blackwell Malden, MA: 2008.

3. Team, R.C. R language definition. *R foundation for statistical computing* 2000.

4. Box, G.E.P.; Cox, D.R. An analysis of transformations. *Journal of the Royal Statistical Society* 1964, 211–252.

5. Ribeiro Jr, P.J.; Diggle, P.J. geoR: a package for geostatistical analysis. *R news* 2001, *1* (2), 14-18.

6. MATLAB - The Language of Technical Computing; https://www.mathworks.com/products/matlab.html.

S5: Model residuals

The residuals of the geostatistical model of BWDO (version C) are plotted against the trend variables used in the model. The residuals are approximately normally distributed around zero.

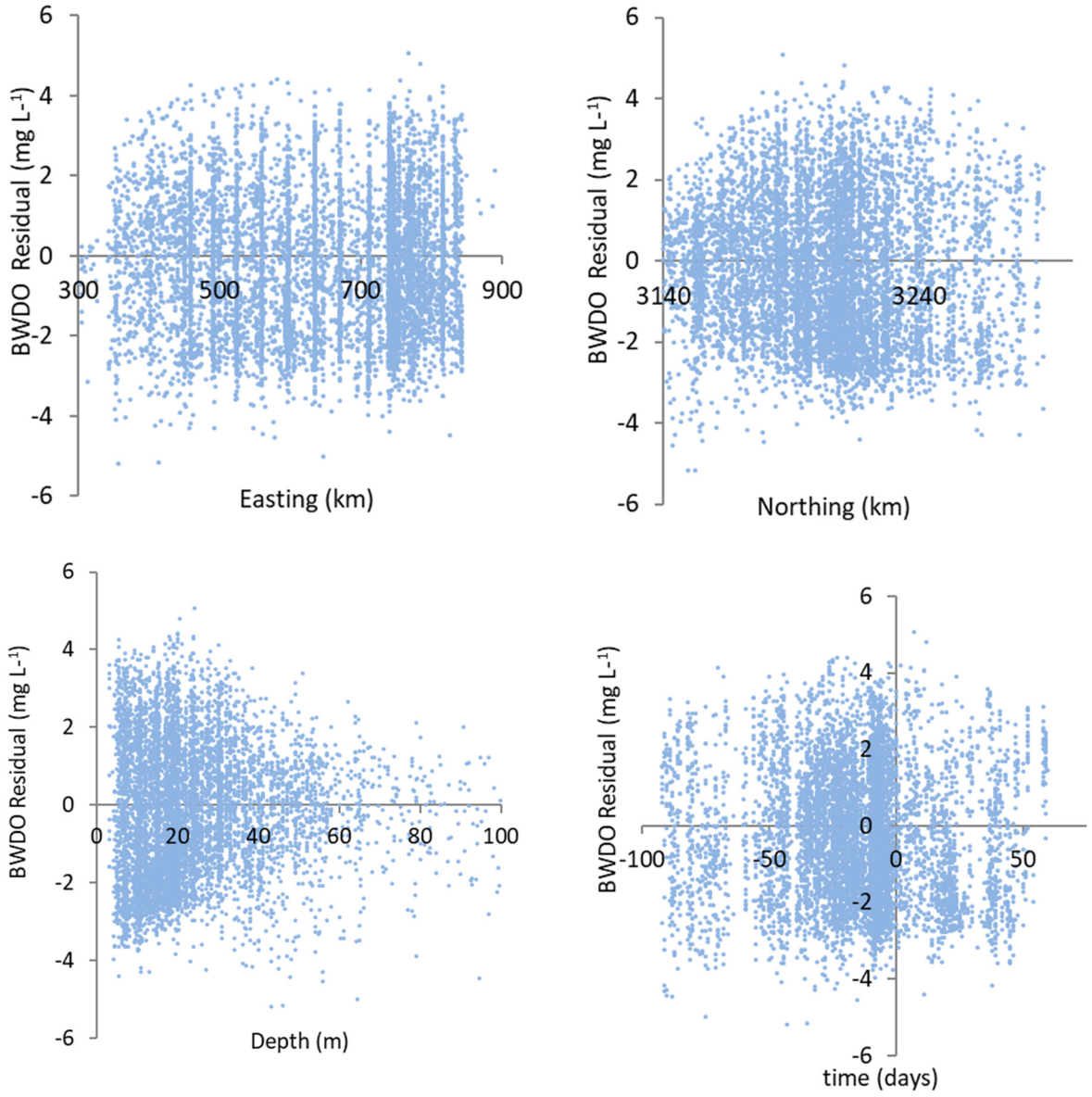

Figure S11. BWDO vs covariates.

S6: Categorical intercepts and trend coefficients for different model versions

Table S2. Cruise specific intercepts from model version A.

date	Intercept	SE	Organization	date	Intercept	SE	Organization
7/18/1985	**2.68**	**0.44**	LUMCON	8/5/1999	2.20	1.00	LDWF
7/11/1986	2.83	0.49	LUMCON	8/24/1999	1.14	1.11	LUMCONT
7/3/1987	3.29	0.51	LUMCON	8/31/1999	3.03	1.04	LDWF
8/14/1988	5.63	0.58	LUMCON	9/9/1999	1.46	1.00	LDWF
8/7/1989	3.58	0.65	LUMCON	9/13/1999	3.27	1.10	LUMCONT
7/25/1990	3.05	0.49	LUMCON	5/10/2000	4.14	1.26	LUMCONT
7/18/1991	2.91	0.49	LUMCON	5/15/2000	5.25	1.15	LUMCONT
5/9/1992	2.96	0.60	NECOP	5/22/2000	5.23	1.00	LDWF
5/18/1992	2.55	0.42	NECOP	6/2/2000	5.69	1.32	LUMCONT
7/4/1992	6.09	0.51	SEAMAP	6/14/2000	6.10	1.10	LUMCONT
7/26/1992	3.01	0.50	LUMCON	6/15/2000	6.25	1.00	LDWF
7/6/1993	1.89	0.39	NECOP	6/27/2000	5.26	1.00	LDWF
7/26/1993	2.17	0.47	LUMCON	7/8/2000	4.59	1.00	LDWF
7/12/1994	3.39	0.41	SEAMAP	7/10/2000	3.02	0.41	SEAMAP
7/26/1994	2.50	0.47	LUMCON	7/13/2000	4.24	1.11	LUMCONT
7/13/1995	2.48	0.41	SEAMAP	7/24/2000	4.33	0.50	LUMCON
7/23/1995	2.17	0.48	LUMCON	7/25/2000	4.45	1.03	LDWF
7/11/1996	2.70	0.41	SEAMAP	8/9/2000	4.32	0.98	LDWF
7/25/1996	1.86	0.48	LUMCON	8/15/2000	3.15	1.11	LUMCONT
7/7/1997	1.88	0.43	SEAMAP	8/18/2000	3.14	1.24	LUMCONT
7/25/1997	2.19	0.48	LUMCON	8/30/2000	3.74	1.04	LDWF
5/12/1998	3.82	1.11	LUMCONT	9/13/2000	5.65	1.10	LUMCONT
5/12/1998	2.32	1.15	LDWF	5/7/2001	6.67	0.75	LUMCONT
5/27/1998	2.47	1.32	LDWF	5/11/2001	6.55	1.01	LDWF
6/10/1998	2.84	1.09	LUMCONT	6/18/2001	3.89	0.99	LDWF
6/23/1998	2.87	1.04	LDWF	6/19/2001	3.83	1.10	LUMCONT
7/11/1998	3.07	0.43	SEAMAP	7/10/2001	2.94	0.44	SEAMAP
7/14/1998	4.52	1.24	LDWF	7/10/2001	2.39	0.45	LUMCON
7/21/1998	2.94	0.48	LUMCON	7/23/2001	1.02	1.07	LDWF
7/23/1998	3.86	1.04	LDWF	8/8/2001	4.54	1.02	LDWF
8/18/1998	2.19	1.04	LDWF	8/16/2001	2.60	1.10	LUMCONT
8/18/1998	1.75	1.11	LUMCONT	9/6/2001	1.51	1.51	LUMCONT
8/25/1998	3.95	0.98	LDWF	9/18/2001	4.90	0.75	LUMCONT
9/22/1998	5.59	1.11	LUMCONT	5/9/2002	5.13	1.10	LUMCONT
9/22/1998	5.96	0.99	LDWF	6/11/2002	5.57	0.75	LUMCONT
5/4/1999	5.00	1.11	LUMCONT	7/9/2002	2.71	0.41	SEAMAP
5/18/1999	4.62	1.04	LDWF	7/24/2002	2.23	0.45	LUMCON
5/25/1999	3.78	1.09	LDWF	8/13/2002	3.04	0.75	LUMCONT
6/3/1999	3.05	1.02	LDWF	8/27/2002	3.94	0.91	LUMCONT
6/8/1999	2.57	1.10	LUMCONT	9/20/2002	4.12	1.11	LUMCONT
6/19/1999	3.67	1.14	LDWF	5/13/2003	5.58	0.78	LUMCONT
7/14/1999	3.75	0.41	SEAMAP	6/6/2003	2.28	1.43	LUMCONT
7/26/1999	1.94	0.46	LUMCON	6/15/2003	2.82	1.11	LUMCONT
7/29/1999	1.39	0.99	LDWF	6/16/2003	3.08	0.51	EPA

date	Intercept	SE	Organization	date	Intercept	SE	Organization
7/14/2003	3.67	0.46	SEAMAP	6/12/2008	3.42	0.77	LUMCONT
7/26/2003	3.78	0.45	LUMCON	7/9/2008	1.58	0.40	SEAMAP
8/2/2003	3.52	0.52	UMCES	7/19/2008	1.19	0.60	TAMU
8/14/2003	3.63	0.85	LUMCONT	7/24/2008	2.40	0.43	LUMCON
9/15/2003	2.67	0.61	TAMU	8/7/2008	2.90	0.70	UMCES
5/5/2004	4.74	1.51	LUMCONT	8/15/2008	3.56	1.29	LUMCONT
5/13/2004	5.08	1.11	LUMCONT	5/26/2009	6.15	1.02	LUMCONT
6/6/2004	5.34	1.50	LUMCONT	8/22/2003	2.76	1.11	LUMCONT
6/16/2004	4.43	0.78	LUMCONT	9/9/2003	5.13	1.10	LUMCONT
6/29/2004	1.75	0.56	TAMU	6/12/2009	2.39	1.11	LUMCONT
7/8/2004	2.29	0.41	SEAMAP	7/6/2009	2.51	0.38	SEAMAP
7/23/2004	2.38	0.47	LUMCON	7/21/2009	4.07	0.44	LUMCON
7/31/2004	4.33	0.59	UMCES	7/29/2009	2.29	0.77	TAMU
8/19/2004	4.80	1.11	LUMCONT	8/11/2009	3.48	0.77	LUMCONT
8/23/2004	1.56	0.58	TAMU	8/25/2009	3.22	1.23	LUMCONT
9/8/2004	4.04	0.77	LUMCONT	9/21/2009	3.33	1.16	LUMCONT
5/11/2005	5.90	1.10	LUMCONT	7/25/2010	2.04	0.45	SEAMAP
5/23/2005	2.55	0.54	TAMU	7/28/2010	2.35	0.43	LUMCON
6/3/2005	4.18	0.77	LUMCONT	9/4/2010	4.11	0.48	UMCES
7/11/2005	2.09	0.57	TAMU	5/23/2011	4.81	0.77	LUMCONT
7/13/2005	3.33	0.52	SEAMAP	6/18/2011	2.39	0.77	LUMCONT
7/27/2005	3.17	0.47	LUMCON	6/26/2011	1.93	0.47	TAMU
7/30/2005	3.14	0.64	SEAMAP	7/10/2011	2.58	0.41	SEAMAP
8/17/2005	2.26	0.77	LUMCONT	7/27/2011	2.79	0.44	LUMCON
8/21/2005	1.38	0.54	TAMU	8/23/2011	1.92	0.96	LUMCONT
9/7/2005	5.37	1.11	LUMCONT	5/2/2012	5.30	0.77	LUMCONT
9/29/2005	5.81	0.72	LUMCONT	6/13/2012	2.34	0.46	TAMU
5/26/2006	3.85	1.10	LUMCONT	6/17/2012	4.97	0.77	LUMCONT
6/6/2006	4.27	1.25	LUMCONT	6/23/2012	4.30	0.46	SEAMAP
6/11/2006	3.95	0.45	EPA	7/25/2012	3.55	0.46	LUMCON
6/27/2006	3.66	0.77	LUMCONT	8/18/2012	3.91	0.80	LUMCONT
7/11/2006	3.07	0.41	SEAMAP	8/21/2012	2.60	0.49	TAMU
7/24/2006	2.70	0.47	LUMCON	6/23/2013	3.07	0.42	SEAMAP
8/9/2006	4.45	0.59	UMCES	7/24/2013	3.02	0.43	LUMCON
9/11/2006	3.30	0.45	EPA	5/26/2014	1.30	1.62	LUMCONT
9/11/2006	3.83	1.15	LUMCONT	6/28/2014	3.05	0.40	SEAMAP
5/5/2007	5.44	0.77	LUMCONT	7/30/2014	3.00	0.46	LUMCON
5/13/2007	4.69	0.45	EPA	6/28/2015	3.48	0.42	SEAMAP
6/6/2007	6.03	1.11	LUMCONT	6/25/2016	2.41	0.36	SEAMAP
7/18/2007	2.11	0.47	SEAMAP				
7/22/2007	2.33	0.68	TAMU				
7/25/2007	2.31	0.44	LUMCON				
8/3/2007	1.91	0.58	UMCES				
8/15/2007	2.80	1.11	LUMCONT				
8/24/2007	3.34	0.45	EPA				
9/8/2007	2.06	0.64	TAMU				
9/12/2007	4.62	0.77	LUMCONT				
5/12/2008	4.07	1.10	LUMCONT				

Table S3. Yearly intercepts from model versions B and C.

Model B		
Year	**Intercept**	**SE**
1985	2.72	1.19
1986	2.88	1.30
1987	3.34	1.35
1988	5.65	1.54
1989	3.58	1.68
1990	3.18	1.30
1991	3.06	1.33
1992	3.66	0.75
1993	2.15	0.91
1994	3.33	0.98
1995	2.52	1.02
1996	2.56	0.99
1997	2.11	0.97
1998	3.38	0.78
1999	3.14	0.77
2000	4.22	0.77
2001	3.91	0.74
2002	3.60	0.75
2003	3.74	0.68
2004	2.98	0.71
2005	3.37	0.67
2006	3.51	0.64
2007	3.65	0.63
2008	2.57	0.78
2009	3.42	0.77
2010	2.97	0.83
2011	2.82	0.75
2012	3.61	0.68
2013	3.22	0.86
2014	3.10	0.83
2015	3.64	1.10
2016	2.51	0.98

Model C		
Year	**Intercept**	**SE**
1985	2.92	1.09
1986	3.05	1.21
1987	3.43	1.25
1988	5.75	1.43
1989	3.76	1.57
1990	3.37	1.21
1991	3.22	1.23
1992	3.25	0.70
1993	2.26	0.83
1994	3.44	0.89
1995	2.67	0.93
1996	2.69	0.90
1997	2.24	0.88
1998	3.26	0.71
1999	3.03	0.70
2000	4.15	0.70
2001	3.65	0.68
2002	3.45	0.68
2003	3.55	0.62
2004	2.91	0.64
2005	3.08	0.62
2006	3.38	0.58
2007	3.20	0.59
2008	2.52	0.71
2009	3.40	0.70
2010	2.95	0.76
2011	2.76	0.68
2012	3.41	0.62
2013	3.25	0.78
2014	3.12	0.76
2015	3.66	1.01
2016	2.47	0.90

Table S4. Regression coefficients (β) with standard errors (σ_β) for normalized, BIC-selected trend variables in different model versions.

Variables	*Parameters*					
	Model A		Model B		Model C	
	β	σ_β	β	σ_β	β	σ_β
E	-0.65	0.05	-0.44	0.06	-0.52	0.06
N	-0.27	0.05	-0.25	0.06	-0.24	0.06
D	-2.47	0.11	-2.42	0.12	-2.41	0.12
D^2	2.64	0.11	2.50	0.12	2.51	0.12
T	n/a	n/a	n/a	n/a	0.15	0.08
T^2	n/a	n/a	n/a	n/a	0.46	0.08

S7: Covariance function for model version C

The figure below illustrates the covariance function used in this study to the covariance parameters selected in model C (space-time geostatistical model with spatial and temporal trends).

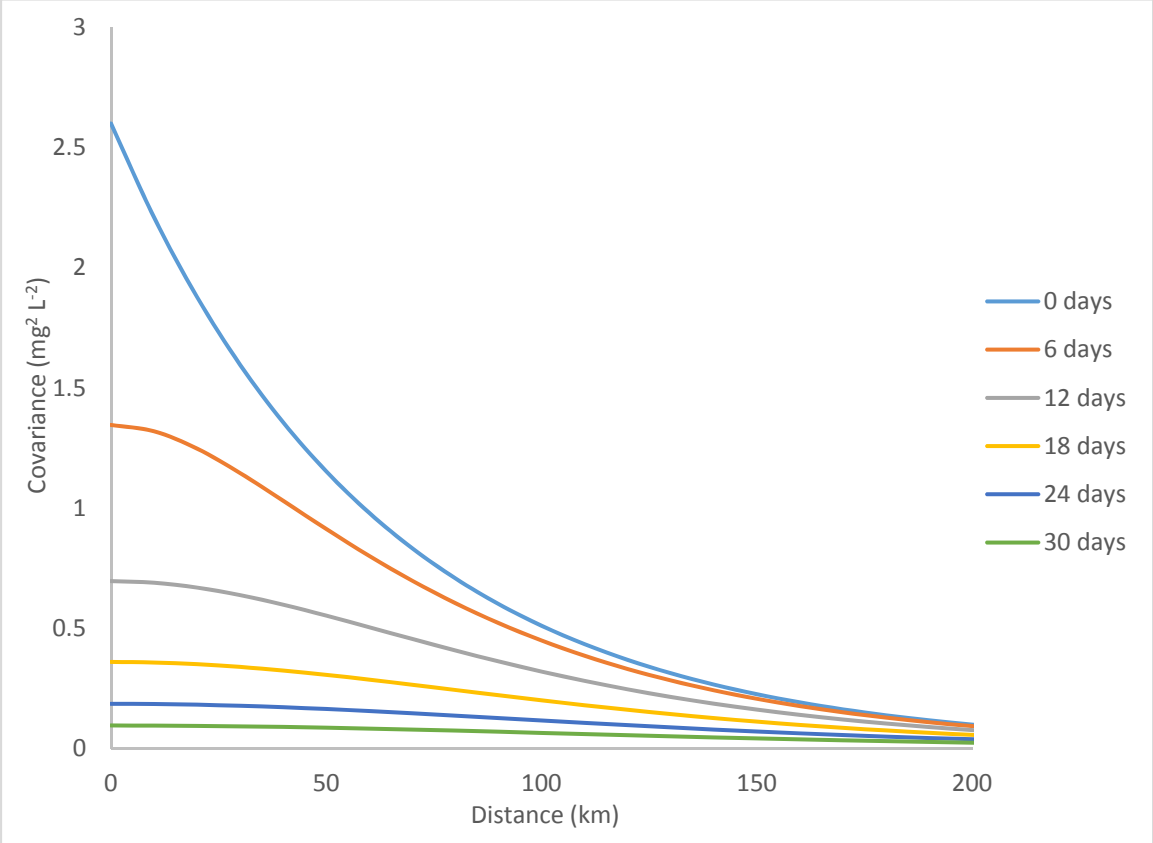

Figure S12. Spatial covariance at different temporal lags (0-30 days) based on covariance function (eq. (2)) for model version C.

Stochasticity of BWDO in our space-time geostatistical model (version C) is found to be spatially and temporally correlated within ranges of 185 km and 28 days, respectively. As noted by an anonymous reviewer, Li et al. (1996) found smaller correlation ranges for hydrographic

variables including salinity, temperature, and geopotential anomaly (though dissolved oxygen was not considered.) In contrast to our study, Li et al. detrended their data using more closely-fitting and temporally-specific trends (based on cruise- and month-specific data). As such, they attributed more variability to trends and less to spatial stochasticity/anomaly, which explains the smaller spatial correlation scales determined in their study. Methods of detrending can vary depending on the objectives of a given study, and the close-fitting trends of Li et al. would not be appropriate for our study due to concerns about over-fitting and the fact that cruise-specific trends could not be used to make estimations between cruises (when no cruise-specific trend is available).

References:

Li, Y.; W. D. Nowlin Jr; R. O. Reid Mean hydrographic fields and their interannual variability over the Texas-Louisiana continental shelf in spring, summer, and fall, *Journal of Geophysical Research: Oceans* 1997, *102*(C1), 1027–1049, doi: 10.1029/96JC03210

S8: Deterministic trends in model version C

Figures below shows the response of BWDO to the deterministic trends selected in model C. Figure S13 shows trends in BWDO in response to location, depth, and day-of-year. Figure S14 shows the aggregation of these deterministic trends mapped over the entire study area.

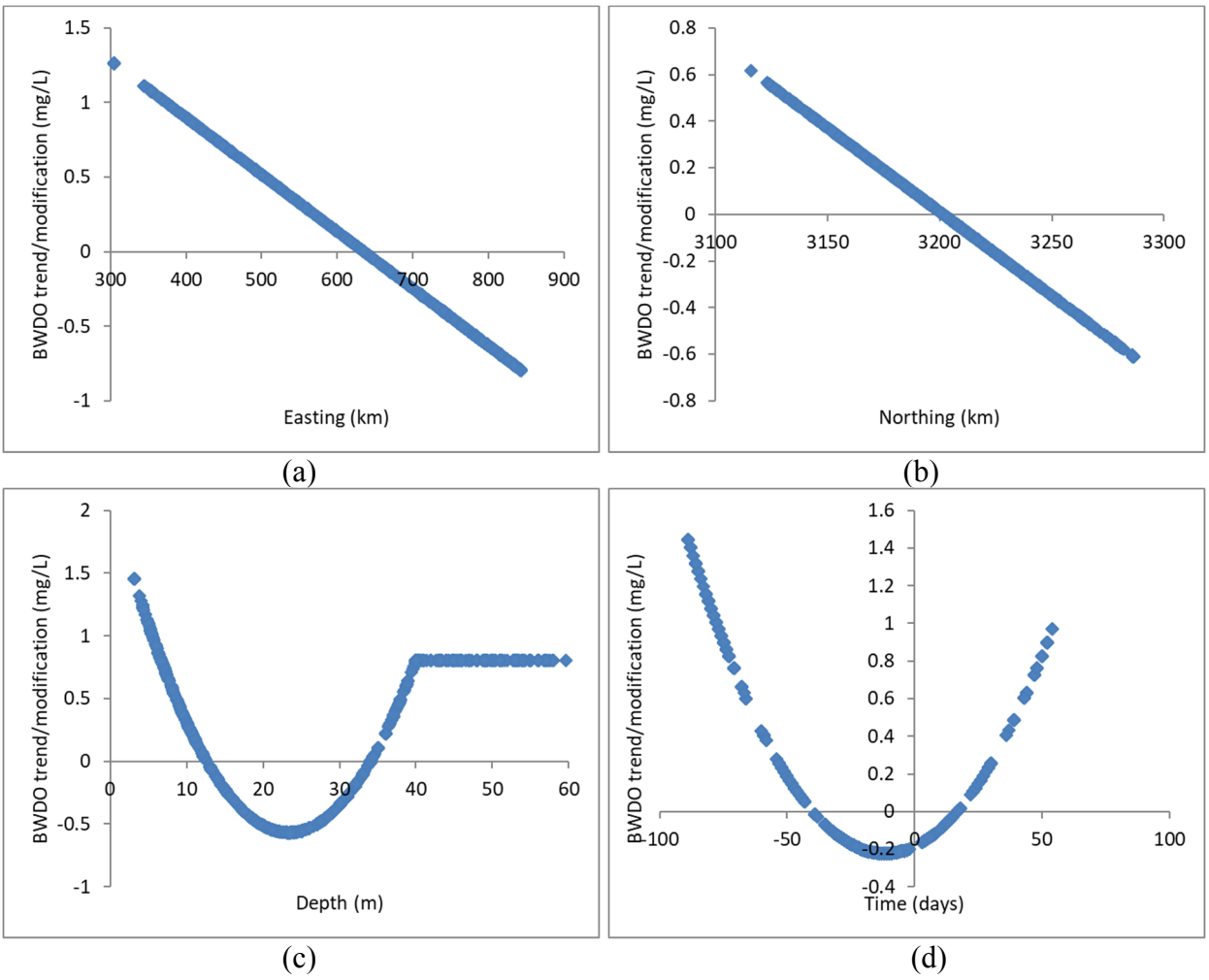

Figure S13. Effect of Deterministic trends on BWDO (a) trends with respect to Easting; (b) trends with respect to Northing; (c) trends with respect to depth; (d) trends with respect to time (where day 0 is August 1).

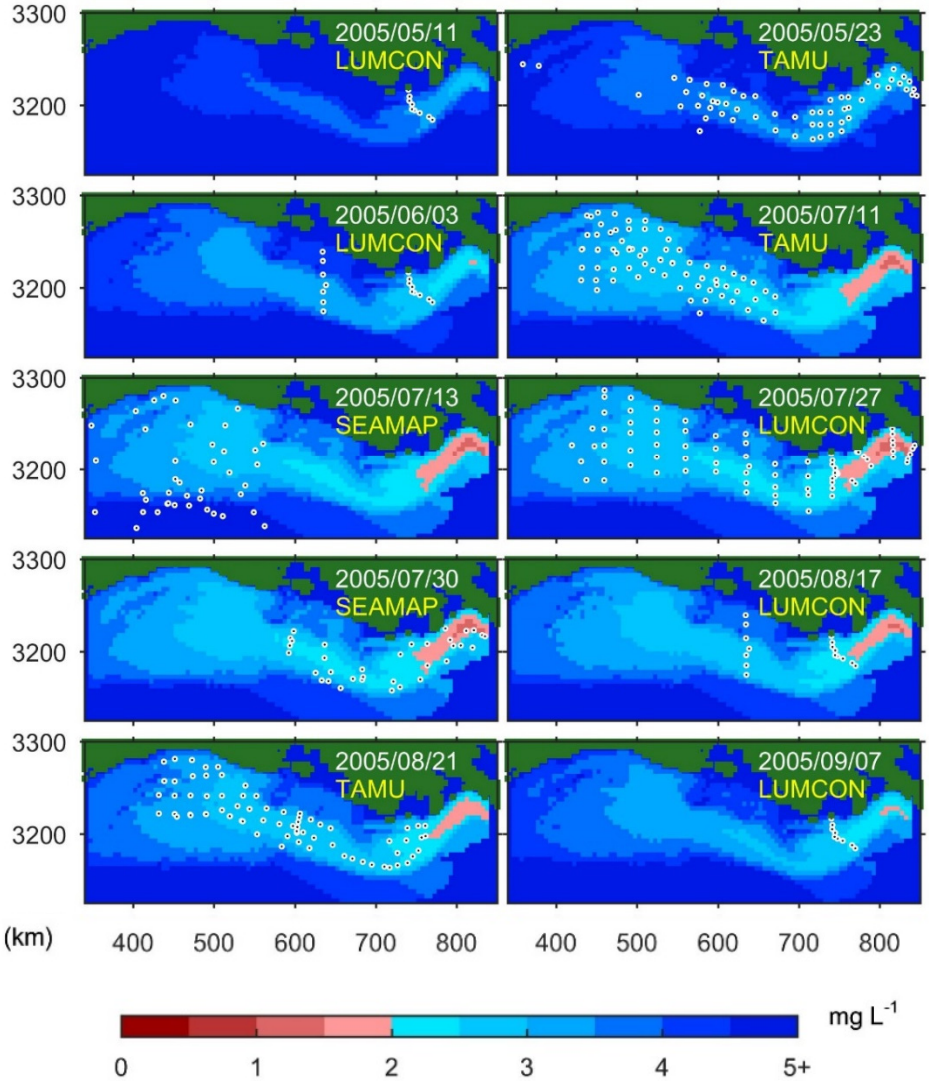

Figure S14. Deterministic trends for cruises in 2005 obtained from model C (spatial and temporal trends with spatial correlation and temporal correlation) using E, N, D, D^2, T and T^2 as trend variables. White dots represent observation locations.

S9: Hypoxic area estimates on cruise mean dates for model versions A, B and C

ORGANIZATION	DATE	MODEL A				MODEL B				MODEL C			
		mean	CI 2.5P	CI 97.5P	CI	mean	CI 2.5P	CI 97.5P	CI	mean	CI 2.5P	CI 97.5P	CI
LUMCON	7/18/1985	14323	10925	18174	7249	14552	10701	19250	8549	14431	10600	19351	8751
LUMCON	7/11/1986	13994	9901	20146	10246	14329	7375	23699	16324	13830	7575	22702	15127
LUMCON	7/3/1987	11049	7025	17272	10247	12704	7376	20998	13623	12200	7299	18876	11577
LUMCON	8/14/1988	630	150	1799	1649	924	101	3200	3099	802	100	2776	2676
LUMCON	8/7/1989	10590	4426	22823	18397	12530	4176	28097	23921	11866	4224	26981	22758
LUMCON	7/25/1990	16782	11100	24449	13349	18264	11775	27774	15999	17693	11773	26413	14640
LUMCON	7/18/1991	17440	12226	24824	12598	18656	12353	27720	15367	20505	13899	30106	16206
NECOP	5/9/1992	15803	6652	28899	22248	15120	7904	24193	16289	8181	3599	14379	10779
NECOP	5/18/1992	16118	11852	21274	9423	14764	10601	19474	8874	10743	7175	15001	7826
SEAMAP	7/4/1992	581	0	2375	2375	3621	400	9174	8774	4245	675	9529	8854
LUMCON	7/26/1992	11595	8375	16596	8221	10506	7726	14875	7149	11136	7999	15678	7678
NECOP	7/6/1993	27442	22826	32549	9723	27734	22300	33599	11299	23824	18775	29426	10651
LUMCON	7/26/1993	23918	18550	31074	12524	24982	19476	33271	13796	24498	19149	31828	12679
SEAMAP	7/12/1994	15571	12126	19399	7274	15322	11201	20373	9171	15486	11024	20526	9501
LUMCON	7/26/1994	18117	13701	24048	10348	17308	13100	22899	9799	17289	13149	22501	9351
SEAMAP	7/13/1995	21217	16901	25774	8874	21424	16051	27525	11474	21270	15699	26951	11253
LUMCON	7/23/1995	23087	17653	30600	12948	22818	17875	28900	11025	22519	17449	28700	11251
SEAMAP	7/11/1996	21321	17225	25600	8375	21818	16327	27472	11145	21680	16350	26877	10527
LUMCON	7/25/1996	25240	19475	33174	13699	23621	18375	31149	12774	23612	18550	30825	12275
SEAMAP	7/7/1997	27182	22650	32249	9599	27869	21629	34200	12571	27660	20848	34180	13333
LUMCON	7/25/1997	19314	14875	25599	10724	20817	15576	27948	12372	21002	16124	27529	11406
LDWF	5/12/1998	7816	626	27074	26449	11651	3826	25247	21421	5738	1850	13180	11330
LDWF	5/27/1998	19825	1852	49721	47869	13295	3976	28248	24272	9235	2724	19628	16903
LUMCONT	6/10/1998	17643	3200	43484	40284	14734	5427	27674	22247	12729	5249	24576	19327
LDWF	6/23/1998	15632	2703	40037	37334	15409	6226	27563	21336	14518	6421	25126	18704
SEAMAP	7/11/1998	13602	9426	18474	9048	13366	8875	18973	10098	13648	8799	18550	9751
LDWF	7/14/1998	4633	50	22849	22799	12930	8626	18025	9399	13253	8875	18578	9703
LUMCON	7/21/1998	12407	9476	17299	7823	12338	9475	17223	7748	12947	9549	18152	8603
LDWF	7/23/1998	8305	525	29764	29239	12489	9276	17124	7848	12687	9774	17851	8076
LUMCONT	8/18/1998	23519	4651	48245	43594	14838	6303	27599	21297	14277	6475	24981	18506
LDWF	8/25/1998	8075	1325	25220	23895	13190	4826	25698	20872	12191	4799	23876	19078
LDWF	9/22/1998	1102	0	6423	6423	8589	1101	21274	20174	3927	225	12051	11826
LUMCONT	5/4/1999	2632	150	11095	10945	11674	2850	25123	22273	4032	725	11307	10582
LDWF	5/18/1999	3952	325	16464	16139	13265	3504	28243	24739	7521	1675	16775	15100
LDWF	5/25/1999	8589	801	25570	24769	14397	4625	28739	24114	9906	3075	20553	17478

ORGANIZATION	DATE	MODEL A				MODEL B				MODEL C			
		mean	CI 2.5P	CI 97.5P	CI	mean	CI 2.5P	CI 97.5P	CI	mean	CI 2.5P	CI 97.5P	CI
LDWF	6/3/1999	13848	2625	35749	33124	15409	5803	30324	24521	12670	4750	23829	19079
LUMCONT	6/8/1999	18634	3329	42971	39641	15076	5850	27843	21993	13480	5349	25326	19977
LDWF	6/19/1999	9227	825	31698	30873	12487	4525	24623	20098	12651	4424	23431	19007
SEAMAP	7/14/1999	7775	5400	11150	5750	8118	4700	12898	8198	9418	5849	13526	7677
LUMCON	7/26/1999	23314	17976	30872	12896	19940	15351	25398	10046	20203	15849	25776	9928
LDWF	7/29/1999	31965	10229	53975	43746	21512	16403	28299	11896	21794	16374	28701	12328
LDWF	8/5/1999	22770	6226	46170	39944	21425	11803	32698	20896	21457	13024	31650	18626
LUMCONT	8/24/1999	35071	10077	56722	46645	19294	8451	31997	23546	17890	8372	31375	23003
LDWF	8/31/1999	15063	2551	38568	36017	18544	7676	32499	24823	16389	7350	28451	21101
LDWF	9/9/1999	31266	9925	53649	43724	18655	8750	33072	24322	14519	6975	26306	19331
LUMCONT	9/13/1999	12855	1676	34947	33271	16942	6927	31324	24397	12299	4625	23929	19304
LUMCONT	5/10/2000	6143	200	24743	24543	5334	775	14197	13422	1878	150	5801	5651
LUMCONT	5/15/2000	1994	0	11946	11946	4777	651	14175	13524	1739	150	6151	6001
LDWF	5/22/2000	1662	0	9793	9793	4365	351	13023	12673	2163	100	7287	7187
LUMCONT	6/2/2000	1655	0	11644	11644	4456	375	13450	13075	2945	300	8754	8454
LUMCONT	6/14/2000	634	0	4049	4049	4411	425	13522	13097	3874	424	10828	10403
LDWF	6/15/2000	521	0	3024	3024	8285	3801	14349	10549	3782	450	10726	10276
LDWF	6/27/2000	1858	101	9274	9174	4765	401	14343	13943	6267	1574	14352	12778
LUMCONT	7/8/2000	3895	250	17291	17041	6378	1576	15125	13549	8365	3673	14800	11127
LDWF	7/10/2000	10955	7376	15299	7923	8402	4401	13500	9099	8467	4350	13626	9276
SEAMAP	7/13/2000	5074	150	21092	20942	8300	4776	12799	8024	8411	4699	12826	8128
LUMCON	7/24/2000	3844	2576	6000	3424	4744	2751	8600	5849	4851	2850	8702	5852
LDWF	7/25/2000	4485	225	18672	18447	4288	2251	8174	5924	4461	2399	8131	5731
LDWF	8/9/2000	4780	350	19345	18995	5138	1100	12024	10924	5167	1275	12303	11028
LUMCONT	8/15/2000	13491	1901	37536	35636	6678	2025	16292	14267	6308	2224	13104	10879
LUMCONT	8/18/2000	12877	975	40775	39800	6728	2000	15399	13399	6476	1998	15102	13104
LDWF	8/30/2000	8027	675	24674	23999	6093	1376	15693	14317	5023	925	13103	12178
LUMCONT	9/13/2000	1074	0	6024	6024	4654	500	13070	12570	2464	175	8178	8003
LUMCONT	5/7/2001	88	0	574	574	3094	176	9949	9773	978	0	3978	3978
LDWF	5/11/2001	273	0	1999	1999	3062	225	10574	10349	1142	25	4729	4704
LDWF	6/18/2001	7707	1200	24399	23199	6309	1700	15574	13874	6828	1874	15377	13503
LUMCONT	6/19/2001	6507	301	24889	24588	6349	1776	15368	13592	6939	2099	15851	13751
LDWF	7/10/2001	15157	10053	20924	10871	10932	5152	19645	14493	11377	5649	19128	13478
LUMCON	7/23/2001	37034	12103	57523	45419	20544	17001	24474	7473	20207	16424	24600	8176
LDWF	8/8/2001	3673	150	15072	14922	12529	3601	24193	20593	12518	4274	23151	18877
LUMCONT	8/16/2001	17371	2351	45222	42871	12173	3851	23974	20124	12043	4650	22403	17753
LUMCONT	9/6/2001	30330	2851	58999	56148	8531	2751	17649	14898	7632	2524	16251	13726

ORGANIZATION	DATE	MODEL A				MODEL B				MODEL C			
		mean	CI 2.5P	CI 97.5P	CI	mean	CI 2.5P	CI 97.5P	CI	mean	CI 2.5P	CI 97.5P	CI
LUMCONT	9/18/2001	1625	126	6371	6246	5102	1000	12999	11999	3173	474	9127	8653
LUMCONT	5/9/2002	2172	100	10468	10368	7186	1151	18149	16998	2827	325	8626	8301
LUMCONT	6/11/2002	1004	201	3125	2924	5221	950	13324	12374	4660	925	12176	11251
SEAMAP	7/9/2002	19238	15276	23625	8349	20094	13950	26100	12150	20617	15100	26879	11779
LUMCON	7/24/2002	22741	19051	27850	8799	21476	17676	25474	7798	21800	17824	26725	8901
LUMCONT	8/13/2002	13501	5176	28631	23455	14353	7100	24122	17022	14181	7150	23350	16200
LUMCONT	8/27/2002	6855	1975	17919	15944	9861	3826	20024	16199	9130	3549	18825	15276
LUMCONT	9/20/2002	6272	450	21723	21273	9284	2401	20623	18221	5080	950	13707	12757
LUMCONT	5/13/2003	1109	225	3474	3249	5480	1226	13391	12166	2649	600	7350	6750
LUMCONT	6/6/2003	21970	1702	53345	51643	10596	4027	21118	17091	9266	3599	17955	14356
EPA	6/15/2003	16452	2676	42421	39745	11354	6526	18949	12423	11019	6225	18176	11951
LUMCONT	6/16/2003	13604	7601	23149	15548	11443	6376	19446	13071	10966	6199	17451	11251
SEAMAP	7/14/2003	8928	4600	14448	9848	9215	4226	15699	11473	10457	5150	17701	12551
LUMCON	7/26/2003	5486	3900	7674	3774	6270	4251	9125	4874	6518	4124	9700	5576
UMCES	8/2/2003	10518	4826	19047	14221	8009	4450	12798	8348	8249	4699	13176	8477
LUMCONT	8/14/2003	7349	1151	20423	19271	8771	3701	16200	12499	8856	4000	15976	11976
LUMCONT	8/22/2003	16815	2476	43619	41143	9852	4003	19621	15618	9749	3925	18578	14653
LUMCONT	9/9/2003	2011	25	10773	10748	10122	3628	18671	15043	7154	2975	12926	9951
TAMU	9/15/2003	17051	8550	28648	20098	11365	6150	18524	12374	7160	3625	12651	9026
LUMCONT	5/5/2004	4178	0	21388	21388	12516	2926	25971	23044	4077	400	12551	12151
LUMCONT	5/13/2004	2439	75	12198	12123	11805	2801	24743	21942	5281	875	13626	12751
LUMCONT	6/6/2004	2400	0	15882	15882	10580	2800	21473	18673	9088	2375	18902	16527
LUMCONT	6/16/2004	3456	600	10648	10048	12208	4251	21598	17347	11587	4449	21926	17476
TAMU	6/29/2004	29540	19500	40996	21496	22190	16902	28174	11273	22418	16549	28701	12152
SEAMAP	7/8/2004	22670	18500	26424	7924	23118	18376	27850	9474	24668	20124	29876	9751
LUMCON	7/23/2004	16466	12650	22346	9696	15657	12526	20824	8298	16391	12825	21004	8179
UMCES	7/31/2004	5943	1301	13899	12598	8688	4025	14975	10950	9384	4524	15777	11253
LUMCONT	8/19/2004	3198	125	15519	15394	18957	10125	30398	20273	18709	10399	29302	18903
TAMU	8/23/2004	31567	19876	43475	23599	22826	14826	33821	18996	20751	13498	30200	16702
LUMCONT	9/8/2004	5044	1225	13000	11775	13748	5053	25849	20796	9815	3549	20126	16577
LUMCONT	5/11/2005	815	0	4925	4925	11005	3251	21497	18246	4727	825	11801	10976
TAMU	5/23/2005	18647	10828	27899	17071	15117	9178	23695	14518	11217	6950	17779	10829
LUMCONT	6/3/2005	4356	876	12666	11790	10988	4251	21049	16798	9479	3325	17754	14429
TAMU	7/11/2005	25029	16252	34772	18520	16153	11526	21724	10199	15274	10999	20500	9501
SEAMAP	7/13/2005	13587	7276	22175	14899	15326	10901	20325	9424	14618	10375	19681	9306
LUMCON	7/27/2005	10289	7826	13824	5998	11192	8526	14700	6174	11373	8824	15301	6478
SEAMAP	7/30/2005	14002	6425	26549	20124	12554	8926	16749	7824	12972	9324	17301	7976

ORGANIZATION	DATE	MODEL A				MODEL B				MODEL C			
		mean	CI 2.5P	CI 97.5P	CI	mean	CI 2.5P	CI 97.5P	CI	mean	CI 2.5P	CI 97.5P	CI
LUMCONT	8/17/2005	22701	9575	39720	30145	25963	19701	33746	14045		18100	30801	12701
TAMU	8/21/2005	34162	25152	44147	18995	24833	18801	32621	13820	24462	18924	31775	12851
LUMCONT	9/7/2005	1650	25	9424	9399	7502	925	17800	16875	9696	2875	19604	16729
LUMCONT	9/29/2005	346	0	1874	1874	12744	3602	24549	20947	2863	175	9201	9026
LUMCONT	5/26/2006	7364	625	26797	26172	8664	2727	18168	15441	6053	1875	13125	11250
LUMCONT	6/6/2006	5401	150	24049	23899	6345	3300	11698	8398	5736	2724	10426	7701
EPA	6/11/2006	5169	3026	8649	5624	6332	3051	11823	8771	6386	3200	10801	7601
LUMCONT	6/27/2006	9762	2800	23321	20521	10010	5126	16273	11147	11380	5648	19276	13628
SEAMAP	7/11/2006	12515	8876	16499	7623	13129	8551	18149	9599	15433	10049	21225	11176
LUMCON	7/24/2006	16803	12776	22748	9973	16281	12350	21448	9098	17234	12575	23250	10675
UMCES	8/9/2006	5637	2425	11197	8772	8953	3975	15947	11972	9472	4123	17300	13177
LUMCONT	9/11/2006	11987	8025	17748	9723	12217	7551	18322	10771	10753	6798	15826	9028
EPA	5/5/2007	1218	225	3798	3573	4647	2275	8649	6374	3811	1949	6651	4701
LUMCONT	5/13/2007	3922	2350	6150	3800	4171	1350	9324	7974	3622	1149	7580	6431
LUMCONT	6/6/2007	649	0	4523	4523	6902	1251	16598	15347	7268	1675	16750	15075
TAMU	7/18/2007	24242	18251	31048	12798	17555	11700	24897	13197	17417	11198	24925	13727
SEAMAP	7/22/2007	22405	11626	35548	23921	19296	13951	25371	11420	19175	13975	25950	11975
LUMCON	7/25/2007	21303	17075	26049	8974	20511	16376	25524	9148	20981	17050	25300	8250
UMCES	8/3/2007	25845	16029	37249	21221	20994	15425	27174	11749	21859	15993	28778	12784
LUMCONT	8/15/2007	16461	3201	40171	36971	16206	9176	24124	14949	16917	10023	25101	15079
EPA	8/24/2007	16231	12476	21999	9523	17522	13325	23149	9824	17456	12899	23077	10178
TAMU	9/8/2007	26257	15276	39748	24473	18132	11301	26374	15073	16121	10225	23876	13651
LUMCONT	9/12/2007	3403	950	8948	7998	14436	7376	22999	15623	11808	5724	19626	13903
LUMCONT	5/12/2008	7102	726	24873	24147	17086	5777	33167	27390	8432	2075	18951	16876
LUMCONT	6/12/2008	9788	3053	22874	19821	17896	8225	29871	21646	16888	7848	28578	20731
SEAMAP	7/9/2008	32284	28077	36298	8221	30712	24352	36549	12197	31207	25224	37201	11976
TAMU	7/19/2008	35795	25276	47699	22423	27767	22927	33469	10542	27476	22175	33201	11026
LUMCON	7/24/2008	21590	18225	25474	7249	22836	19226	27349	8123	23089	19424	27126	7702
UMCES	8/7/2008	16612	7075	31494	24419	17085	8277	27648	19371	17207	9274	27250	17976
LUMCONT	8/15/2008	9719	376	36424	36049	19832	9401	31998	22596	20040	9625	33301	23676
LUMCONT	5/26/2009	504	0	3271	3271	8450	1476	18998	17523	4884	525	14981	14456
LUMCONT	6/12/2009	19139	3301	43445	40144	14428	5427	26547	21120	12936	4850	24508	19658
SEAMAP	7/6/2009	15955	12751	19399	6649	14491	8951	20697	11746	16627	10873	22676	11804
LUMCON	7/21/2009	6948	5551	8550	2999	8250	6226	11174	4948	8828	6649	12076	5426
TAMU	7/29/2009	22163	9376	40575	31199	9327	6100	13949	7849	9559	6075	14301	8226
LUMCONT	8/11/2009	9010	2451	22896	20445	9288	3901	17921	14019	9634	4324	18353	14028

ORGANIZATION	Date	Model A				Model B				Model C			
		mean	CI 2.5P	CI 97.5P	CI	mean	CI 2.5P	CI 97.5P	CI	mean	CI 2.5P	CI 97.5P	CI
LUMCONT	8/25/2009	13189	1050	40647	39597	10913	2951	22449	19499	10226	3549	21754	18204
LUMCONT	9/21/2009	11273	1051	35224	34173	11582	3026	25271	22246	6377	1325	15552	14227
SEAMAP	7/25/2010	21760	15176	28724	13548	17751	12401	23850	11449	18733	13149	25050	11901
LUMCON	7/28/2010	16281	12526	20249	7724	18716	14901	23047	8146	19703	15549	24375	8826
UMCES	9/4/2010	7700	3977	12574	8598	11983	3376	23743	20367	9759	5471	15801	10329
LUMCONT	5/23/2011	3810	550	12497	11947	10359	5551	17173	11623	7570	1775	16901	15126
LUMCONT	6/18/2011	21421	8480	38548	30068	21904	13800	31972	18172	19527	12325	28726	16401
TAMU	6/26/2011	26494	20276	34700	14424	24243	19026	30500	11474	21789	16749	27651	10901
SEAMAP	7/10/2011	19056	14500	23624	9124	21513	16225	27474	11249	21407	16199	27676	11476
LUMCON	7/27/2011	16515	13950	19325	5375	17453	14626	20999	6373	17580	14574	21203	6629
LUMCONT	8/23/2011	25088	8254	46639	38386	18320	8754	30049	21296	16564	8199	28181	19982
LUMCONT	5/2/2012	1432	225	4971	4746	6519	1575	15224	13649	2056	375	5526	5151
TAMU	6/13/2012	20054	14326	27072	12746	15302	11226	20199	8973	12750	9000	17301	8301
LUMCONT	6/17/2012	2149	376	6574	6198	9413	5650	13900	8250	8217	4849	12552	7703
SEAMAP	6/23/2012	3715	1226	7873	6647	4679	1800	8500	6700	4835	2000	8876	6876
LUMCON	7/25/2012	7077	4825	10075	5250	7694	5026	11248	6223	7855	4924	11526	6601
TAMU	8/18/2012	5903	1325	15839	14514	14490	10000	21248	11248	12226	8724	17553	8828
LUMCONT	8/21/2012	18173	12325	25921	13596	13076	8151	20298	12147	10841	6899	15927	9028
SEAMAP	6/23/2013	14719	9578	20149	10572	14610	8100	22298	14198	14025	7699	20378	12679
LUMCON	7/24/2013	14616	12226	17649	5424	14877	11976	18398	6423	14924	12174	18178	6003
LUMCONT	5/26/2014	32940	3051	60623	57573	16309	5552	29549	23997	11477	3549	24378	20829
SEAMAP	6/28/2014	13032	9704	16549	6845	13618	8650	18975	10325	16619	10899	23131	12233
LUMCON	7/30/2014	11943	9476	15074	5599	12443	9375	16225	6850	13178	9699	17876	8177
SEAMAP	6/28/2015	7158	4150	10999	6849	8340	3925	13950	10025	8217	3724	13528	9803
SEAMAP	6/25/2016	19792	15926	23998	8072	19485	14401	25345	10944	19624	14493	26001	11509
AVERAGE	--	12868	--	--	17390	13274	--	--	13846	12142	--	--	12009

S10: BWDO maps for cruise dates using model version C

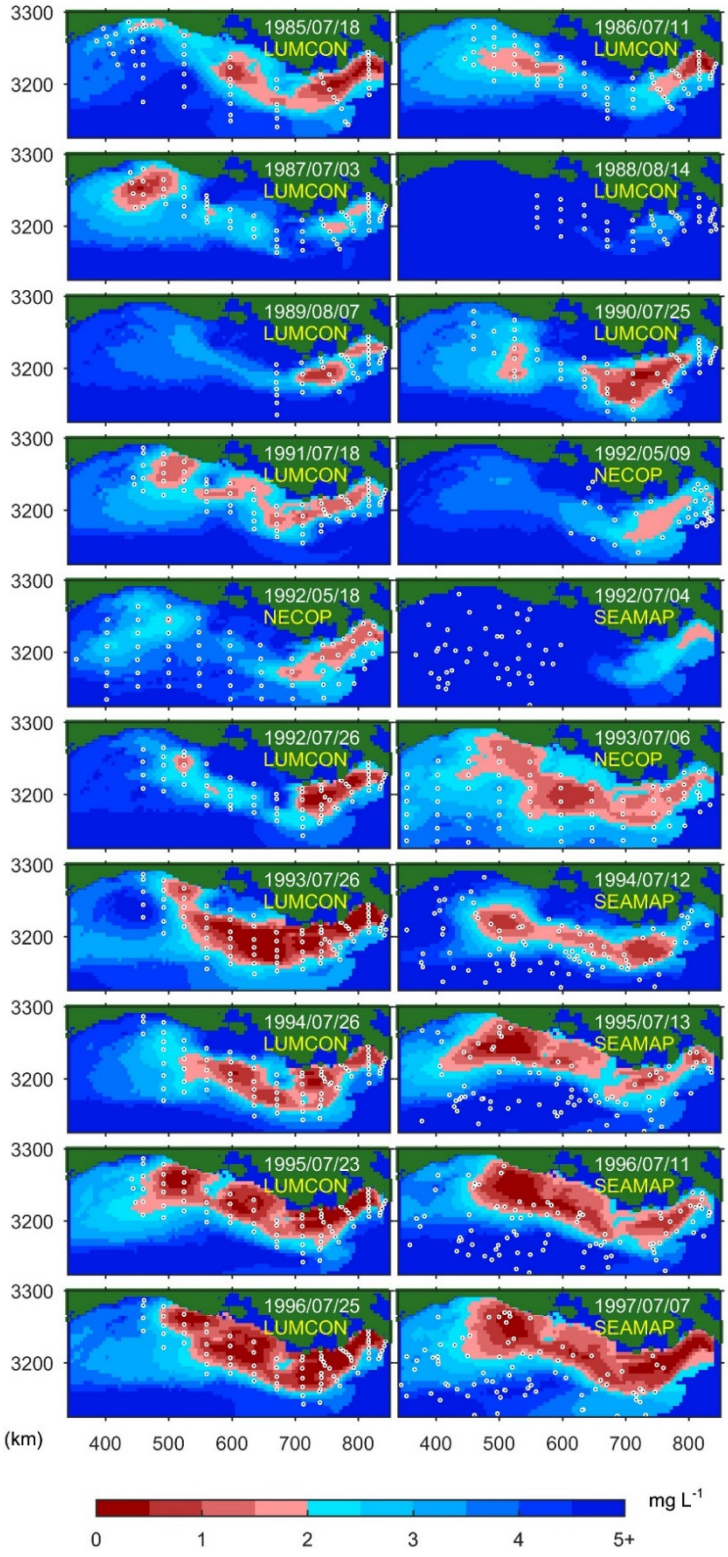

Figure S15. BWDO maps for cruises between 07/1985 and 07/1997 obtained from model C.

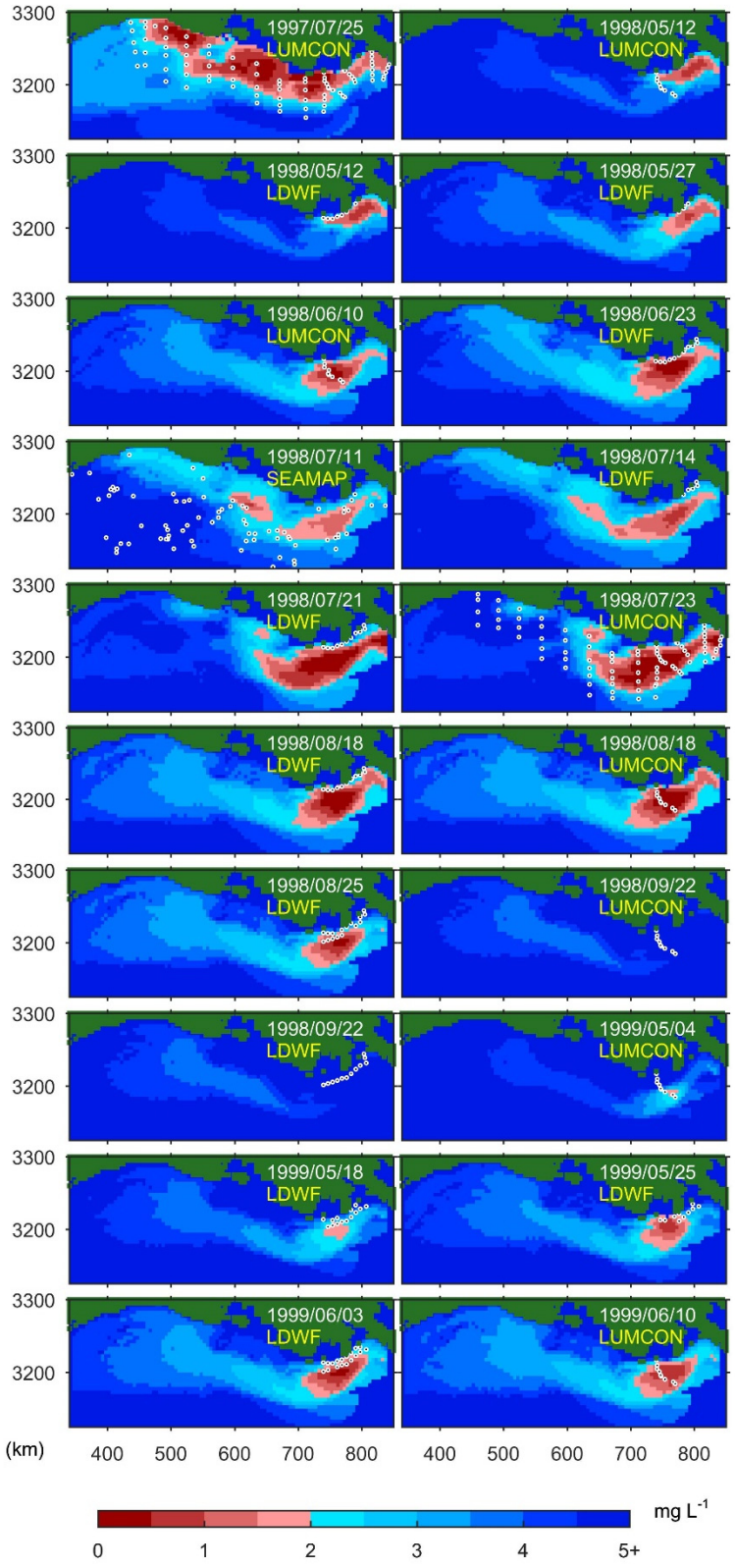

Figure S16. BWDO maps for cruises between 07/1997 and 06/1999 obtained from model C.

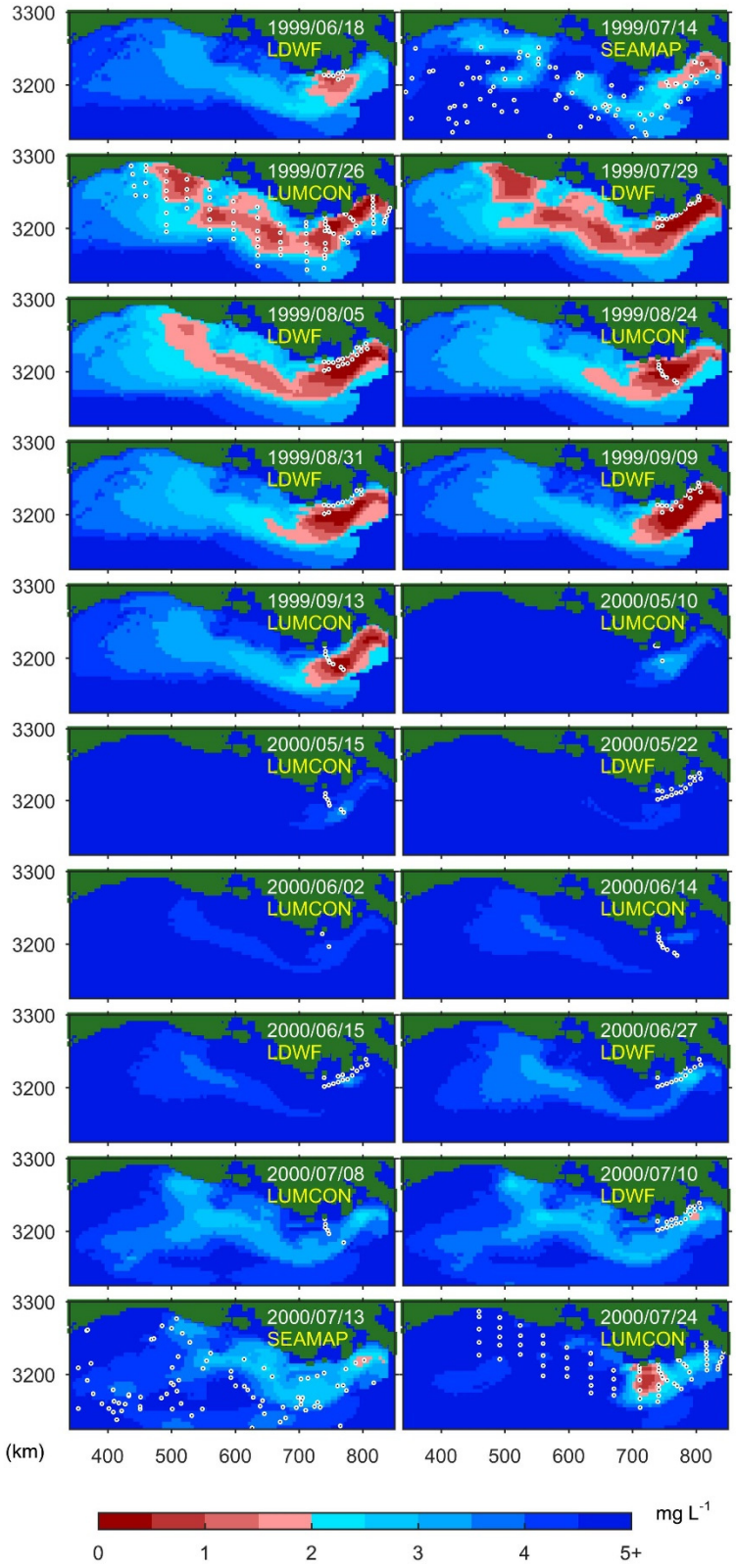

Figure S17. BWDO maps for cruises between 06/1999 and 07/2000 obtained from model C.

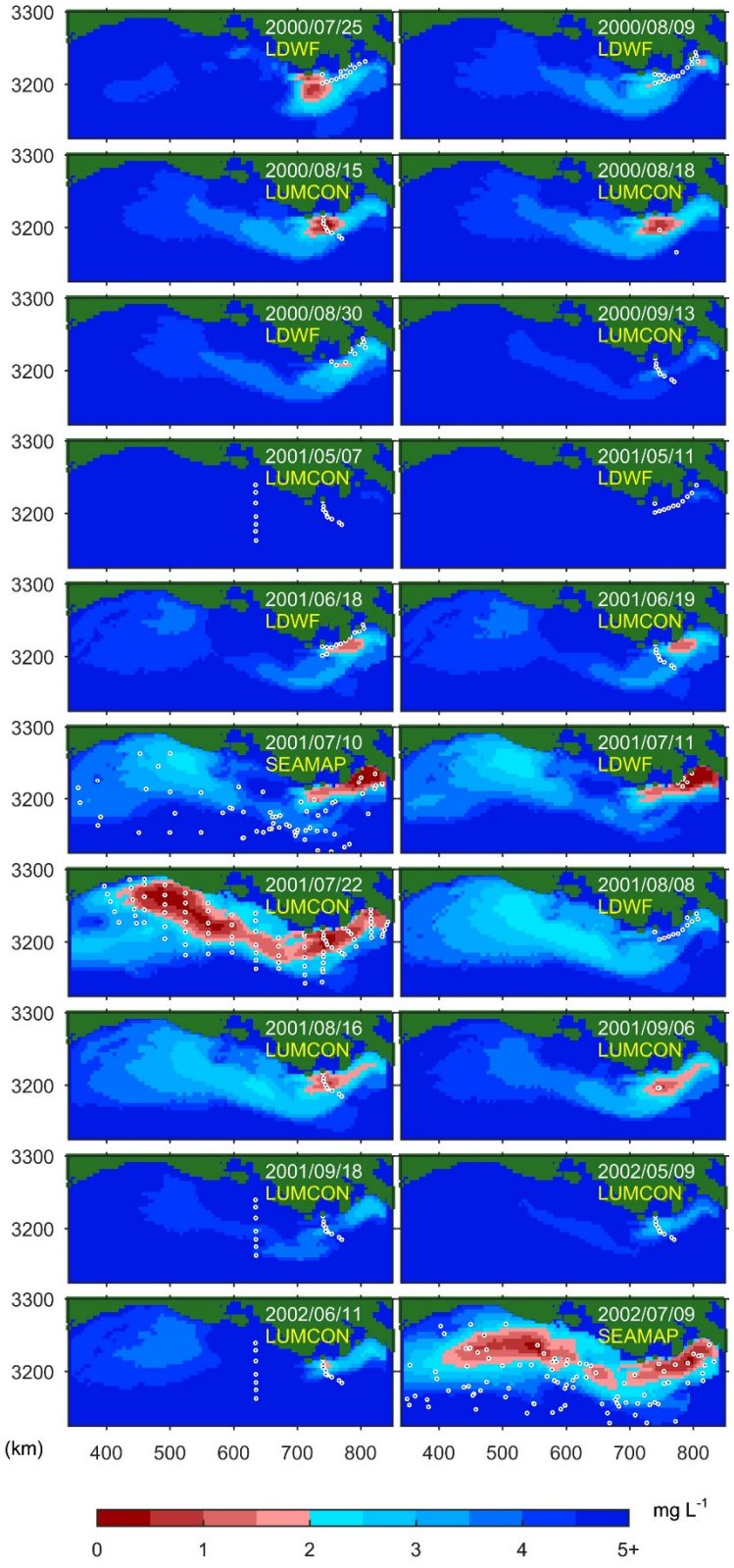

Figure S18. BWDO maps for cruises between 07/2000 and 07/2002 obtained from model C.

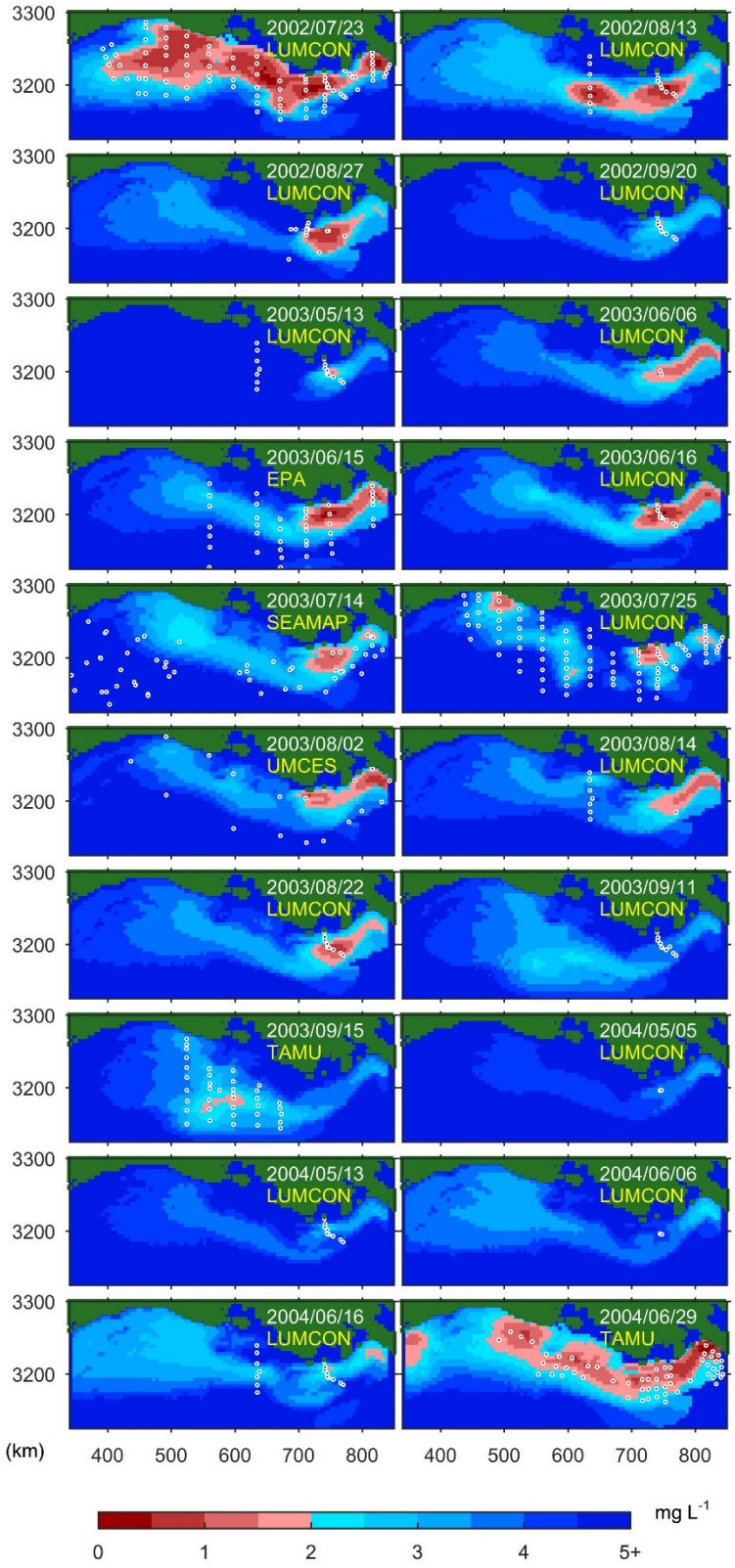

Figure S19. BWDO maps for cruises between 07/2002 and 06/2004 obtained from model C.

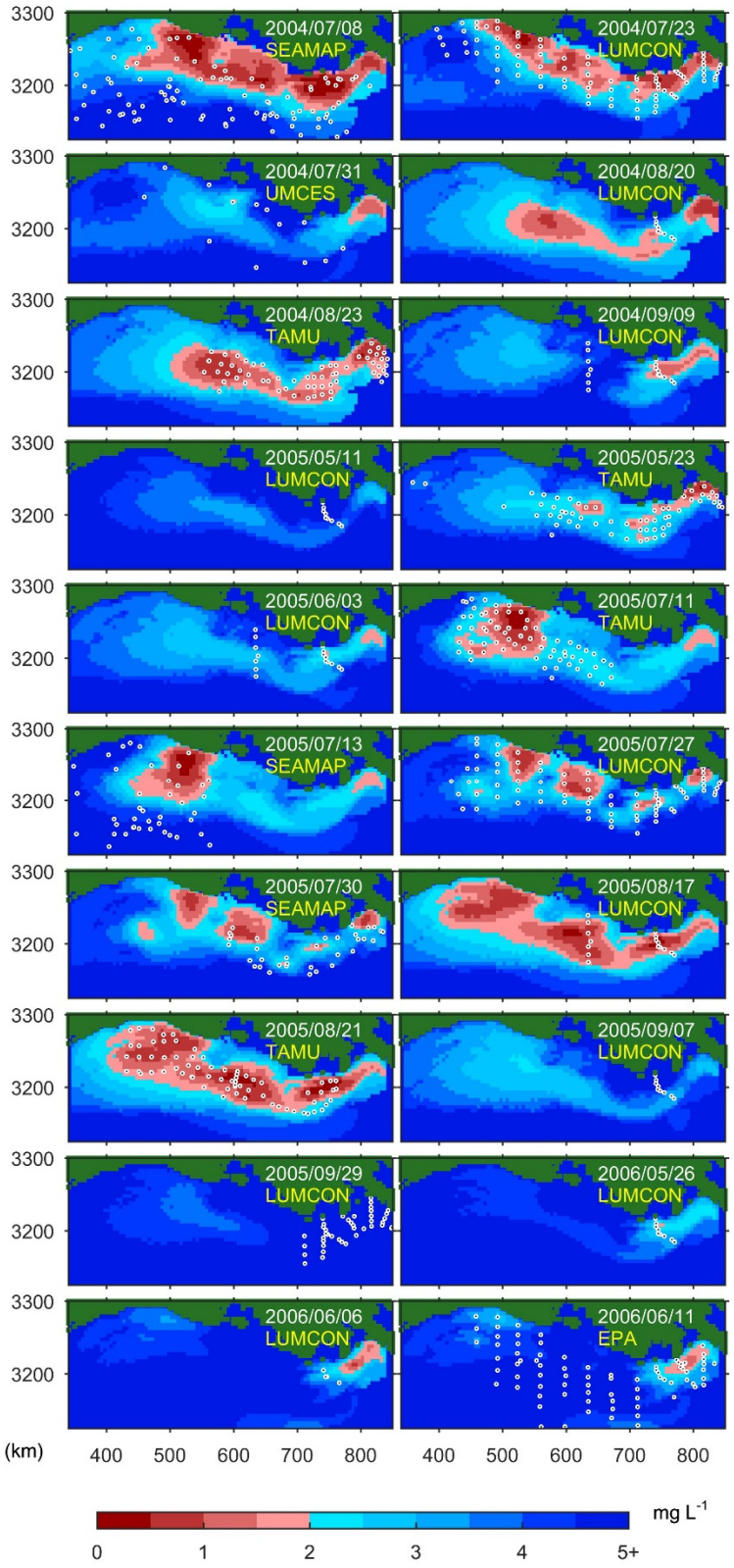

Figure S20. BWDO maps for cruises between 07/2004 and 06/2006 obtained from model C.

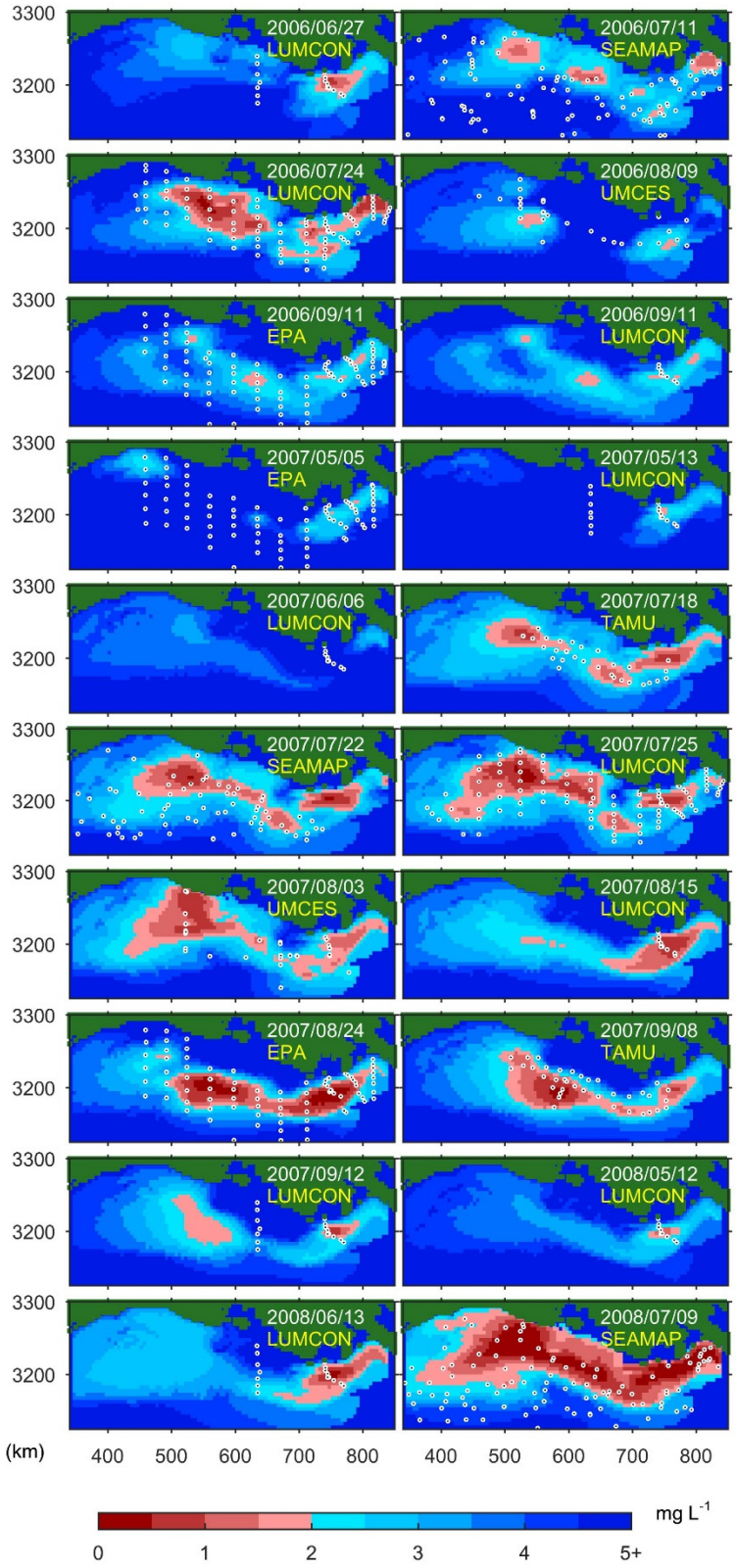

Figure S21. BWDO maps for cruises between 06/2006 and 07/2008 obtained from model C.

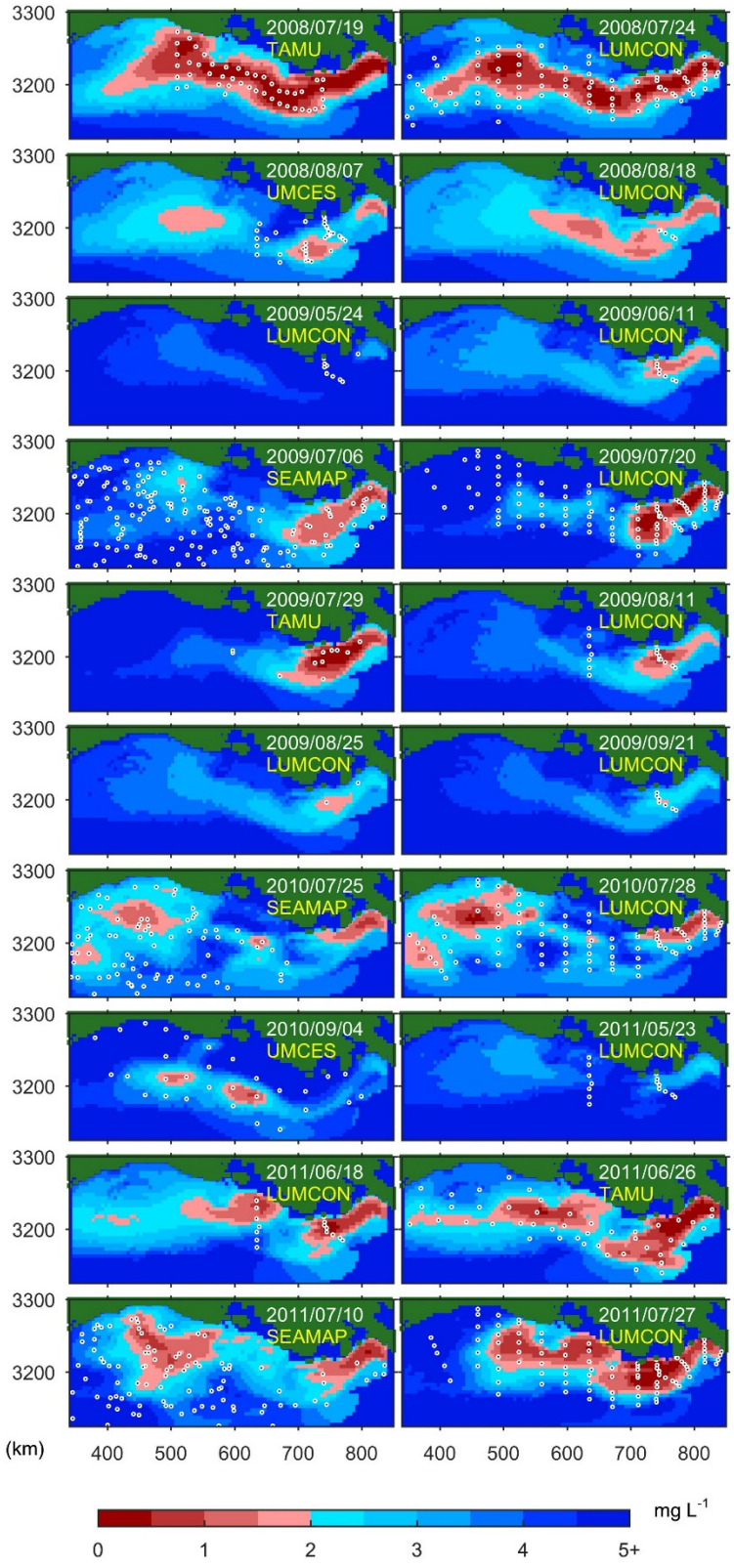

Figure S22. BWDO maps for cruises between 07/2008 and 07/2011 obtained from model C.

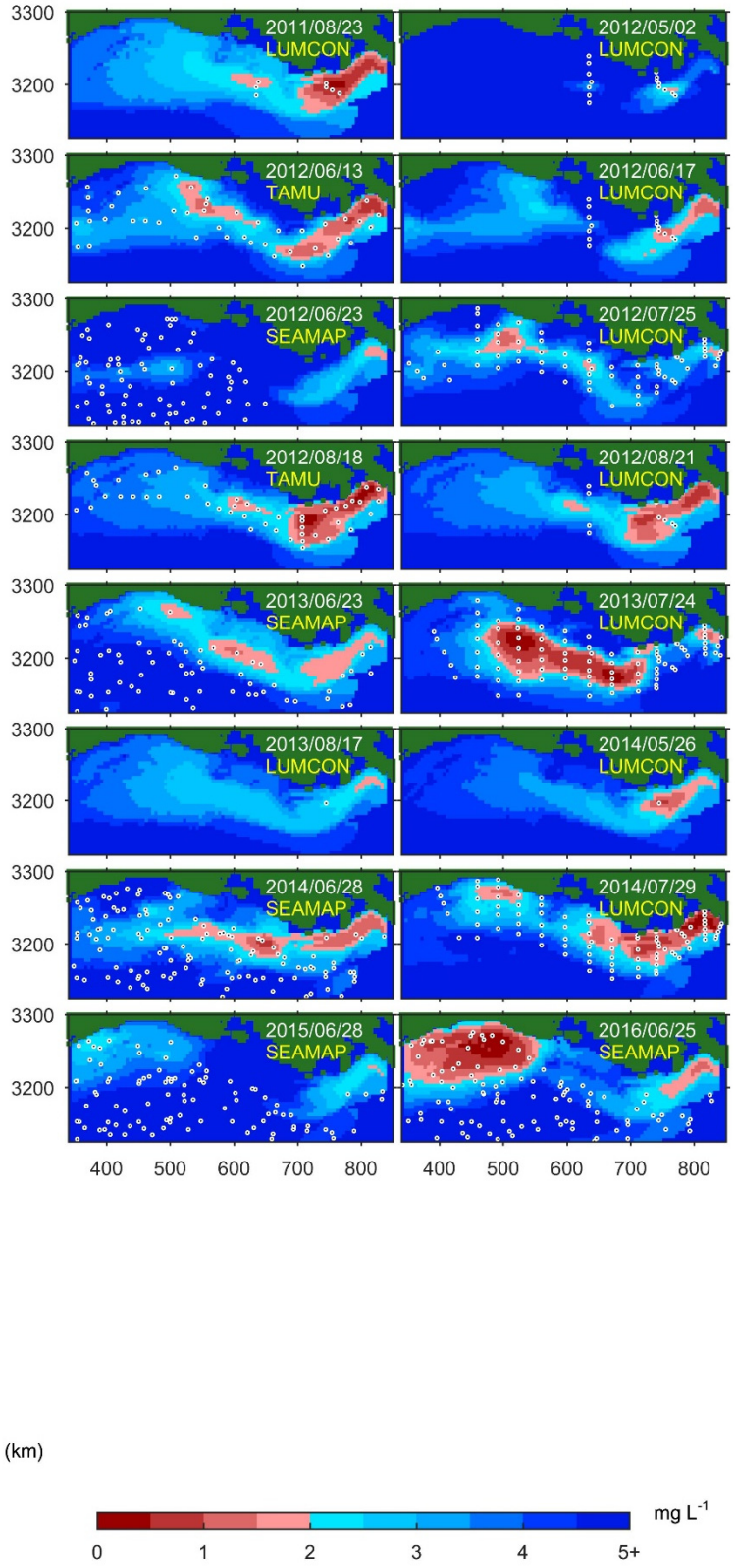

Figure S23. BWDO maps for cruises between 08/2011 and 06/2016 obtained from model C.

S11: Summer-wide hypoxic area estimates for model version C, 1985-2016

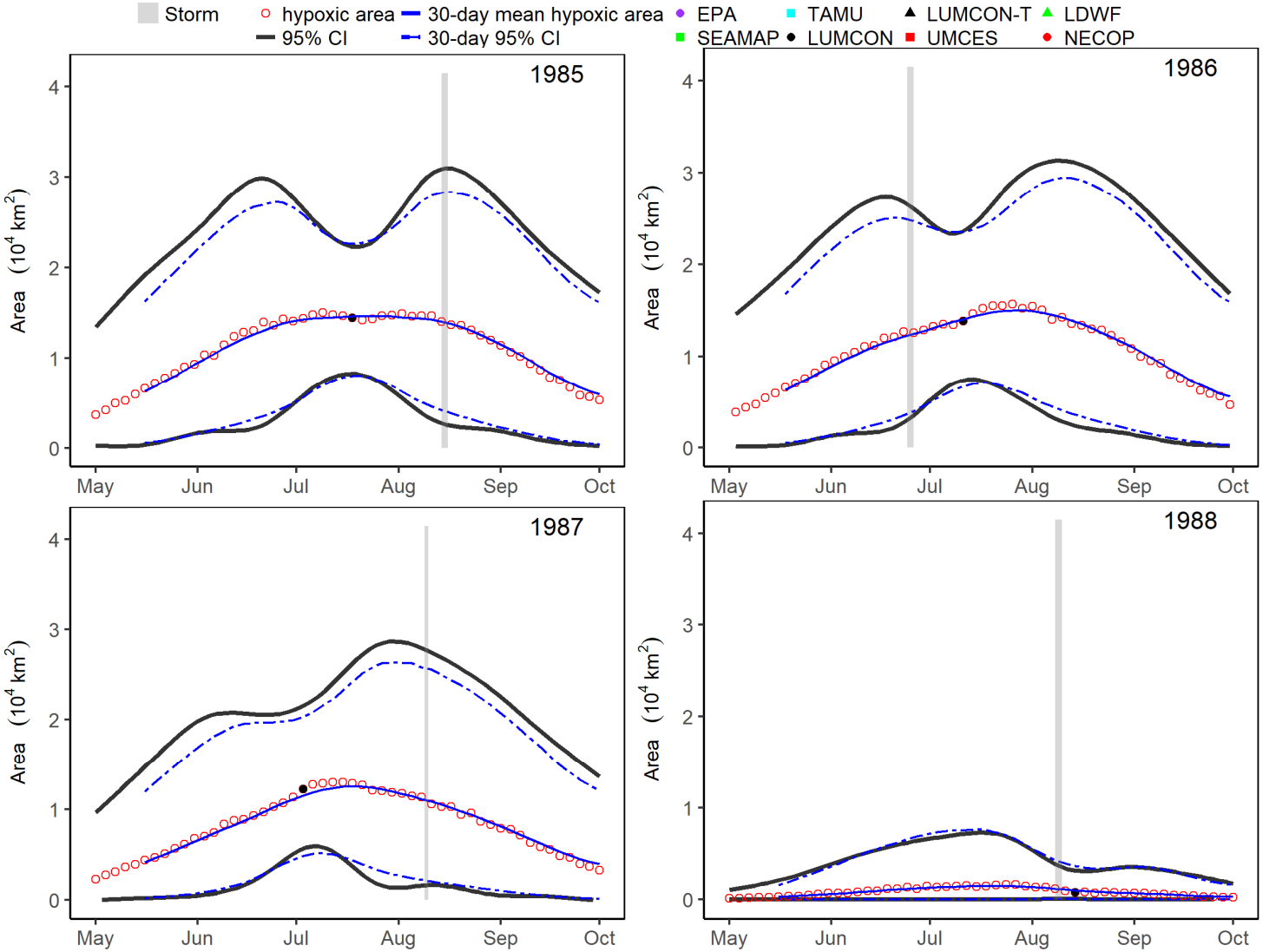

Figure S24. Summer-wide daily estimates and 30-day means with their respective 95% CI for 1985-1988.

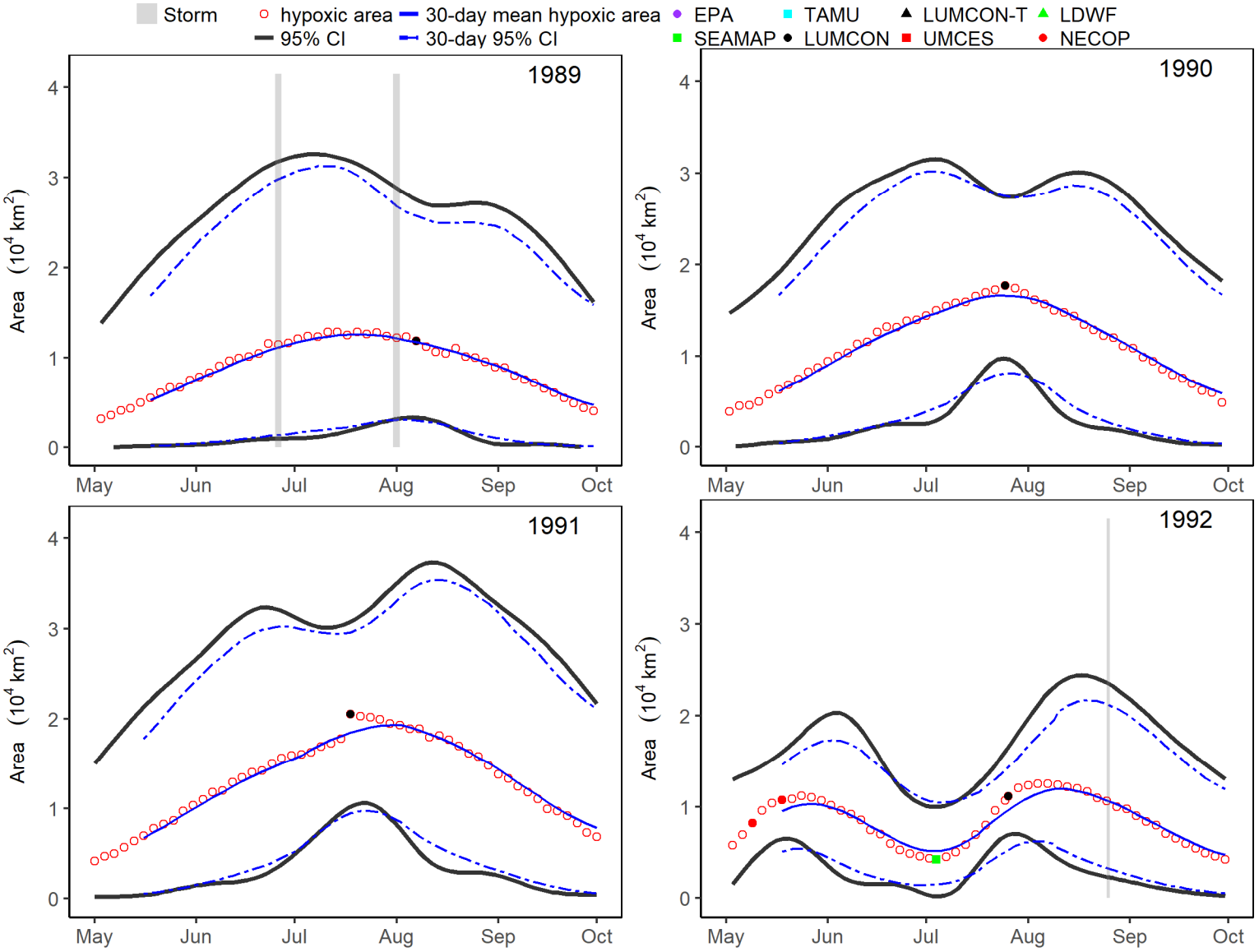

Figure S25. Summer-wide daily estimates and 30-day means with their respective 95% CI for 1988-1992.

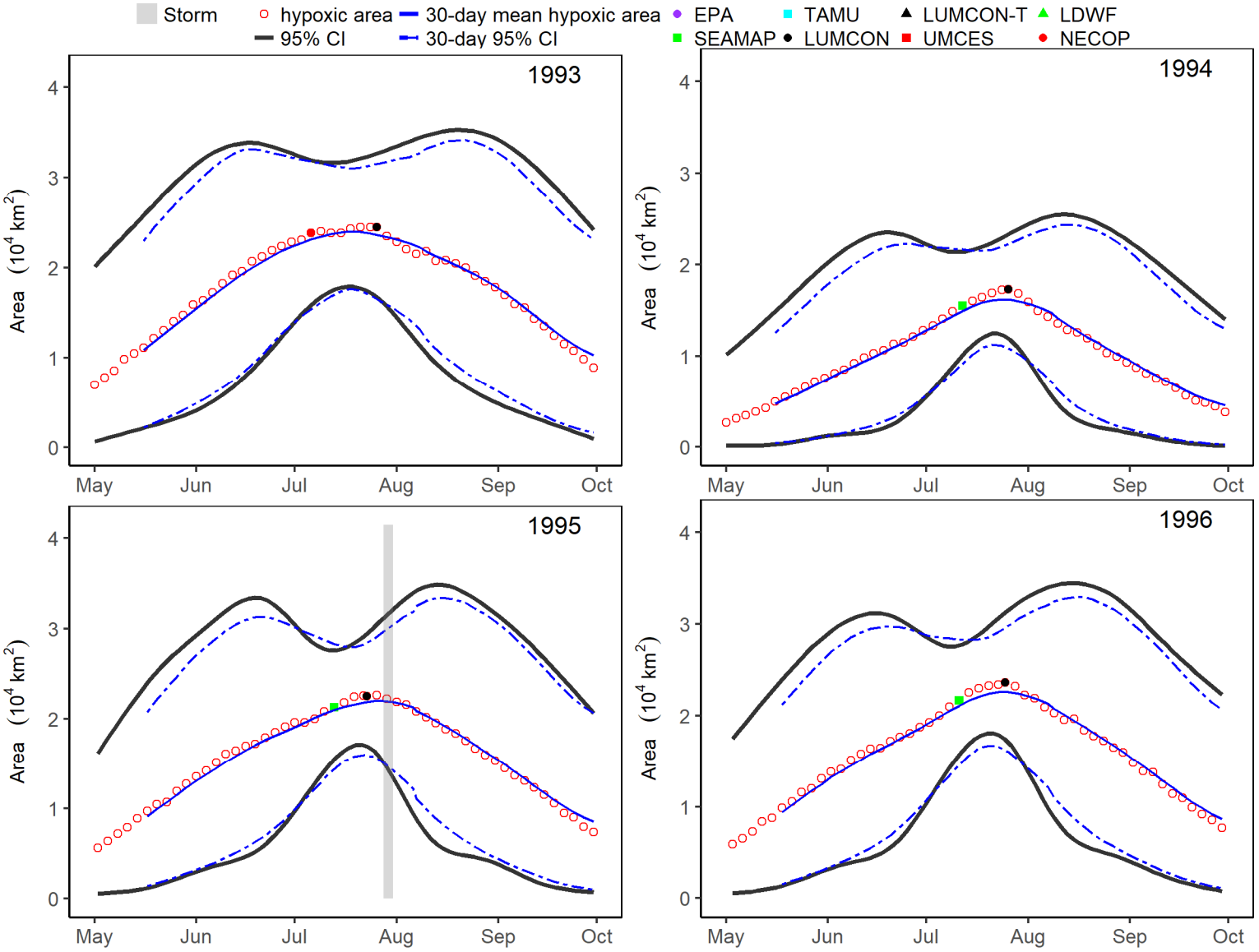

Figure S26. Summer-wide daily estimates and 30-day means with their respective 95% CI for 1993-1996.

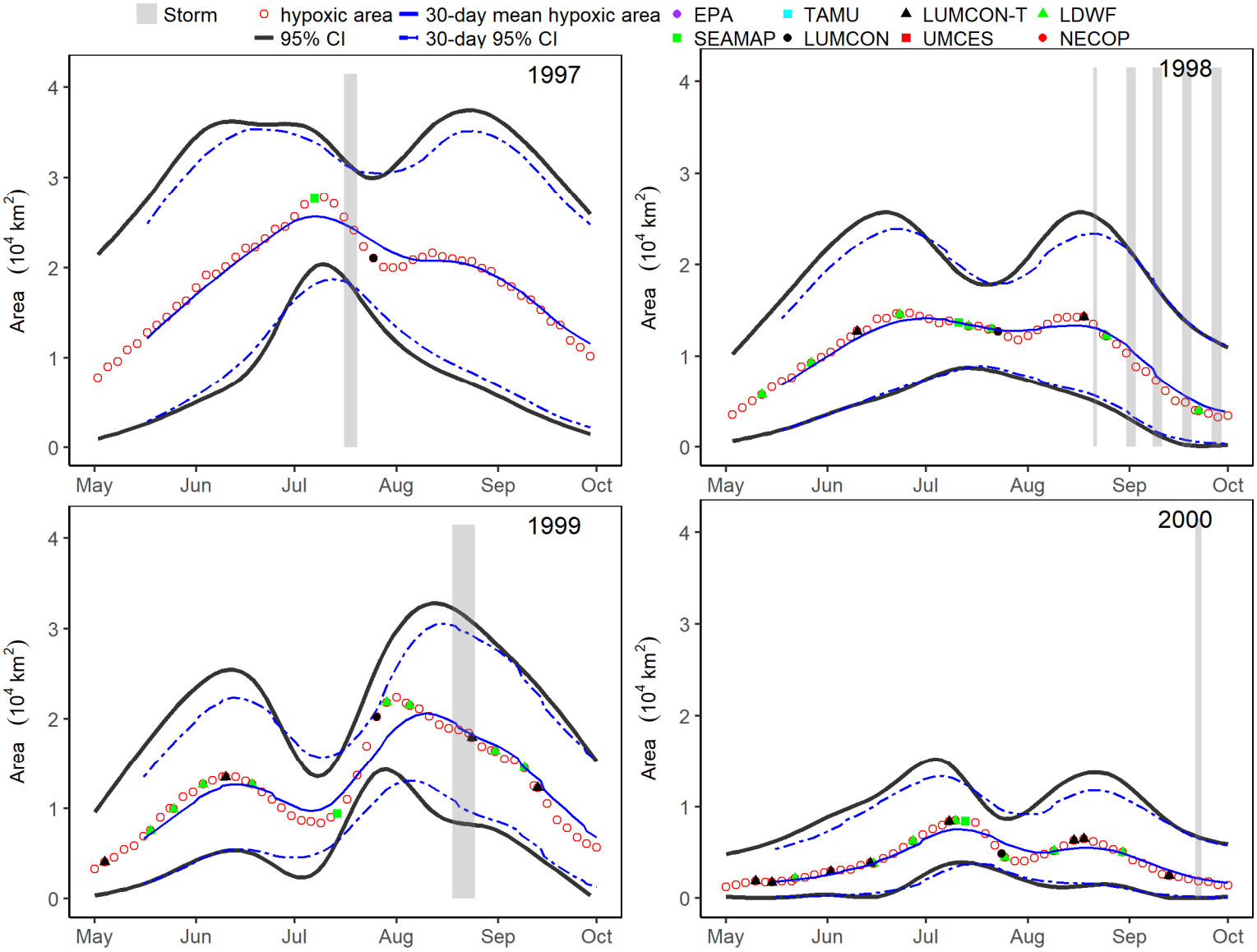

Figure S27. Summer-wide daily estimates and 30-day means with their respective 95% CI for 1997-2000.

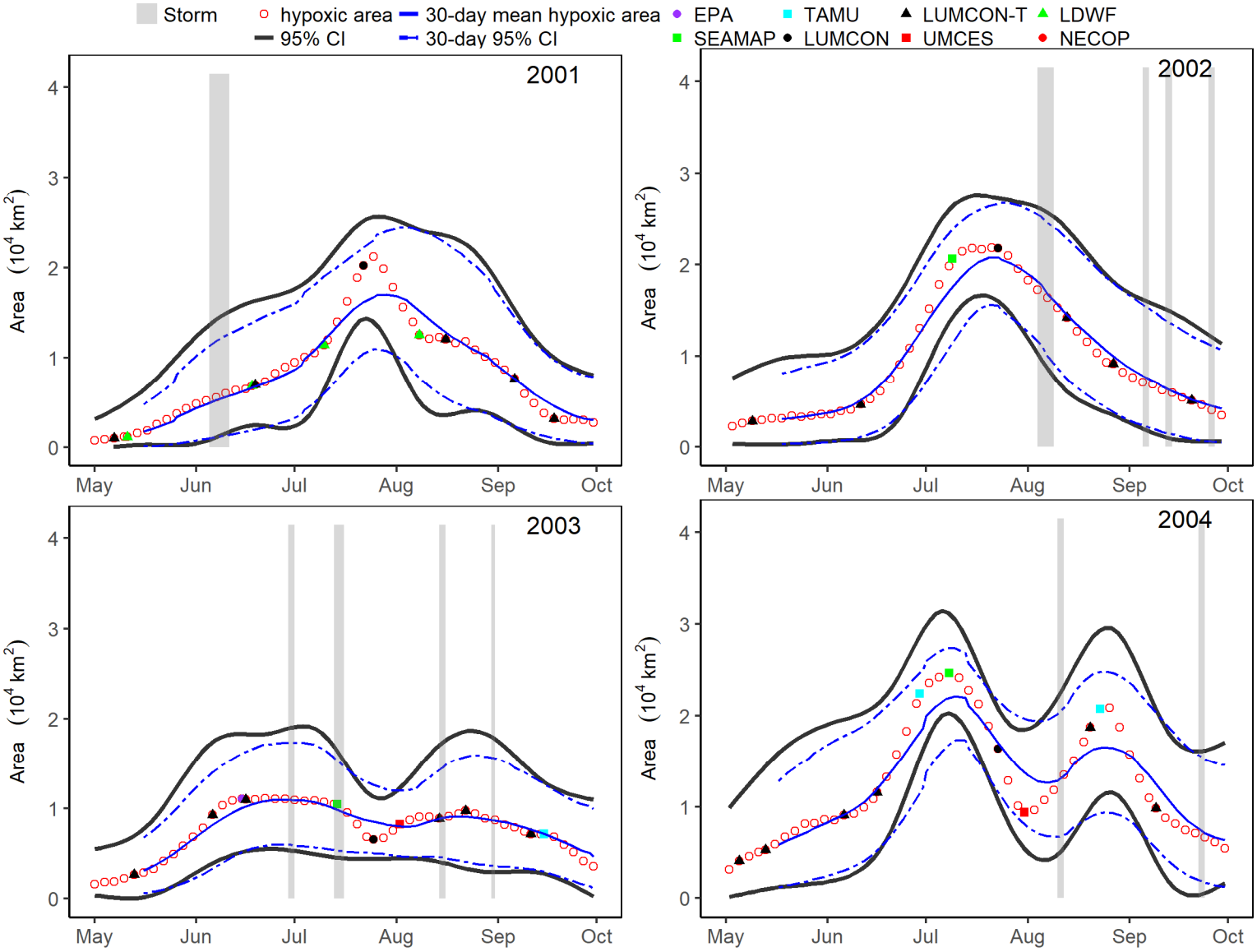

Figure S28. Summer-wide daily estimates and 30-day means with their respective 95% CI for 2001-2004.

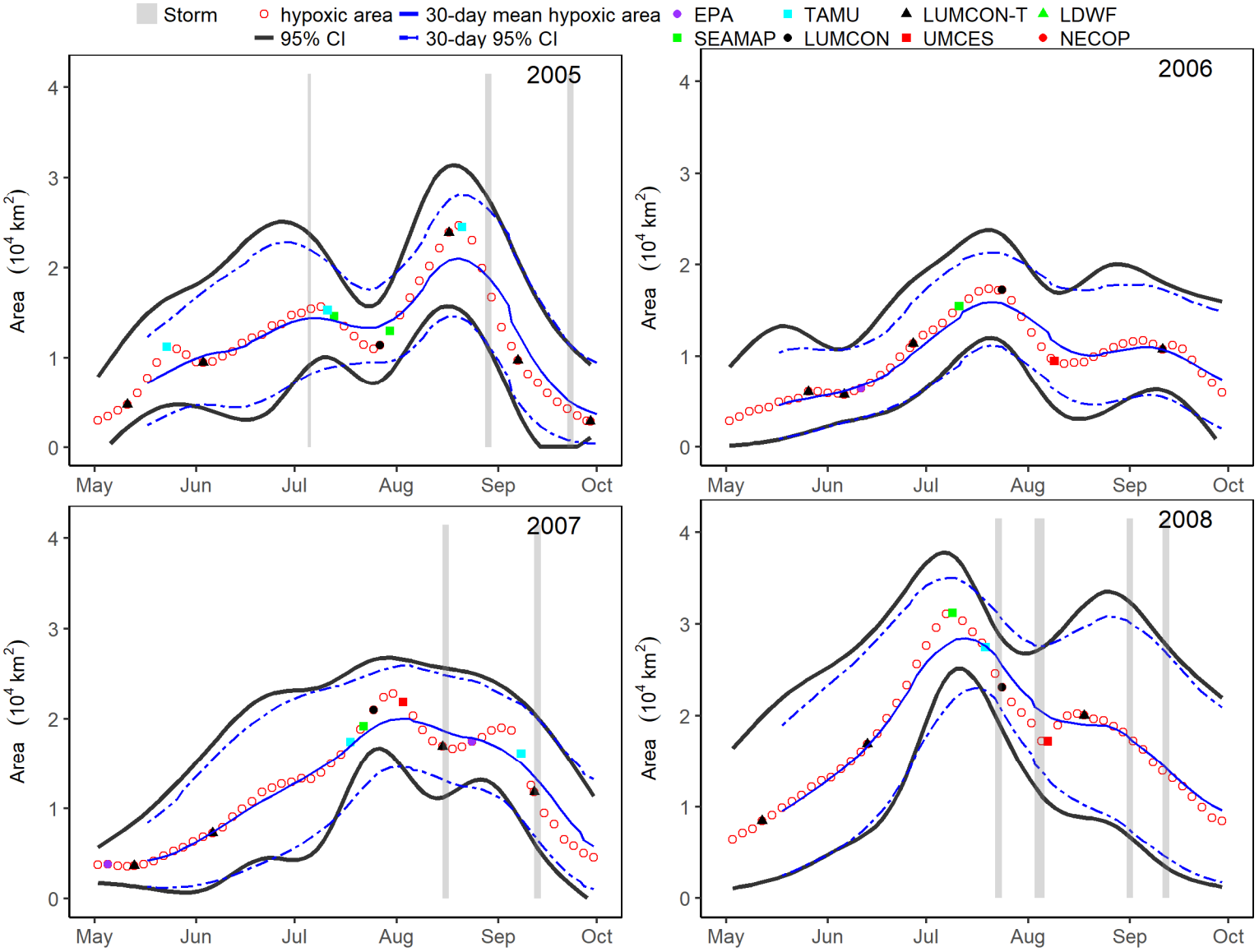

Figure S29. Summer-wide daily estimates and 30-day means with their respective 95% CI for 2005-2008.

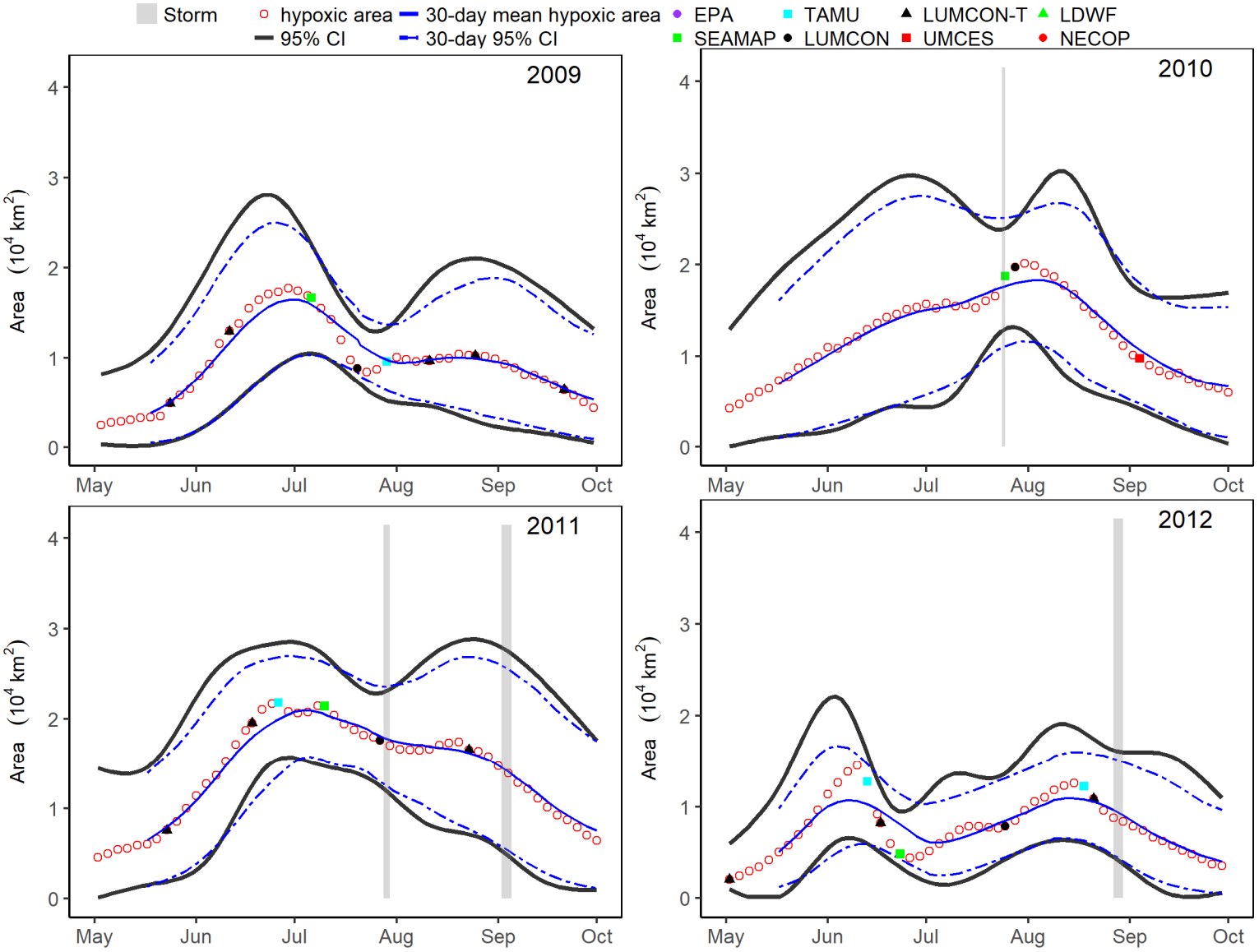

Figure S30. Summer-wide daily estimates and 30-day means with their respective 95% CI for 2009-2012.

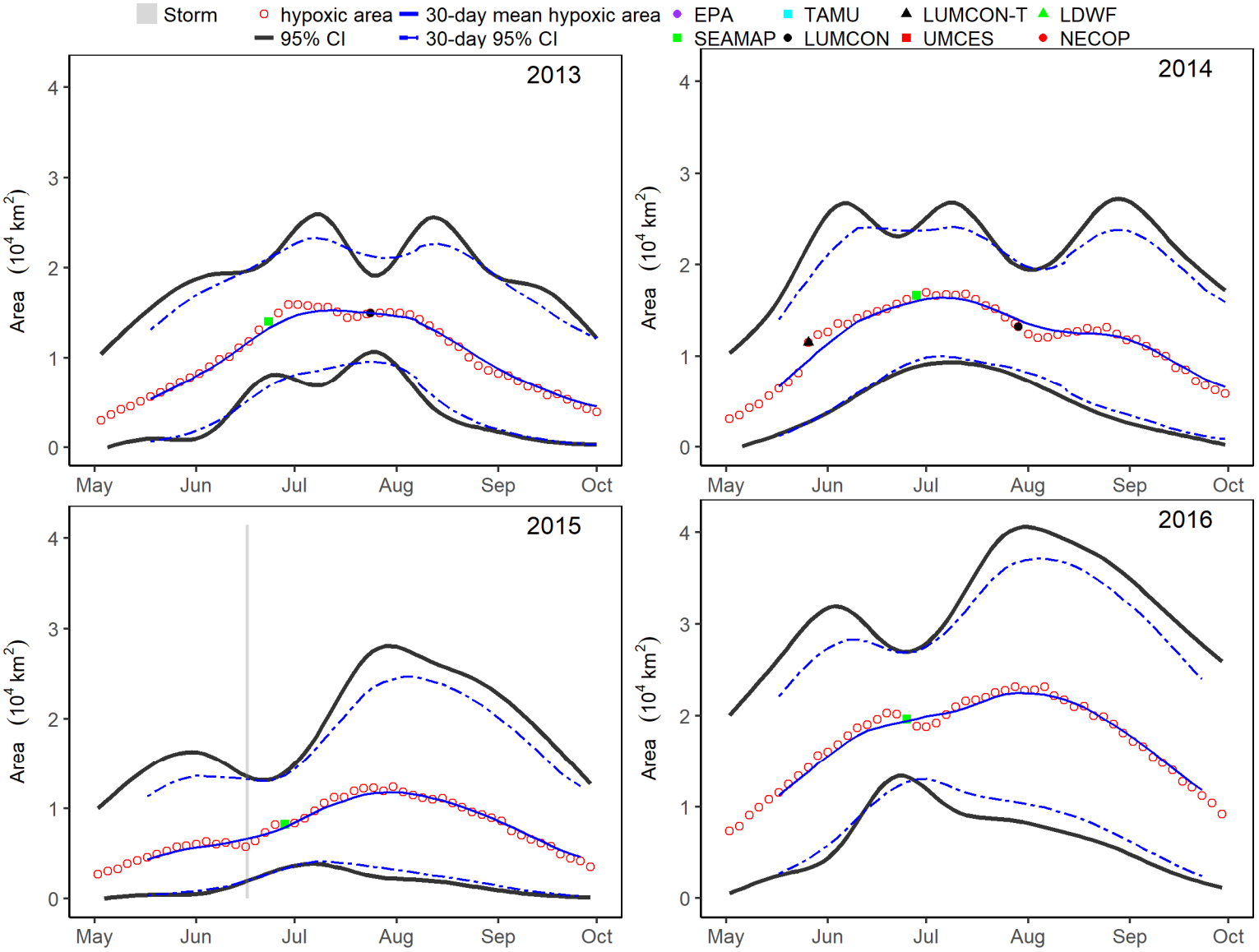

Figure S31. Summer-wide daily estimates and 30-day means with their respective 95% CI for 2013-2016.

S12: Monthly averages of hypoxic area from model version C, 1985-2016

Daily estimates of hypoxia (determined at 3-day intervals) were averaged over each summer month (May-September) from 1985-2016.

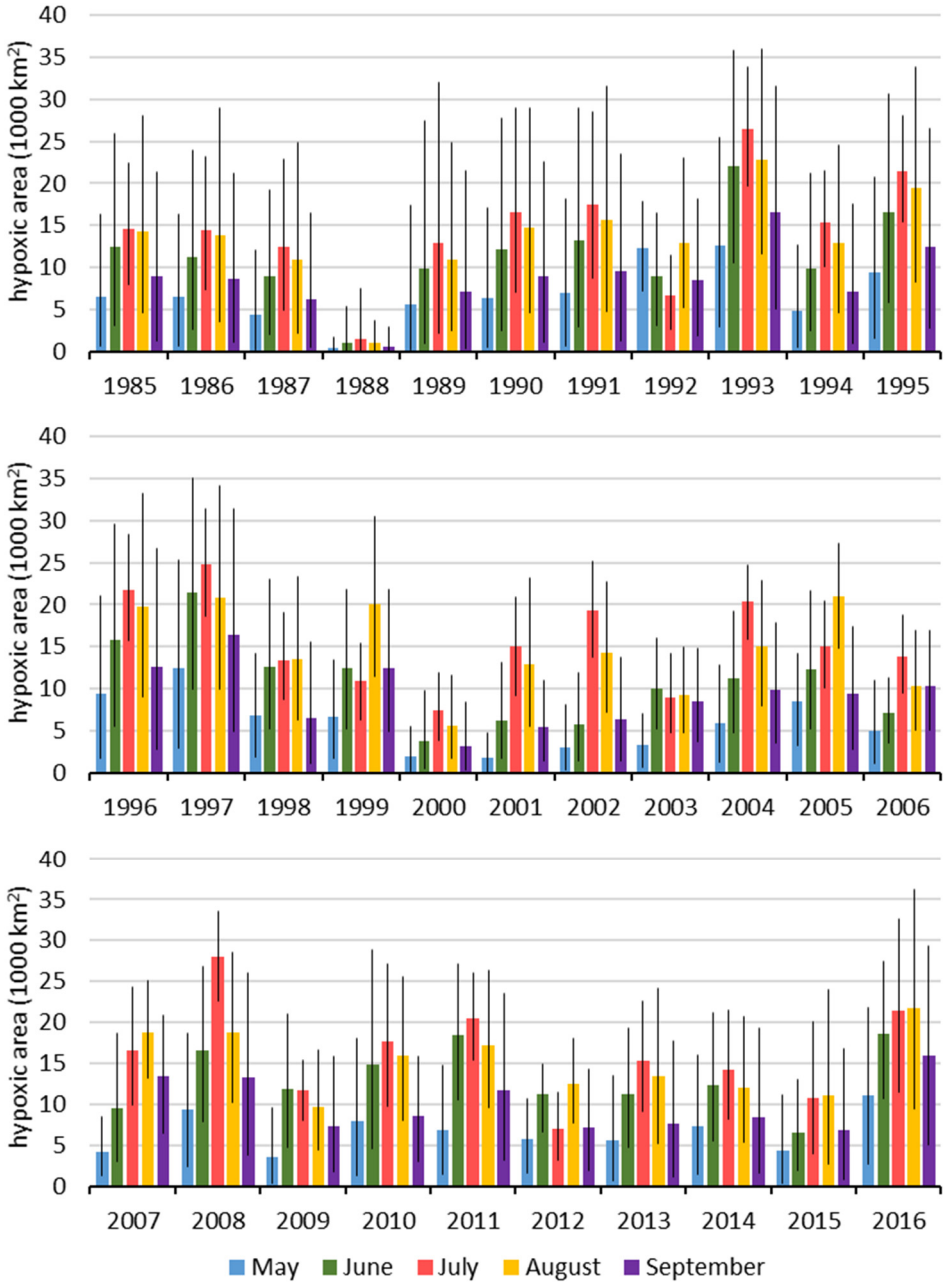

Figure S32. Comparison of monthly averages of hypoxic area obtained from model version C for the years 1985-2016.

Table S5. Monthly averages of hypoxic area obtained from model version C for the years 1985-2016.

YEAR	MAY			JUNE			JULY			AUGUST			SEPTEMBER		
	mean	CI 2.5	CI 97.5	mean	CI 2.5	CI 97.5	mean	CI 2.5	CI 97.5	mean	CI 2.5	CI 97.5	mean	CI 2.5	CI 97.5
1985	6565	669	16261	12377	3121	25897	14556	8003	22457	14310	4557	27986	9004	1299	21322
1986	6427	612	16385	11166	2667	23980	14403	7313	23222	13767	3594	28915	8698	1162	21140
1987	4291	226	11998	8866	2064	19249	12513	4863	22929	10846	2128	24918	6236	529	16538
1988	342	0	1762	976	2	5399	1500	17	7432	1066	63	3741	528	0	2935
1989	5517	175	17389	9853	943	27376	12937	2174	32070	10974	2485	24791	7172	388	21447
1990	6338	446	17047	12159	2388	27687	16530	7067	29000	14667	4645	28995	9008	1086	22601
1991	6963	597	18121	13262	2960	29045	17449	8638	28537	15700	4704	31608	9543	1220	23438
1992	12292	7194	17919	8937	3005	16531	6646	2628	11387	12843	5161	23023	8538	1903	18228
1993	12646	2940	25423	22073	10461	35843	26463	19701	33788	22799	11639	35982	16611	4981	31563
1994	4828	414	12597	9879	2392	21274	15403	10062	21505	12957	4545	24564	7105	937	17473
1995	9351	1561	20782	16550	5870	30621	21408	15396	28029	19473	8195	33775	12490	2702	26473
1996	9459	1641	21069	15784	5493	29549	21680	15651	28288	19773	8979	33300	12620	2835	26744
1997	12430	2849	25272	21392	9946	35122	24802	18594	31392	20868	9856	34189	16375	4848	31384
1998	6862	1910	14161	12583	5178	22965	13421	8679	19125	13569	6333	23409	6529	1110	15578
1999	6668	1711	13453	12381	5267	21845	10907	6244	15394	20025	11445	30470	12410	4968	21738
2000	1872	164	5583	3706	530	9820	7373	3837	11851	5540	1692	11610	3123	377	8375
2001	1750	89	4753	6144	1647	13054	14957	9118	20922	12950	5484	23111	5458	1348	11047
2002	3048	319	8027	5773	1383	11846	19285	13802	25144	14288	7250	22773	6321	1430	13806
2003	3295	681	6974	10008	5167	15961	8974	4768	14144	9249	4775	14925	8548	3666	14864
2004	5821	1179	12826	11278	4745	19187	20305	15930	24643	15101	7930	22945	9820	3490	17876
2005	8482	3198	14169	12293	5140	21722	14994	10051	20433	20986	14827	27244	9404	2723	17454
2006	4956	1059	11024	7061	3575	11283	13866	9436	18730	10276	4995	16961	10350	5094	16877
2007	4227	1284	8459	9540	2953	18708	16651	9928	24406	18805	13217	25064	13463	6476	20875
2008	9412	2471	18762	16506	7863	26819	27963	22642	33539	18693	10304	28627	13293	3795	26059
2009	3639	403	9645	11887	4824	20983	11654	8034	15389	9689	4469	16726	7320	1845	15880
2010	7972	1259	18042	14838	4634	28833	17681	9790	27139	16008	8099	25516	8644	3083	15928
2011	6858	1437	14732	18438	10579	27088	20518	15384	26115	17234	9646	26398	11742	3217	23623
2012	5813	1556	10701	11251	6698	14966	6955	3208	11515	12579	7740	18018	7156	1909	14305
2013	5684	719	13551	11255	4762	19328	15328	9197	22580	13394	5218	24176	7648	1167	17787
2014	7404	1512	15973	12308	5518	21168	14211	8250	21458	11986	5337	20659	8501	1632	19279
2015	4294	347	11128	6592	1947	13126	10854	4009	20056	11144	2637	23974	6918	860	16868
2016	11156	2711	21770	18645	10702	27510	21391	11529	32630	21688	9377	36294	15957	5022	29391

S13: Hypoxic Area versus Nutrient Loading

The table below contains the data used in examining the correlations between hypoxic area estimates and nutrient loadings. Midsummer (cruise) hypoxia estimates are most strongly correlated with February through June loads (r^2=0.48), and average summer-wide estimates are most strongly correlated with November-June loads (r^2=0.66).

Table S6. Estimates of hypoxic area (midsummer cruise and summer-wide) determined from geostatistical model results and average nutrient loadings from Mississippi and Atchafalaya rivers (1998-2014).

YEAR	AVERAGE LOAD FROM FEBRUARY TO JUNE (Mg/Month)	AVERAGE LOAD FROM NOVEMBER TO JUNE (Mg/Month)	MIDSUMMER CRUISE ESTIMATE (km^2)	SUMMER-WIDE HYPOXIA ESTIMATE (km^2)
1998	140712	107730	12621	13173
1999	152943	118143	20273	14268
2000	67971	50369	4777	5442
2001	137814	99067	20744	11532
2002	117897	92958	21566	13471
2003	82971	68359	6575	9316
2004	105673	86703	16091	15152
2005	99287	97882	11453	15650
2006	89115	67006	16498	10601
2007	116923	97211	21002	15127
2008	168972	126625	23068	21347
2009	133379	104295	8373	11074
2010	127876	115044	18855	16176
2011	149507	110280	17758	18749
2012	70181	66287	8004	10209
2013	130514	94474	14971	13449
2014	91495	73500	12625	12835